TTI: 0-1244

Influence of Coarse Aggregate Shape and Surface Texture on Rutting of Hot Mix Asphalt Concrete

Research Report 1244-6

Cooperative Research Program

in cooperation with the
Federal Highway Administration and the
Texas Department of Transportation

Technical Report Documentation Page

1. Report Number	2. Government Accession No.	3. Recipient's Catalog No.
FHWA/TX-94/1244-6		

4. Title and Subtitle	5. Report Date
INFLUENCE OF COARSE AGGREGATE SHAPE AND SURFACE TEXTURE ON RUTTING OF HOT MIX ASPHALT CONCRETE	March 1994 Revised: October 1994
	6. Performing Organization Code
7. Author(s) Mohan Yeggoni, Joe W. Button, and Dan G. Zollinger	8. Performing Organization Report No. Research Report 1244-6
9. Performing Organization Name and Address Texas Transportation Institute The Texas A&M University System College Station, Texas 77843-3135	10. Work Unit No.(TRAIS) 11. Contract or Grant No. Study No. 0-1244
12. Sponsoring Agency Name and Address Texas Department of Transportation Research and Technology Transfer Office P. O. Box 5080 Austin, Texas 78763-5080	13. Type of Report and Period Covered Interim: September 1990 - August 1993 14. Sponsoring Agency Code

15. Supplementary Notes

Research performed in cooperation with the Texas Department of Transportation and the U.S. Department of Transportation, Federal Highway Administration.

Research Study Title: Evaluation of the Performance of Texas Pavements Made with Different Coarse Aggregates

16. Abstract

The objectives of this study were to: 1) evaluate the influence of coarse aggregate shape and surface texture on deformation characteristics of asphalt concrete, 2) characterize aggregate elongation, shape, and texture using fractal dimensional analysis, and 3) study the correlation between the physical properties of coarse aggregates and the permanent deformation characteristics of asphalt concrete. In order to study the influence of coarse aggregate type on the properties of asphalt concrete mixture, seven different blends of aggregates of the same gradation were prepared using three types of aggregates: 1) uncrushed river gravel, 2) crushed river gravel, and 3) crushed limestone. These seven aggregate blends were used to prepare specimens for a laboratory testing program.

The laboratory investigation was conducted in two phases: 1) an asphalt concrete mixture study and 2) the characterization of coarse aggregate elongation, shape, and surface texture using fractal dimensional analysis. The asphalt concrete mixture analysis focused on evaluating permanent deformation characteristics of mixtures made with different percentages of crushed coarse aggregate. An increase in the percentage of crushed coarse aggregate resulted in increased Hveem and Marshall stability and increased resistance to creep and permanent deformation of hot mix asphalt concrete. Resilient modulus of the specimens was also enhanced by increasing the amount of crushed aggregate in the mix at high temperature (115°F [or 40°C]). Fractal dimension analysis was shown to be a viable technique for characterizing aggregate particle shape and surface texture. Researchers found a direct correlation between permanent deformation of asphalt concrete mixtures and shape characteristics of coarse aggregate particles used in the mixtures.

17. Key Words	18. Distribution Statement
Asphalt Concrete Mixtures, Coarse Aggregates, Mix Design, Rutting Model, Permanent Deformation, Fractal Analysis, "p" Value.	No restrictions. This document is available to the public through NTIS: National Technical Information Service 5285 Port Royal Road Springfield, Virginia 22161

19. Security Classif.(of this report)	20. Security Classif.(of this page)	21. No. of Pages	22. Price
Unclassified	Unclassified	147	

Form DOT F 1700.7 (8-72)

INFLUENCE OF COARSE AGGREGATE SHAPE AND SURFACE TEXTURE ON RUTTING OF HOT MIX ASPHALT CONCRETE

by

Mohan Yeggoni
Graduate Assistant
Texas Transportation Institute

Joe W. Button
Research Engineer
Texas Transportation Institute

and

Dan G. Zollinger
Assistant Research Engineer
Texas Transportation Institute

Research Report 1244-6
Research Study Number 0-1244
Research Study Title: Evaluation of the Performance of Texas Pavements Made with Different Coarse Aggregates

Sponsored by the
Texas Department of Transportation
In Cooperation with
U.S. Department of Transportation
Federal Highway Administration

March 1994
Revised: October 1994

TEXAS TRANSPORTATION INSTITUTE
The Texas A&M University System
College Station, Texas 77843-3135

IMPLEMENTATION STATEMENT

A comprehensive laboratory test program was performed primarily to ascertain the influence of *coarse* aggregate shape and surface texture on rutting resistance of asphalt paving mixtures. A companion laboratory/field study was conducted during 1987 through 1991 in which the influence of *fine* aggregate shape and surface texture on rutting was assessed (Research Report 1121-2F, "Identifying and Correcting Rut-Susceptible Asphalt Mixtures"). In fact, the use of fractals for objectively measuring aggregate shape and surface texture, and the "p" value concept were first introduced to the Texas Department of Transportation in that study. This complementary study of creep/permanent deformation as a function of coarse aggregate properties adds further credence to the earlier conclusion that these new laboratory procedures (fractal dimension analysis and the "p" value concept), if properly applied in the laboratory, can minimize the placement of rut-susceptible asphalt mixtures in the field.

The "p" value is based on a hyperbolic mathematical model that provides an excellent predictor of actual creep and recovery of asphalt mixtures. It is an improvement over other models because it is based on the properties of the complete paving mixture and not just the binder properties alone. TxDOT Study 455 has incorporated this model into the Texas Flexible Pavement System to provide for more realistic prediction of rutting from laboratory tests and, therefore, is available for immediate implementation.

Fractal dimension analysis of coarse aggregate exhibited excellent correlation with permanent deformation characteristics of asphalt mixtures. Fractal analysis has been demonstrated to be a very practical but robust technique for objectively quantifying particle shape and surface texture of coarse aggregates and, with magnification, even fine aggregates. The importance of this finding lies in the fact that no standard method exists for directly measuring aggregate particle shape (i.e., angularity) or surface texture. ASTM D4791 measures flatness and elongation of aggregate particles, but it is tedious and time consuming. With relatively little additional research effort, fractal dimension analysis could be developed into an implementable procedure. It could become an integral part of a new

classification system for asphalt and portland cement paving aggregates.

The requirement of 85 percent crushed faces for gravel aggregate retained on the No. 4 sieve in the current TxDOT specification for Item 340, "Hot Mix Asphaltic Concrete Pavement," was primarily established to afford adequate skid resistance. However, findings of this study indicate that this value is also optimum for cost-effective, rut-resistant mixtures. This practice should be continued.

The use of 85 to 100 percent crushed coarse aggregate in asphalt mixtures resulted in laboratory mixture properties indicative of adequate resistance to rutting when the mixture contains the proper asphalt content as determined by standard TxDOT hot mix asphalt design methods. Asphalt content should not be arbitrarily increased in the field merely to obtain the required density. If design density is difficult to achieve and aggregate gradation is acceptable, the size and number of compaction devices and mat temperature should be carefully scrutinized before asphalt content is increased over the optimum design value. Difficulty in compaction of a mixture may indicate the resulting pavement will also be difficult to deform by heavy traffic loads.

DISCLAIMER

The contents of this report reflect the views of the authors who are responsible for the facts and accuracy of the data presented herein. The contents do not necessarily reflect the official view or policies of the Texas Department of Transportation (TxDOT) or the Federal Highway Administration (FHWA).

ACKNOWLEDGMENT

The authors wish to acknowledge the guidance and assistance of several individuals who made positive contributions to this work.

Mr. Jim Nitsch of TxDOT served as chairman of the Technical Panel.

Mr. Greg Poirier of Holnam Inc. served as the industrial liaison for the Panel.

Mr. Paul Chan of TTI collected and analyzed all data in relation to fractal dimension analysis.

Final typing of the manuscript was performed by Ms. Cathy Bryan.

The work was sponsored and funded by the Texas Department of Transportation in cooperation with the Federal Highway Administration.

TABLE OF CONTENTS

TABLE OF CONTENTS (Continued)

LIST OF FIGURES

LIST OF FIGURES (Continued)

LIST OF FIGURES (Continued)

LIST OF TABLES

LIST OF TABLES (Continued)

SUMMARY

In 1987 to 1991, a laboratory and field investigation was conducted to determine the influence of sand-size (minus No. 10 sieve) aggregate particles on rutting of asphalt paving mixtures. The culmination of that work was Report No. FHWA/TX-91-1121-1F, "Identifying and Correcting Rut-Susceptible Asphalt Mixtures." This study was a follow-up to that work to determine the effect of coarse aggregate (defined herein as that retained on a No. 4 sieve) properties on permanent deformation characteristics of asphalt concrete mixtures. This study consisted only of a laboratory investigation.

Specific objectives of this study include: 1) evaluate the influence of coarse aggregate shape and surface texture on deformation characteristics of asphalt concrete, 2) characterize aggregate elongation, shape and texture using fractal dimensional analysis, and 3) study the correlation between the physical properties of coarse aggregates and the permanent deformation characteristics of asphalt concrete. In order to study the influence of coarse aggregate type on the properties of asphalt concrete mixtures, seven different blends of aggregates were prepared using various percentages of three different types of aggregates: 1) crushed river gravel, 2) crushed limestone, and 3) uncrushed river gravel. These seven aggregate blends, ranging from uncrushed to fully crushed, were used to fabricate test specimens for the experiments.

This investigation was conducted in two phases: 1) an asphalt concrete mixture study and 2) the characterization of coarse aggregates elongation, shape, and surface texture using fractal dimensional analysis. The asphalt concrete mixture analysis focused on evaluating permanent deformation characteristics of mixtures made with different percentages of crushed coarse aggregate. Fractals are a family of mathematical functions that describe natural phenomena and shapes. The fractal dimension of a surface corresponds closely to the intuitive notion of roughness. This work demonstrated that fractal dimension analysis is a suitable objective technique for characterizing aggregate shape and surface texture. This is significant because there are currently no standard tests in AASHTO or ASTM for directly and objectively measuring aggregate particle shape and surface texture.

Furthermore, direct correlation was observed between permanent deformation of asphalt concrete and shape/texture measurements of coarse aggregate particles used in the mixture.

Based on the laboratory evaluation of the mixes prepared using different amounts of crushed coarse aggregates and objective measurement of aggregate shape and surface texture, the researchers concluded:

1. Long-term static and cyclic creep (unconfined compression) tests were sensitive to changes in coarse aggregate surface characteristics. Both static and dynamic creep tests showed a decrease in creep and permanent deformation with increase in the amount of crushed coarse aggregate in asphalt mixtures of the same gradation.
2. Hveem stability increased consistently with an increase in the percentage of crushed coarse aggregate.
3. At high pavement service temperatures, an increase in the percentage of crushed coarse aggregate increased resilient modulus. At low temperatures, aggregate type had little effect on resilient modulus.
4. Marshall stability increased with an increase in the amount of crushed coarse aggregate in the mixture.
5. The fractal dimension number has potential to be a practical measure of shape and texture of aggregate particles. The fractal number for texture correlated with deformation behavior of asphalt mixtures.
6. A test property termed "p" value correlates with creep compliance of the mixture and accounts for the influence of aggregate shape and texture on permanent deformation of asphalt concrete. The "p" value decreased with an increase in percentage of crushed coarse aggregate.
7. The "p" value increased with a decrease in the fractal number which indicates that rutting susceptibility increases with a decrease in the fractal dimension number.
8. The amount of crushed coarse aggregate is a major factor that should be considered when designing rut-resistant hot mix asphalt concrete.
9. This work provides evidence that the requirement of 85 percent crushed faces in TxDOT standard specification for Item 340, hot mix asphalt concrete, is about optimum for rut resistance and economy.

CHAPTER 1
INTRODUCTION

BACKGROUND

Rutting or permanent deformation in asphalt concrete pavement has been one of the major concerns of highway engineers for many years (1, 6, 10). Premature failure of asphalt pavements due to rutting has occurred in all states in the U.S. (10). Tire pressures used in current asphalt pavement design are in the range of 70 to 80 psi (4.8×10^5 to 5.5×10^5 pascal); whereas, future and present truck tire pressures have been estimated to be more than 100 psi (6.9×10^5 pascal) (19). Excessive tire pressures are a major cause of rutting (1, 6, 9, 10). In addition to excessive loading, improper mixture preparation that provides higher or lower asphalt content than required and improper material selection, (i.e., grade of asphalt, type of aggregate, and excessive moisture content) contribute to the rutting problem (6, 9, 10, 20).

Many highway engineers believe that in the future, tire pressures will increase further, thus, worsening the rutting distress facing the highway agencies (10). Others indicate there will certainly be no reduction in truck tire pressures in the future (21, 22). Since higher tire pressures applied on pavements appear to be inevitable, it is necessary for materials engineers to consider the asphalt concrete mixture and its components in order to formulate a rut-resistant asphalt mixture.

Proper selection of materials is one of the most important tasks in developing an asphalt mixture that shows improved resistance to permanent deformation. Results of investigations to determine the type of aggregates that provide better resistance to permanent deformation show that crushed aggregates play a major role in contributing to greater stability (resistance to deformation and plastic flow) of hot mix asphalt concrete (1-15). Previous studies show that crushed aggregate, through interlocking and shear resistance, can improve the mix strength which is a measure of load bearing capacity and resistance to rutting and shoving (horizontal displacement of an asphalt mixture) (1-15).

PURPOSE AND SCOPE

A main objective of this study was to evaluate the properties of aggregate particles to examine their influence on the behavioral and performance characteristics of asphalt concretes. The ultimate goal was to determine shape and surface texture of aggregate particles and evaluate the permanent deformation performance of asphalt concrete mixtures in relation to the physical properties of the coarse aggregates.

A permanent deformation model developed by Button et al. (6) was used to determine "p" value which is considered to be an aggregate related material characteristic of the asphalt concrete. A revolutionary technique, fractal dimension (fd) analysis, was used in the second phase to quantify aggregate particle shape (angularity) and texture (measure of surface roughness). In order to correlate aggregate properties with asphalt concrete mix permanent deformation characteristics, researchers studied the influence of crushed coarse aggregate on the properties of asphalt concrete mix and determined the permanent deformation factor, the "p" value, and the fractal dimension for aggregates of different shapes and surface textures. This work provides a basis to develop aggregate-related specifications to improve the quality (level of stability and strength) of asphalt concrete to withstand the stresses in asphalt concrete pavements. The objective characterization of aggregate shape and surface texture could be used in an aggregate classification system for improved aggregate specifications.

CHAPTER 2
LITERATURE REVIEW

Many studies have been conducted to investigate the causes of rutting and to suggest various remedies for its prevention (1-27). Researchers have experimented with aggregates of different gradations, shape, and surface texture and with different types of asphalt binders to investigate their influence on the permanent deformation characteristics of asphalt concrete. Research findings reviewed in this chapter can be categorized as follows:

1) Types and causes of rutting,
2) Measures to reduce rutting, and
3) Characterization of aggregate properties.

TYPES AND CAUSES OF RUTTING

A US DOT ad hoc task force, lead by Mendenhall et al. (10), on asphalt pavement rutting and stripping identified the following types of rutting:

1) Plastic deformation - a depression in asphalt pavement near the center of the applied load with slight humps on either side of the depression.
2) Consolidation - a depression in asphalt pavement near the center of the applied load without accompanying humps.
3) Structural deformation - a subsidence in the base, subbase, and/or subgrade, as well as the pavement, accompanied by a distress cracking pattern in the pavement.

Warburton et al. (17) stated that consolidation in asphalt concrete pavements was the result of excessive traffic load on the pavement and that plastic deformation was due to the inadequate stability of asphalt concrete mixture.

Krutz and Stroup-Gardiner (12) reported that stripping in asphalt concrete due to moisture susceptibility is a major cause of rutting. Stripping in an asphalt mixture can be defined as a phenomenon that causes asphalt to lose its cohesive strength and bond to aggregate particles due to the presence of moisture. Researchers observed that severe rutting occurred during the first warm weather following the application of a chip seal in Nevada. The chip seal trapped moisture inside the pavement which caused stripping. Examination of cores collected from severely rutted pavements revealed that a considerable amount of stripping occurred in the asphalt concrete layers. A hypothesis was made that the low shear resistance, due to the presence of moisture, caused high levels of stripping which eventually caused permanent deformation in the asphalt concrete pavements. In order to verify this hypothesis, specimens were prepared using loose asphalt concrete samples collected from the field during construction. Some of these samples were conditioned in accordance with Lottman's moisture conditioning procedure (18). Both normal and moisture conditioned samples were tested for creep. Creep results of these tests showed that moisture conditioning played a significant role in increasing the susceptibility of asphalt concrete to permanent deformation. A statistical test (Student's t-test) was used to find the significance of the difference in the means of creep values before and after moisture conditioning. It was found that the difference was statistically significant at 95 percent confidence interval, but was not significant at 99 percent confidence interval.

Consolidation of asphalt concrete in the upper layer is mainly due to high truck loads and tire pressures applied on the pavement surface (10, 19). Research at Texas A&M University and the University of Texas indicated that higher tire pressures and axle weights caused fatigue cracking and rutting at early ages of the pavement life (21, 22). Researchers reported that traffic volume on highways could not be controlled, but recommended that higher loads and tire pressures should be controlled through legislation (6, 10). Several State Highway Agencies (SHA's) anticipate worsening of rutting due to:

1) The increase in volume of traffic (ESAL),
2) The increase in number of truck over loads (number of trucks that utilize tire pressures higher than the tire pressure used in the pavement design), and

3) Switching tire axles on trucks from duals to super singles which increases the stress in the pavement under the wheel (9, 10).

A major cause of plastic flow and consolidation of asphalt concrete pavement is inappropriate selection of aggregates and binders for asphalt concrete mixtures. Use of poorly graded aggregates having smooth, subrounded particles and a high percentage of natural, rounded sand contribute to the loss of shear resistance of asphalt concrete mix (6). Use of low viscosity asphalt in hot regions promotes plastic flow (10). Asphalt content above the optimum required for asphalt concrete also causes inadequate stability of concrete mix. A combination of low viscosity asphalt, smooth rounded aggregates, and a high percentage of natural sand can make a highly rut-susceptible asphalt concrete mixture due to its high temperature susceptibility and low shear resistance (6).

Huber and Heiman (14) conducted an investigation to find factors that influenced rutting in some severely rutted pavements. Data regarding asphalt content, Hveem stability, air voids, and fractured aggregate surfaces in asphalt concrete pavement immediately after construction were defined as the post-construction data. It was assumed that changes in the properties of asphalt concrete in the center portion of a lane were minimal and that measured properties of cores could be considered as post-construction data. On the other hand, properties of the asphalt concrete mix in the wheel path were considered as present data. Data regarding asphalt content, air voids, fractured faces, Hveem stability, Marshall stability, and viscosity of the asphalt at the time of analysis were determined by analyzing the cores collected from wheel paths. Rutting performance of the pavement was analyzed to determine if there was a correlation to the post-construction data and the present data. Rut depth could not be correlated to any of the asphalt concrete properties. However, rate of rutting was correlated to asphalt content and Hveem stability from the present data. Additionally, rate of rutting could be correlated to the voids in mineral aggregate asphalt content, air voids, and Hveem stability from post-construction data.

Examination of cores collected from rutted pavements showed low average Marshall stability, excessive asphalt content, a higher percentage material passing No. 200 sieve (75 μm), and low viscosity asphalt. Researchers found that rutting was mainly a result of low

stability, low air voids, and low viscosity. Percentage air voids in the mix was low due to the presence of a high amount of fines and asphalt in the mixture which filled the voids.

REDUCING RUTTING

Various steps have been taken by many SHA's in the U.S. to address rutting distress in asphalt concrete pavements. Many SHA's have specified a minimum of 85 percent crushed particles in the total aggregate blend in an effort to reduce rutting. The Iowa DOT (1, 23) has reduced rutting by implementing the following asphalt concrete mixture design specifications:

1. Maximum size of aggregate is 3/4 inch (19 mm),
2. Minimum laboratory air voids in the asphalt concrete mixture as 3.5 percent and maximum as 6.0 percent,
3. Minimum of 13.5 percent voids in mineral aggregates (VMA),
4. Marshall compaction of 75 blows, and
5. Minimum of 85 percent crushed particles in the aggregate.

The Illinois Department of Transportation (25) has also taken measures to reduce rutting in asphalt pavements. These measures include:

1) Increase VMA from 11-13 percent to a minimum of 15 percent,
2) Increase design air void content from 2.5 percent to 4 percent,
3) Replace 100 percent of natural sand with coarser crushed sand size particles,
4) Increase aggregate fines (-No.200) from 0-6 percent to 0-8 percent, and
5) Change asphalt type from AC-10 to AC-20 .

These new specifications reduced rutting in the state.

Studies have been conducted to determine the effectiveness of large-stone (maximum size of aggregate over 1 inch [25 mm]) asphalt mixes (7, 11). It was found that large-stone

asphalt concrete mixtures were very effective in reducing rutting. Kandhal (7) stated that the use of large-stone mixtures is appropriate to address severe rutting conditions in asphalt concrete pavements. The Marshall asphalt mixture design procedure (ASTM D1559-82) currently specifies use of 4-inch (10.16 cm) diameter samples. However, specimens of 4-inch diameter cannot be prepared using stone larger than one inch (25 mm). Kandhal (7) developed a draft standard for Marshall design using 6-inch (152 mm) diameter samples and recommended that this be standardized as there will be extensive use of large-stone mixes to reduce rutting potential of asphalt concrete.

Mahboub and Allen (11) recommended the use of large-stone asphalt concrete mixes for construction of highly rut-resistant asphalt concrete pavements. The authors stated that large-stone mixes reduce rutting susceptibility of asphalt concrete by dissipating the compressive and shear stresses through stone on stone contact. A series of large-stone aggregate gradations were used in the mix design using the Marshall design procedure. Samples six inches (152 mm) in diameter and 3-3/4 inches (95 mm) in height were used in the mix design. Air void contents determined for these samples showed that the desirable density of the mix can be easily obtained using large-stone mixes. Compressive strength, resilient modulus, and static and dynamic creep tests were performed on the samples prepared with large-stone asphalt concrete mix. Results of these tests indicated that large-stone asphalt concrete mixtures showed better stability, compressive strength, resilient modulus, and resistance to creep than conventional mixes. The authors recommended the standardization of the Marshall procedure with 6-inch (152 mm) diameter samples.

Three types of large-stone mixes have been evaluated in addressing rutting under heavy loads and high tire pressures: 1) dense graded, 2) stone filled, and 3) open graded. Acott (24) describes dense graded material as a blend that primarily develops strength from aggregate interlock and the viscosity of the binder. The introduction of large-stones increases volume concentration of coarse aggregate in the mix which, in turn, improves its load bearing capacity. This type of mix is characterized by high stability and air void levels typically between four and eight percent.

A stone filled asphalt concrete mix may contain large single sized stone of maximum size 1 to 1-1/2 inches (2.54 cm to 3.81 cm) in the base layer of the pavement and a

maximum size of 1 inch (25 mm) for the asphalt concrete used in the top or surface layer of the pavement. In the stone filled asphalt concrete mix, a stone matrix is formed by the largest stones, and voids between the stones are filled with asphalt and fine aggregate mixture. Due to the bridging effect of the large stone skeleton, the mix is resistant to rutting and densification under traffic. The introduction of higher proportions of large size stone increases the volume concentration of aggregate, reduces aggregate surface area per unit weight, and reduces the optimum asphalt content (24).

A large-stone open graded asphalt concrete mix may contain top size aggregate of 2-1/2 inches (64 mm), low asphalt cement content (typically 2.0 percent), and voids in the 15 to 30 percent range (6, 30).

Bayomy and Guirguis (26) reported that coating of aggregate particles with a film of portland cement provides higher load bearing capacity and stability to asphalt concrete than conventional uncrushed aggregates. Aggregate particles were coated with portland cement, allowed to cure, and then used in the preparation of asphalt concrete mixtures. An illustration of the cement coating concept is shown in Figure 2.1. Specimens were prepared using cement coated aggregates. Laboratory tests were performed on these specimens to estimate rutting, stripping, and ravelling susceptibility. Experimental results showed that the specimens with cement coated particles displayed more resistance to permanent deformation, better performance in the fatigue test, and a sizeable improvement in indirect tensile strength than did the samples prepared with conventional asphalt concrete mix.

Based on the guidelines for cement coating of aggregates developed by Bayomy and Guirguis (26), a research study was conducted by Button and Jagadam (27) to determine the changes in properties of asphalt concrete when prepared with cement coated aggregates. Laboratory and field experiments were conducted using natural, uncrushed aggregates with and without cement coating. Specimens were tested to determine stability and creep resistance. Findings of the experimental program showed that there was an improvement in creep resistance and Hveem stability of the mixture. However, about 95 percent of the cement coating was lost due to abrasion during the plant mixing process.

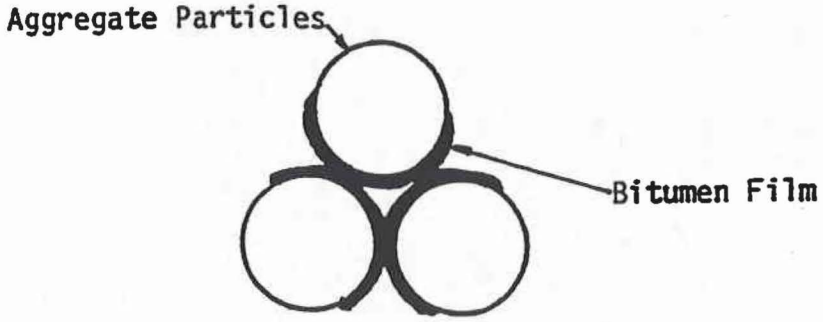

Uncoated Particles in Bituminous Mixtures

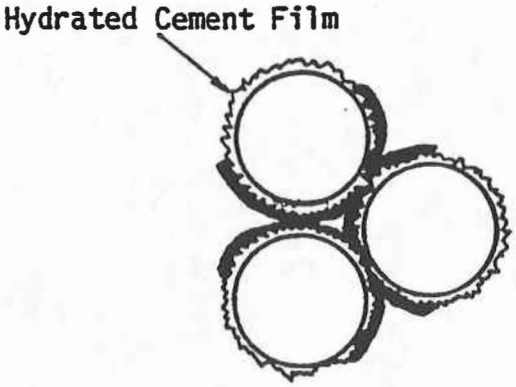

Cement Coated Particles in Bituminous Mixtures

Figure 2.1. Cement Coating Concept (After Reference 26).

CHARACTERIZATION OF AGGREGATE PROPERTIES

Characterization of aggregate physical properties has been done by using various techniques in the past. Characterization of aggregate particle shape (angularity), size, and texture is very useful as they play a major role in the mix design, workability, and performance of asphalt concrete.

Roughness Estimation

Mather (35) reported that roughness, or surface texture, can be estimated by determining deviation of the surface from mean surface level. ASTM D3398 (36) gives the procedure for the determination of particle index of aggregate particles. Particle Index can be characterized as an overall representation of particle shape and texture. Particle Index is determined by estimating voids in an aggregate system at a certain level of compaction.

Barksdale et al. (37) used a rather simple imaging and digitizing technique to characterize the aggregate particle shape. Images of aggregate particles were obtained using a standard office copying machine. The longest dimension of the particle was considered as length of the particle, and width of the particle was considered as the average dimension in the direction perpendicular to the length. Thickness of the particle was taken as the average dimension in the direction perpendicular to the length and the width. Ratios of thickness to width and width to length were determined. A plot of width to length ratio against the ratio of thickness to width (Figure 2.2) was used for aggregate shape classification.

Wilson et al. (38) also used image processing to determine the angularity of aggregates. Angularity is computed by an algorithm which accounts for the change in slope of the periphery of the aggregate particle image. Images of the aggregate particles were taken using a video camera and these images were digitized into pixels. A grey scale of 0 to 68 was used, with 0 representing the darkest and 68 representing the brightest color of the image. Periphery of the particle was identified by checking for the highest difference in grey levels of two adjacent pixels. Change in slope from pixel to pixel on the edge was studied. Angularity of the particle was determined as the ratio of difference in the number

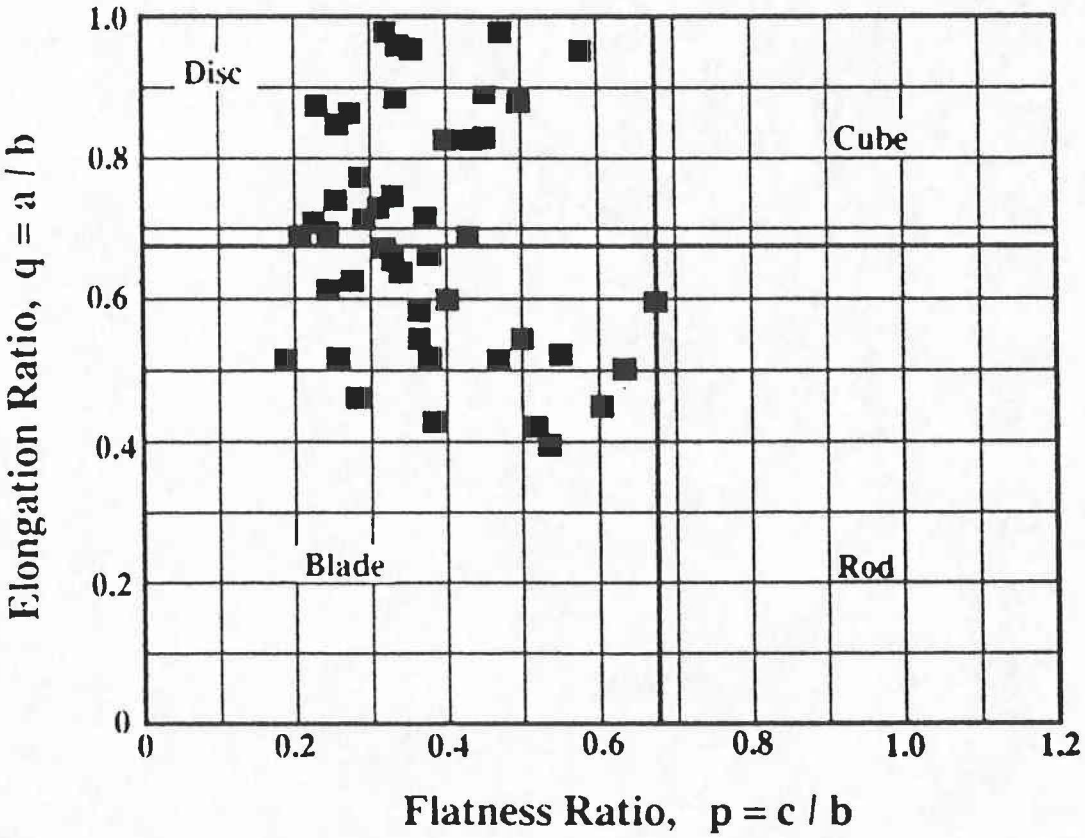

Figure 2.2. Typical Shape Classification Diagram (After Reference 37).

of pixels with a slope change and the number of pixels with the same slope to the total number of pixels forming the edge. The authors recommended that a large-scale study linking aggregate particle properties such as shape, size, and texture with mechanical properties of asphalt concrete such as creep would lead to models for the prediction of pavement performance.

Fractal Dimension Analysis

A revolutionary and promising concept in the characterization of aggregate physical properties is fractal dimension (fd) analysis. This concept has received widespread attention in several fields for characterization of irregular natural shapes and particles. Several studies using fractal dimension analysis to characterize aggregates have been conducted. This concept is explained in a greater detail in Chapter 3 of this report.

Carr et al. (39) reported the use of fractals for characterization of aggregate shape. In this study, the fractal number was determined to represent the shape or angularity of the particle. The authors gave ratings for regular or smooth shapes to irregular (natural) shapes. Fractals concepts were also used for determination of surface area of the particles of size 1 mm or larger (40). Three images of the particle in mutually orthogonal perspectives in silhouette were taken to compute the fractal dimension of the surface of the particle. Areas calculated from these surfaces were then summed to determine the total surface area of the particle.

Leblanc et al. (41) used fractals for analysis and generation of pavement distress images. The fractals concept was used to compress and regenerate the distress data of a pavement. This compression and regeneration is required to reduce space required for storage. This data may be applicable to a pavement management system for evaluation purposes.

Surface texture of particles can be computed using fractals. Box counting was the technique used to determine the fractal dimension number (33). Roughness of the particle was observed to be a direct measure of the rate of increase in non-empty boxes on box-count plot. This plot is explained in Chapter 3 of this report. Roughness of the particles determined using fractals was used to correlate with the cleanability of the metal finishes.

Mandelbrot et al. (42) used the fractals method to estimate fractal dimension number 'D' of the fracture surfaces of metals. Fractal dimension number 'D' was observed to follow the trend of values obtained by another similar study, fracture profile analysis. The authors stated that the fractal dimension number 'D' could be correlated to the toughness of metal.

Fractals are also used in physiology. A study performed by West and Goldberger (43) explains that this concept can be used to study the structure, growth, and function of the particles. In the words of the authors, "the mathematical concept of fractal brings an elegant new logic to the irregular structure, growth, and function of complex biological forms" (43). The authors used this concept to study the relation between form and function of a biological system.

In an effort to develop a criterion that links aggregate properties to Portland Cement Concrete (PCC) mixture design, Ribble et al. (44) used the fractals concept to study the macro shape and micro texture of aggregate particles and their relation to workability of concrete mix. The authors concluded that:

1) Workability of concrete mixture is directly dependent on the fractal dimension number of the aggregates,
2) Fractal dimension of intermediate aggregates compound with coarse aggregate fractal dimensions, and
3) Macro shape and micro texture need to be considered in the workability of mix design.

Perdomo and Button (46) used fractal analysis to rank particle shape and surface texture of crushed and uncrushed aggregates in a study of the influence of fine aggregate particles on rutting of asphalt paving mixtures. This early work concluded that fractals analysis is a viable procedure for characterizing shape and texture of aggregate particles. They pointed out that contrasting colors within some aggregate particles yielded an unrealistically high fractal dimension value.

CHAPTER 3
MATERIALS AND TEST METHODS

The prime goals of this research work were to investigate the influence of coarse aggregate shape (angularity) and texture on rutting characteristics of the asphalt concrete. The laboratory investigation in this research work was conducted in two phases. The first phase of the investigation consisted of the evaluation of asphalt mixtures including Hveem and Marshall stability, resilient modulus, and creep/permanent deformation tests. The second phase of testing focused on the determination of aggregate particle shape and texture using fractal dimension analysis. This chapter discusses experimental procedures and the details of materials used in this research program. A flow chart of the testing program is included in Figure 3.1.

ASPHALT

Since the prime goal of this testing program was to investigate the influence of aggregate shape and texture on rutting characteristics of asphalt concrete mixtures, asphalt was limited to one type and, thus, was not a factor in the results obtained from this study. Consequently, this reduced the number of factors affecting the test results. The asphalt used in the laboratory program was Texaco AC-20. Properties of this asphalt are included in Table 3.1.

AGGREGATES

Seven different aggregate blends of the same grading with varying amounts of crushed coarse aggregate particles were prepared using three types of aggregates: 1) crushed limestone from Brownwood, Texas, 2) crushed river gravel, and 3) uncrushed river gravel from San Antonio, Texas. The fine aggregate portion (- #4 sieve) of all the aggregate blends used in this work was kept constant to study the effect of coarse aggregate properties on performance of asphalt concrete. Fine aggregate was 50 percent by weight of the total

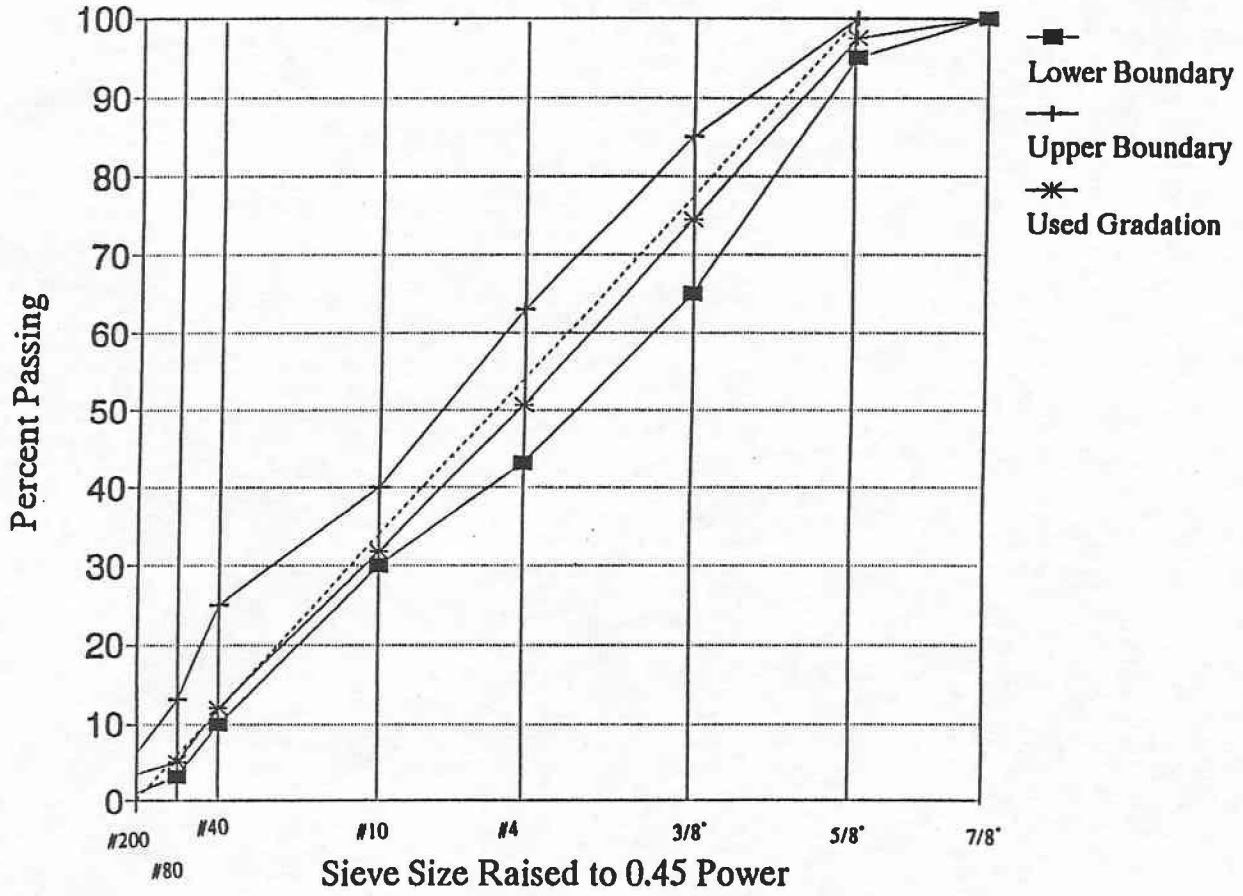

Figure 3.1. Aggregate Gradation Used in this Program with Type C Gradation.

Table 3.1. Properties of the Asphalt Cement Used in the Testing Program.

Asphalt Source & Grade	Texaco AC-20
Viscosity at 140°F (60°C), p	2293
Viscosity at 275°F (135°C), cst	478
Penetration at 77°F (25°C), 100 g, 5s, dmm	74
Penetration at 39.2°F (4°C), 100g, 5s, dmm	26
Softening Point, °F (°C)	119 (48)
Temperature Susceptibility[1], 140°F to 275°F (60-135°C)	-3.34
PVN[2]	-0.30
PVN*[3]	-0.37
P.I.[4] from penetration at 77°F (25°C) and softening point	-0.76
Penetration ratio	35
After Rolling Thin Film Oven Test Viscosity at 140°F (60°C), P Viscosity at 275°F (135°C), cSt Penetration at 77°F (25°C), 100g, 5s, dmm Penetration at 39.2°F (4°C), 100g, 5s, dmm	 3515 722 46 19
Ductility, cm	120+

1 Temperature susceptibility = $(\log\eta_2 - \log\log\eta_1) / (\log T_2 - \log T_1)$, where η = viscosity in poises, T = absolute temperature.

2 PVN = [4.258 - 0.7967 log P - log X) / (0.7951 - 0.1858 log P)]*(11.5), where P = penetration at 77°F (25°C), dmm and X = viscosity at 275°F (135°C), centistokes.

3 PVN* = [(6.489 - 1.590 logP - log X^1) / (1.050 - 0.2234 log P)] (-1.5), where P = Penetration at 77°F (25°C), dmm and X^1 = viscosity at 140°F (60°C), poise.

4 P.I. = (20 - 500α) / (1+50α) where,
α = [log 800 - log pen (25°C)] / (T_{sp} - 25), where T = temperature, °C.

aggregate and was composed of 15 percent natural sand, 14 percent crushed limestone, and 21 percent crushed river gravel.

Details of the aggregate blends prepared using these aggregates are included in Table 3.2. Aggregate blends given in Table 3.2 were used in all the tests explained in the subsequent sections. The aggregates were blended to meet Type C specifications. The gradation ranges are given in Table 3.3, and a 0.45 power chart showing the aggregate gradation along with the specification limits is given in Figure 3.2.

Table 3.2. Details of Aggregate Blends Prepared.

Aggregate Types	Percent Crushed Faces on #4 Sieve			
	0	50	85	100
A. Gravel + Crushed Gravel + 15% Natural Sand	X	X	X	X
B. Gravel + Crushed Limestone +15% Natural Sand		X	X	X

* X indicates tests were performed on the mix with this aggregate blend.

Table 3.3. Aggregate Gradation of Type C Specifications - 1992.

Sieve size	% Passing
7/8 inch (22 mm)	100
5/8 inch (16 mm)	95-100
3/8 inch (9.5 mm)	65-85
#4 (4.75 mm)	43-63
#10 (2.00 mm)	30-40
#40 (425 μm)	10-25
#80 (180 μm)	3-13
#200 (75 μm)	1-6

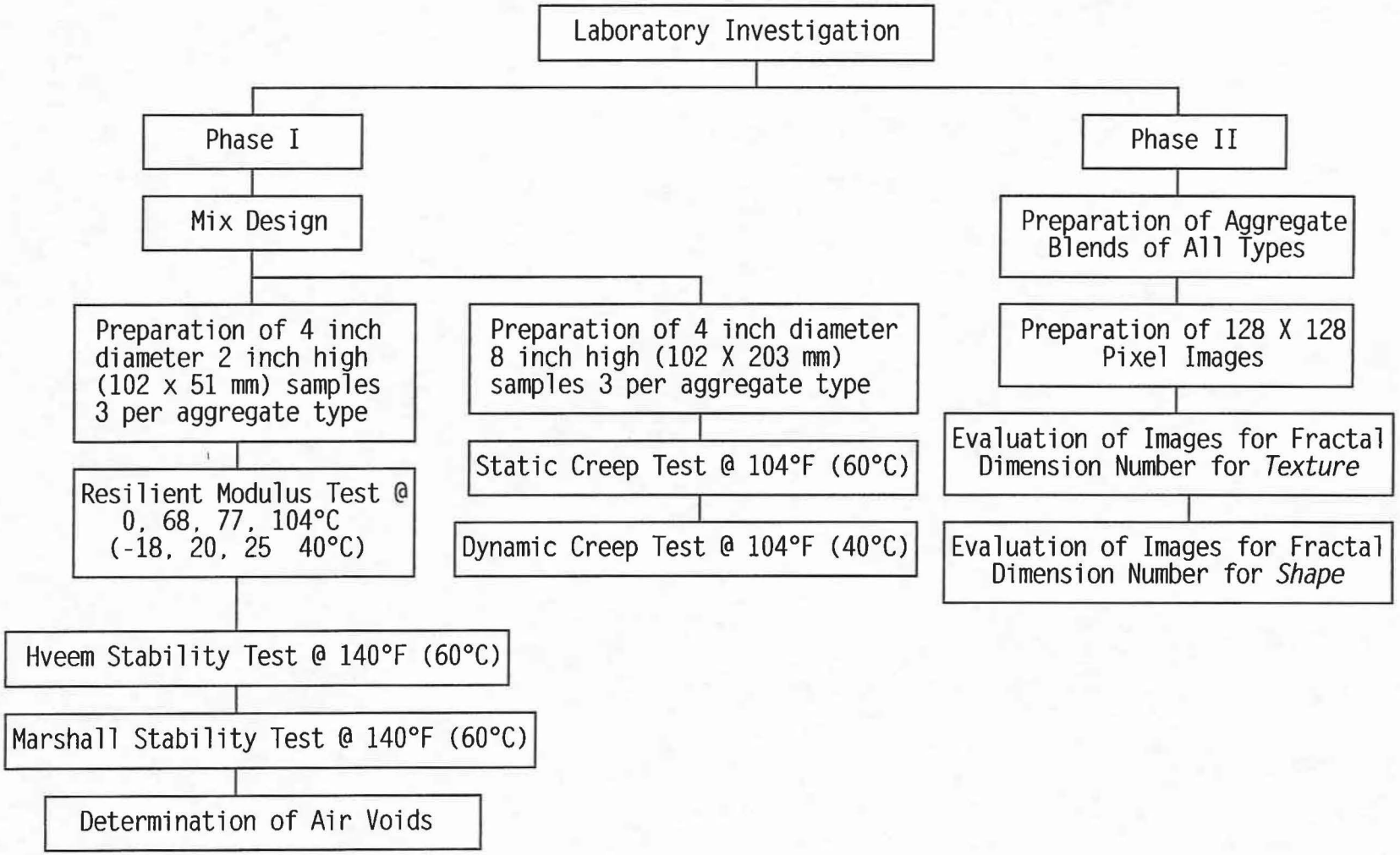

Figure 3.2. Laboratory Test Program.

ASPHALT MIX DESIGN

The Texas Department of Transportation (TxDOT) mixture design method, as described in construction bulletin C-14 (28), was used to determine the optimum asphalt content. Samples for mixture design were prepared using the gyratory compactor for four asphalt contents. Asphalt contents used were in the range of four to seven percent. Density and Hveem stability of the samples were determined and plotted against asphalt content. Optimum asphalt content was determined at 96 percent density (four percent air voids) with a minimum of 35 percent Hveem stability. Optimum asphalt contents for asphalt concrete mixtures with different aggregate blends were determined and used in the fabrication of specimens for all the tests performed in this research program.

SPECIMEN PREPARATION

For Hveem stability, Marshall stability, and resilient modulus tests, samples were prepared using a gyratory compactor. These samples were two inches (50 mm) in height by four inches (102 mm) in diameter. Samples for creep and permanent deformation were prepared using a Cox kneading compactor. These samples were four inches (102 mm) in diameter and eight inches (203 mm) in height. Care was taken to obtain approximately the same amount of air voids for all the aggregate blends. The target air void content was from five to six percent. In order to obtain air voids in the above specified range, compactive efforts were determined by preparing a number of trial samples. Table 3.4 gives the compactive efforts used for the different aggregate blends. Samples were compacted in three layers to provide uniform density. The number of tamps were increased with each successive layer to achieve uniform density. The following compaction combination was used to give uniformity:

First layer:	30 tamps
Second layer:	60 tamps
Third layer:	140 tamps

Table 3.4. Compactive Efforts for Different Percentages of Coarse Crushed Aggregate.

Crushed Aggregate (percent)	Compactive effort (psi) (kPa)
0	300 (2069)
50	300 (2069)
85	350 (2413)
100	350 (2413)

EXPERIMENTAL PROCEDURES

Phase one of the experimental program included:

1. Hveem and Marshall stability testing,
2. Resilient Modulus testing, and
3. Static and Dynamic creep testing.

Phase two included the determination of a fractal dimension value for shape and texture of the coarse aggregate particles used in the asphalt concrete mixture preparation.

Hveem Stability

Test method Tex-208-F (29) was followed in Hveem stability testing. The samples used in this test were four inches (102 mm) in diameter and two inches (51 mm) high. These samples were compacted using the Texas gyratory compactor with a four percent air void target. After conditioning a minimum of five days at room temperature, the samples were placed in a 140°F (60° C) oven for a minimum of two hours before testing. Hveem stability represents a measure of resistance to deformation of the material.

Resilient Modulus

Resilient modulus is a measure of resistance of asphalt concrete to permanent deformation, or its ability to recover from elastic deformation. ASTM method D 4123-82

(31) describes this test in detail. The Schmidt Mark IV pneumatic resilient modulus device was used in this testing program. Resilient modulus for the mixes with each of the aggregate blends was determined at four different temperatures (0, 68, 77, and 115°F) (-17.7, 20, 25, and 46.1°C). Determination of resilient modulus at a range of temperatures allows for the evaluation of temperature susceptibility of the mixtures. A diametral load was applied while measuring the deformation in the plane perpendicular to the loading plane. The duration of loading was 0.1 seconds, and the amount of load was varied depending on the test temperature to get the lateral deformation in the range of 15-80 micro inches. Higher loads were applied at low temperatures and low loads were applied at high temperatures due to the hard and soft nature of asphalt concrete at the respective temperatures.

Marshall Stability

Marshall stability was performed in accordance with ASTM procedure D1559 (30). Samples used for Marshall stability were the same samples used in Hveem stability and resilient modulus testing. Samples were cured in a water bath which was maintained at 140° ± 1.8°F (60±1°C) for 30 minutes. Marshall stability value is the number of newtons required to fail a sample.

Creep and Permanent Deformation

Creep and permanent deformation tests were conducted on samples four inches (102 mm) in diameter by eight inches (203 mm) in height. Density of compacted specimens was maintained in a range from 94-95 percent which gave an air void content of 5-6 percent. A range of compactive efforts were used on each aggregate type to obtain a reasonably constant air void content as previously discussed under sample preparation. Researchers found that coarse aggregate particles fractured under compaction loads above 400 psi (2760 kPa). River gravel particles fractured more than limestone at that level. Fracturing of aggregates was eliminated by reducing the compactive effort below 400 psi (2760 kPa). Another problem faced in the compaction process was the compaction of mixes with 100 percent coarse, uncrushed river gravel which shifted laterally under the compaction foot due

to the lack of aggregate interlocking and, thus, low shear resistance. This plastic flow of mixture was minimized by using a wider compaction foot developed at TTI.

The VESYS (32) creep testing procedure was followed in the two types of creep tests performed on asphalt concrete samples and with all seven different types of aggregate blends:

1) Static creep testing, and
2) Dynamic creep testing.

The test setup shown in Figure 3.3 was used for both creep tests. Load was applied uniaxially, and deformation measurements were made using linear variable differential transducers (LVDT's) with a gauge length of four inches (102 mm). A test load of six psi (41.3 kPa) was determined to be appropriate through pre-stressing of the sample at 104°F (40°C). Loads in the range of 5 to 10 psi (34 to 69 kPa) were used at 104°F (40°C) for VESYS creep testing in the other investigations (6, 27) at TTI. Preconditioning was performed before starting the actual creep testing: two ramp loads were applied on the sample for a duration of 10 minutes each with a minimal unloading time. A third conditioning load was then applied for ten minutes.

Static creep testing began at least one hour after the preconditioning loads were applied. A standard static creep testing procedure (32) was followed in this test. This procedure follows:

1) A ramp load of six psi (41 kPa) was applied for 0.1 second, and the permanent deformation was measured after two minutes of recovery.
2) A second ramp load of six psi was applied for a second, and the permanent deformation was measured after two minutes of recovery.
3) A third ramp load of six psi was applied for 10 seconds, and the permanent deformation was measured after two minutes of recovery.

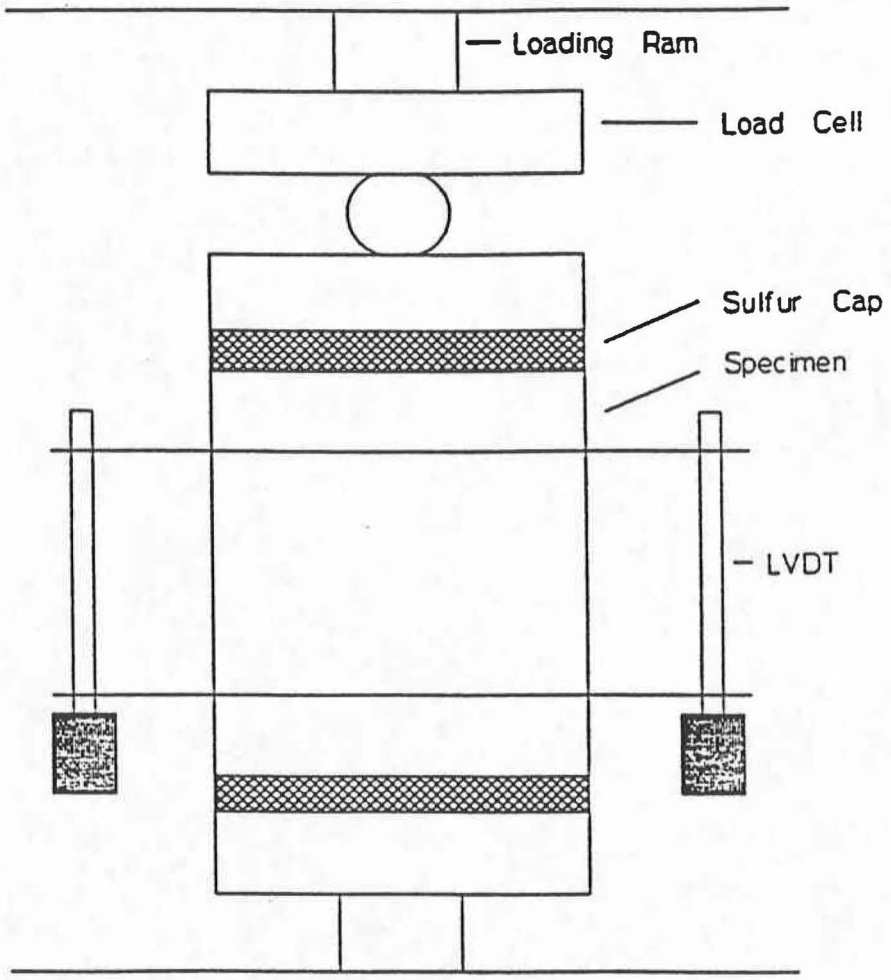

Figure 3.3. Setup for Static and Dynamic Creep Testing.

4) A fourth ramp load of six psi was applied for 100 seconds, and the permanent deformation was measured after an unloading period of four minutes.
5) A fifth ramp load of six psi was applied for 1000 seconds, and the magnitude of creep deformation was measured after 0.03, 0.1. 0.3, 1.0, 3.0, 10.0, 30.0, 100.0 and 1000.0 seconds. Total permanent deformation was measured eight minutes after unloading the sample.

In the dynamic creep testing, a repeated haversine load with the magnitude of 6 psi (41 kPa) and duration of 0.1 second was applied on the specimen. A rest period of 0.9 seconds followed each load application. Total number of load applications was 10,000, and the accumulated permanent deformation was measured at 1, 10, 100, 200, 1000, and 10,000 seconds. Elastic strain was measured at the 200th cycle for determination of dynamic modulus.

Evaluation of Test Methods for Rutting Prediction

Performance of asphalt concrete can be predicted by various test methods. As explained in the previous chapters, four tests were performed in this research program to study the behavior of asphalt concrete made with varying amounts of crushed coarse aggregates. This section discusses the potential of each of the test methods in predicting the performance of asphalt concrete.

Hveem Stability

The Hveem stability test simulates confined compressive stresses of a pavement in the field. The stresses in the field are repeated with moving wheel loads; whereas, in the Hveem stability test, the stress is applied only once. Hveem stability represents the resistance to deformation; but, it does not clearly indicate the permanent deformation or creep behavior of asphalt concrete pavement. However, Hveem stability values can be used for preliminary design of the asphalt concrete mixture which can later be tested for rutting behavior through advanced creep testing procedures. Very poor asphalt concrete mixtures can usually be identified by the Hveem stability test.

Marshall Stability

Marshall stability is considered as a measure of the resistance to plastic flow of asphalt concrete mixture. This test fails the sample in a complex mode of tension and shear. Marshall stability value cannot be directly used to predict permanent deformation or creep behavior of asphalt concrete. Marshall stability can be used to identify unacceptable mixtures which possess very poor stability.

Resilient Modulus

Resilient modulus is a measure of asphalt mixture stiffness. Resilient modulus in the diametral mode is a binder sensitive value. Stiffness of the mix increases with a decrease in the temperature due to the temperature susceptibility of asphalt cement. Resilient modulus is normally used to determine the load carrying capacity of the pavement layer but cannot accurately predict rutting.

Creep and Permanent Deformation

Static creep tests simulate the deformation characteristics of asphalt concrete under heavy loads; whereas, dynamic creep tests simulate the passage of moving wheels on a pavement. Creep compliance is a reasonably good measure for estimating the permanent deformation characteristics of an asphalt concrete mixture. Permanent deformation characteristics (alpha, gnu) calculated from creep testing data can be used in pavement design to predict rutting potential of asphalt concrete.

Fractal Dimensional Analysis

The shape and texture of natural objects such as trees, mountains, clouds, rivers, and rocks cannot be analyzed in an objective manner using simple geometry due to their complexity and non-uniformity. Analyzing these shapes and textures would enable engineers and scientists to utilize their characteristics in engineering applications. Mandelbrot (45, 47) introduced the concept of fractals which has been adapted by some engineers and scientists for characterizing shape and texture of irregular objects and surfaces, such as stones.

A family of mathematical functions developed to describe natural phenomena and shapes were called fractals. The defining characteristic of fractals is the fractal dimension. Fractal dimension closely describes the level of roughness of a surface. The fractal dimension of an object is computed with the aid of a two-dimensional black and white image of the object and an algorithm that studies the variation of grey level on the image. This image is digitized so that it contains a large grid of picture elements called pixels (the dots in a newspaper photo or TV screen). Each pixel on the grid is assigned a grey level using a grey scale. The range of the grey scale is zero to 255, where zero represents pitch black and 255 represents the brightest light color. Using this concept of fractals with grey levels, the following physical properties of an aggregate particle can be determined:

1) Aggregate shape,
2) Aggregate elongation, and
3) Aggregate surface texture.

Aggregate Shape or Angularity

There are three distinct steps in the process of determination of shape of an aggregate particle:

1) Extraction of edge (shape of 2-dimensional image),
2) Plotting slope density function, and
3) Box counting and determination of fractal dimension.

Detection of the edge of an aggregate particle is necessary to evaluate shape of an aggregate particle. An image (a video frame) of an aggregate particle is made on a contrasting background. Usually, light color background is used for the dark color aggregates and vice versa. This image is then digitized into pixels, and these pixels are assigned grey levels. Rate of change in the grey levels of adjacent pixels is then observed. There will be a rapid change of grey level along the edge of the particle due to the contrasting background. The edge of the particle is enhanced by determining the gradient

of the pixels with the help of a Sobel Gradient Operator. The gradient of a pixel is determined by combining the horizontal and vertical masks of the Sobel Operator. Extraction of the edge from its image is done through the application of an extraction algorithm which searches for boundary pixels in a series of directions which are on the order of N, NE, E, SE, S, SW, W, and NW (33). The original image and the extracted edge of a circle are shown in Figures 3.4a and 3.4b. Original images and corresponding edge images of crushed limestone and river gravel particles are included in Appendix C (Figures C1a-b and C3a-b).

The next step in shape determination is utilization of the slope density function (SDF). Li et al. (33) stated that "the SDF is the histogram or frequency of the angles collected over the boundary of a given shape." Angularity of an object is described by the degree of jagged nature of the SDF curve. The SDF curve of a triangular blob is also shown in Figure 3.5a. The SDF of a circle in Figure 3.5b is flat due to the constant change in the angle. The SDF curve of an ideal square has four peaks that represent the four straight edges, as shown in Figure 3.5c. Some jagged nature can be observed in the SDF of a circle in Figures 3.6a-b. This jagged nature is due to imperfect digitization and representation of a circle's pixels. SDF and box count plots of crushed limestone and river gravel aggregate particles are given in Appendix C (Figures C2a-b and C4a-b). It can be observed that the SDF of a crushed limestone particle yields a higher number of peaks which represent straight edges and sharp corners than that of subrounded river gravel aggregate particles. Since the SDF of a particle closely describes its angularity, fractal dimension of the shape of the particle is obtained based on the SDF using the box counting method as explained in the next section.

Use of box dimension is a way to determine the fractal dimension of a shape (33). In this method, a series of grids of different box sizes are laid on the SDF plot, and the non-empty boxes are counted (Figure 3.7). A plot of the number of non-empty boxes against the box size on a log-log scale is called the box count plot. Fractal dimension number of a shape is defined as the absolute value of the box count plot slope. For perfectly smooth surfaces, the fractal dimension is one, and for extremely jagged surfaces, the fractal dimension approaches two.

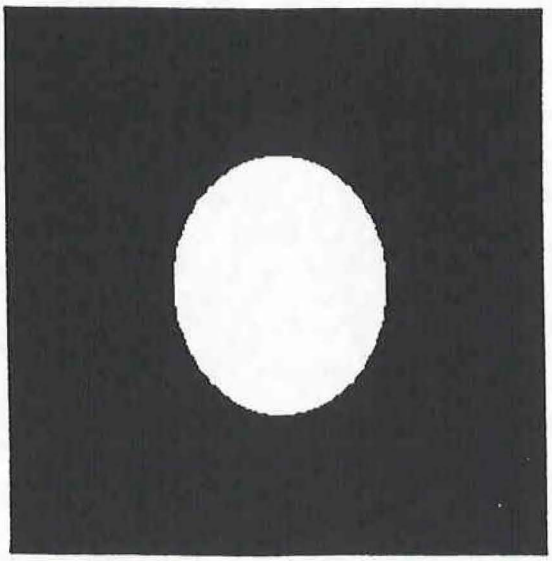

Figure 3.4a. Original Image of an Ideal Circle (After Reference 33).

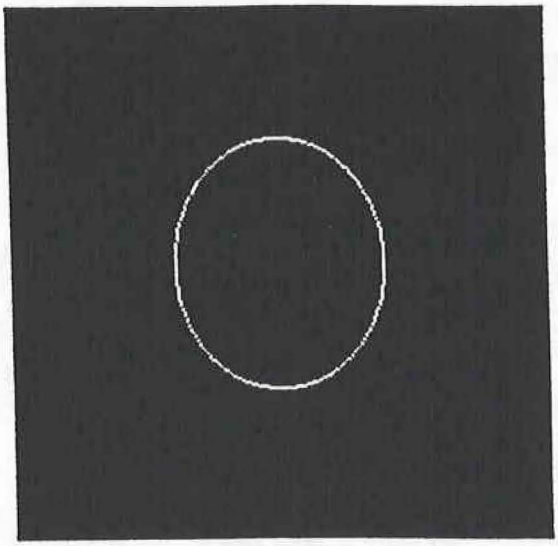

Figure 3.4b. Extracted Edge Image of an Ideal Circle (After Reference 33).

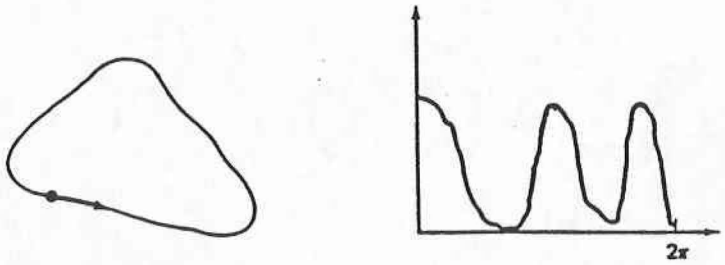

Figure 3.5a. SDF Curve of a Triangular Blob (After Reference 33).

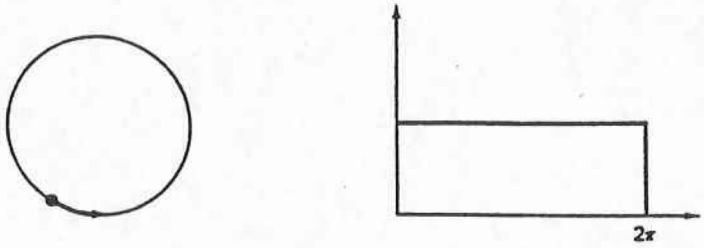

Figure 3.5b. SDF Curve of a Circle (After Reference 33).

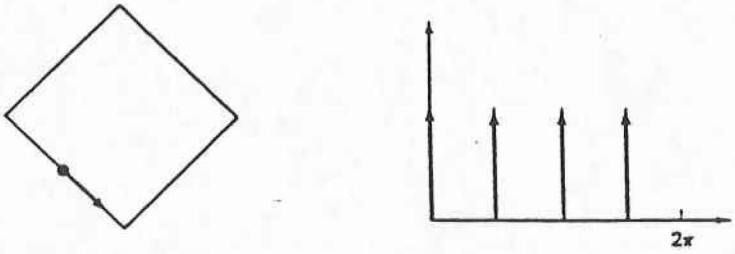

Figure 3.5c. SDF Curve of a Square (After Reference 33).

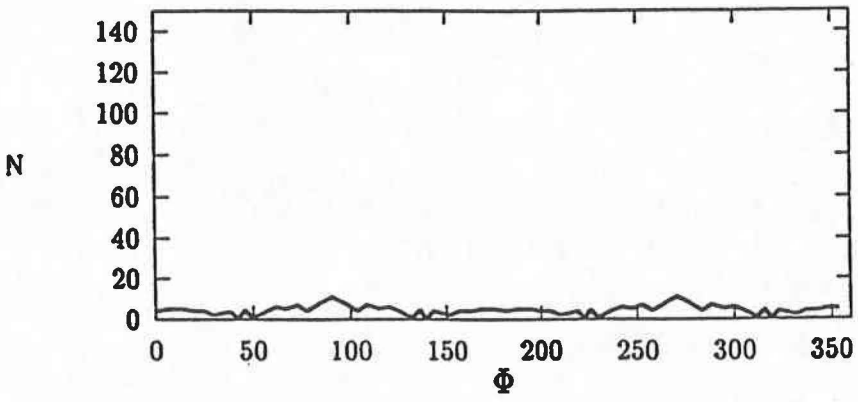

Figure 3.6a. SDF Curve of a Circle (After Reference 33).

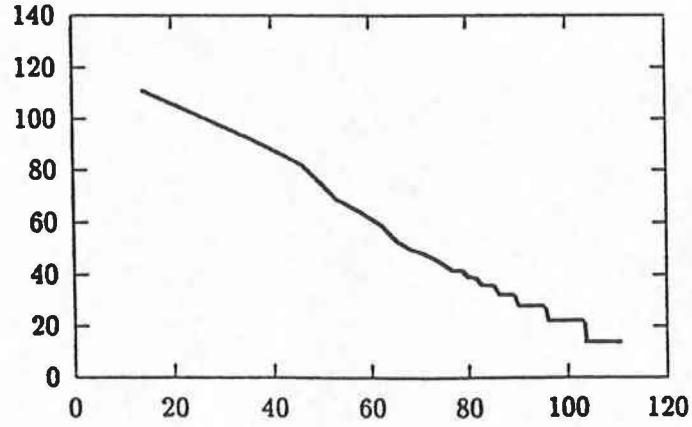

Figure 3.6b. Box Count Plot of a Circle (After Reference 33).

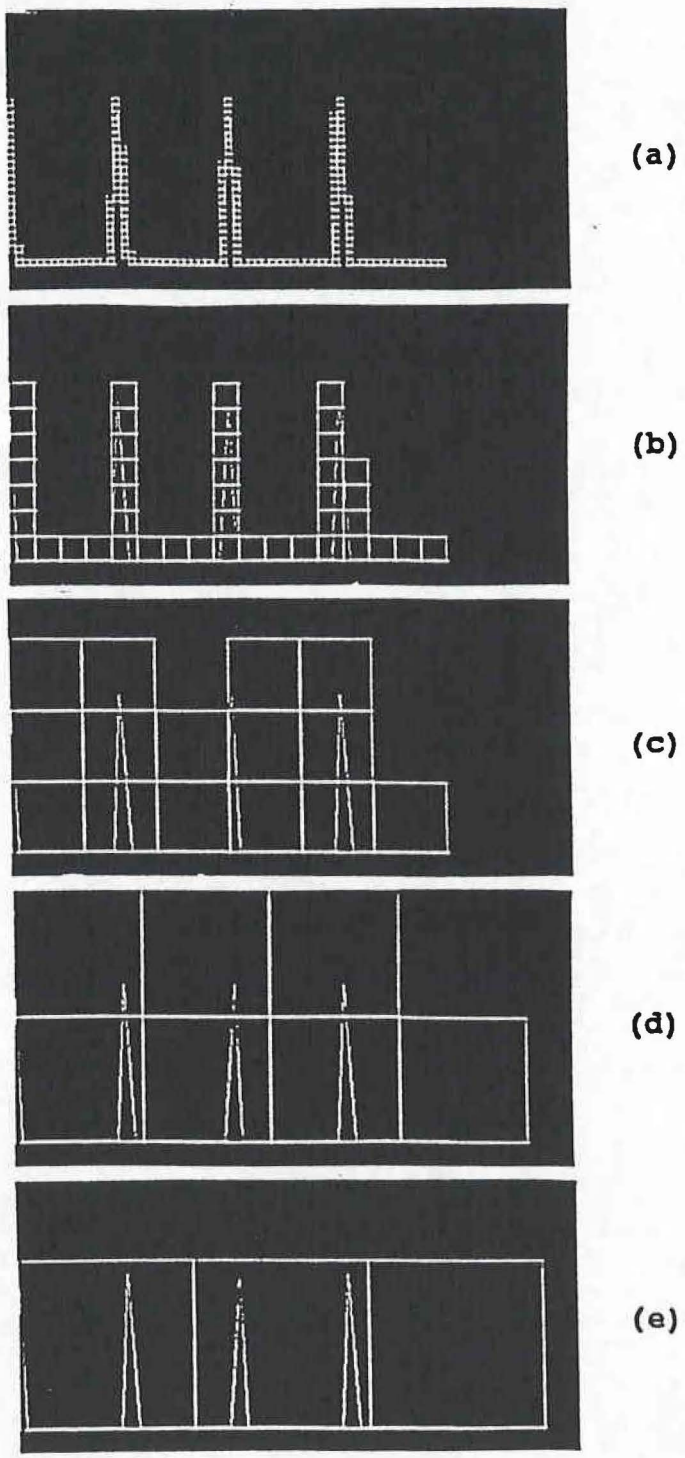

Figure 3.7 Over Laid of Grids of Five Different Box Sizes with a SDF Curve (After Reference 33).

Aggregate Elongation

Elongation of an aggregate particle can be considered a relative measure of its shape. The longest dimension of a 2-dimensional image of a particle is considered the major axis of the particle, and the average dimension in the direction perpendicular to the major axis is considered the minor axis. Elongation of a particle can be computed as the ratio of major axis length to the minor axis length. An algorithm measures the longest dimension on the image and considers it the major axis, which is shown in Figures 3.8a-b for a limestone particle. The average dimension in the direction perpendicular to the major axis is computed to determine the elongation of these particles.

Aggregate Surface Texture

Surface texture of an aggregate particle is determined by measuring the rate of variation of grey levels of the adjacent pixels on its image. The rougher the surface of the particle, the higher the variation in grey levels of the image. The fractal dimension number for texture increases with the increase in the variation of grey levels or roughness. For calibration purposes, a cardboard surface was used for a smooth surface texture, cork particle board was used for intermediate surface texture, and carpet material was used for a rough surface texture. The fractal dimension numbers for cardboard, cork, and carpet were determined to be 0.04, 0.17, and 0.40 (averages of three samples), respectively. Video images of cardboard, cork surface, carpet material, limestone, and river gravel are given in Figures 3.9, 3.10, 3.11, 3.12, and 3.13, respectively. The fractal dimension number for texture was determined for all the aggregate blends used in the experimental program. Images of all the seven aggregate blends are given in Appendix C (Figures C5a-g).

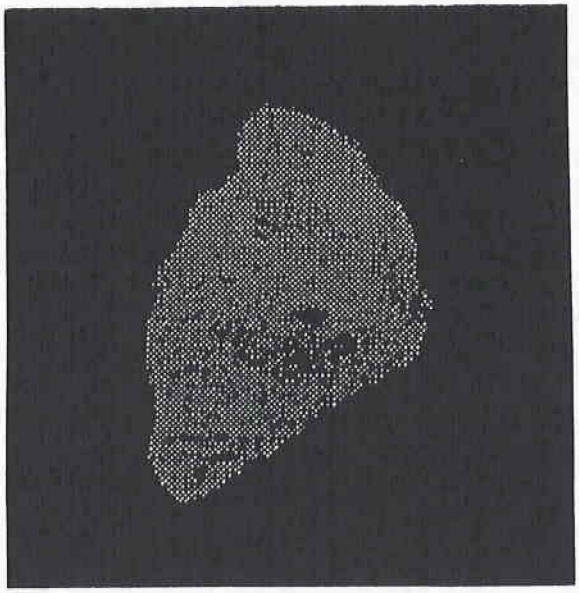

Figure 3.8a. Original Image of Limestone Aggregate Particle (After Reference 33)

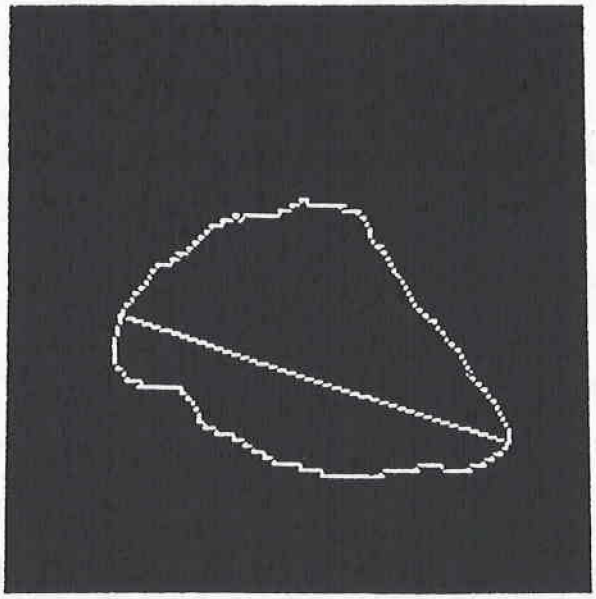

Figure 3.8b. Extracted Major Axis of Limestone Aggregate Particle (After Reference 33).

Figure 3.9. Image of Card Board for Texture.

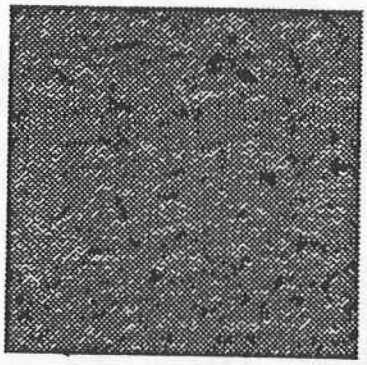

Figure 3.10. Image of Cork Surface for Texture.

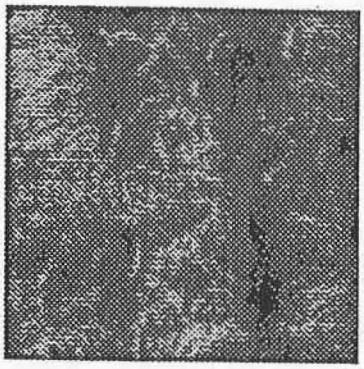

Figure 3.11. Image of Carpet Material for Texture.

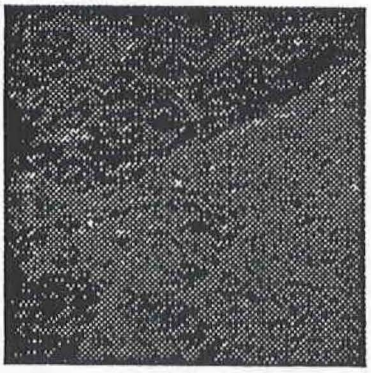

Figure 3.12. Image of Limestone Aggregate Particle Surface for Texture.

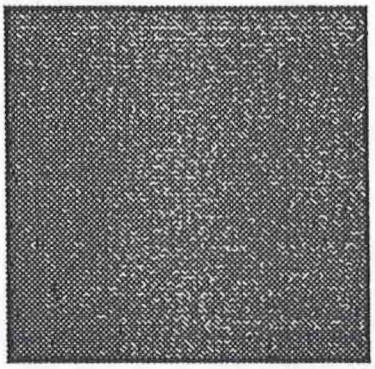

Figure 3.13. Image of River Gravel Aggregate Particle for Texture.

CHAPTER 4
TEST RESULTS AND ANALYSIS

The tests explained in Chapter 3 were performed to determine both asphalt concrete mixture and aggregate properties. Findings of the testing program are discussed in this chapter. Results obtained for mixtures made with different amounts of coarse aggregates are analyzed for statistical significance of the change in asphalt concrete properties with a change in amount of crushed coarse aggregate. Relationships between creep compliance of the asphalt mixture and texture of the aggregates used is also discussed.

MIXTURE DESIGN

Mixture design was performed on the aggregate blends containing 100 percent crushed coarse limestone, 100 percent crushed coarse river gravel, and 100 percent uncrushed or smooth river gravel. Optimum binder content for the mixture with zero percent crushed coarse aggregate (100 percent uncrushed gravel) was determined to be 5.2 percent by weight of the mixture. Optimum asphalt content for mixtures containing 100 percent crushed limestone and 100 percent crushed river gravel were 5.5 and 5.4 percent, respectively. Assuming a linear correlation of asphalt content with percentage crushed aggregate, optimum binder contents for mixes with 50 and 85 percent crushed aggregate were estimated.

Optimum binder contents of mixtures with 50 and 85 percent crushed limestone were estimated to be 5.35 and 5.45 percent, respectively. For mixes with 50 and 85 percent crushed coarse river gravel, optimum asphalt content was estimated to be 5.30 and 5.35 percent, respectively. Table 4.1 shows optimum asphalt contents.

Figure 4.1 shows densities for 100 percent crushed limestone, river gravel, and uncrushed river gravel with different binder contents. Figure 4.2 shows Hveem stabilities for mixes with zero and 100 percent crushed coarse aggregate and for different binder contents.

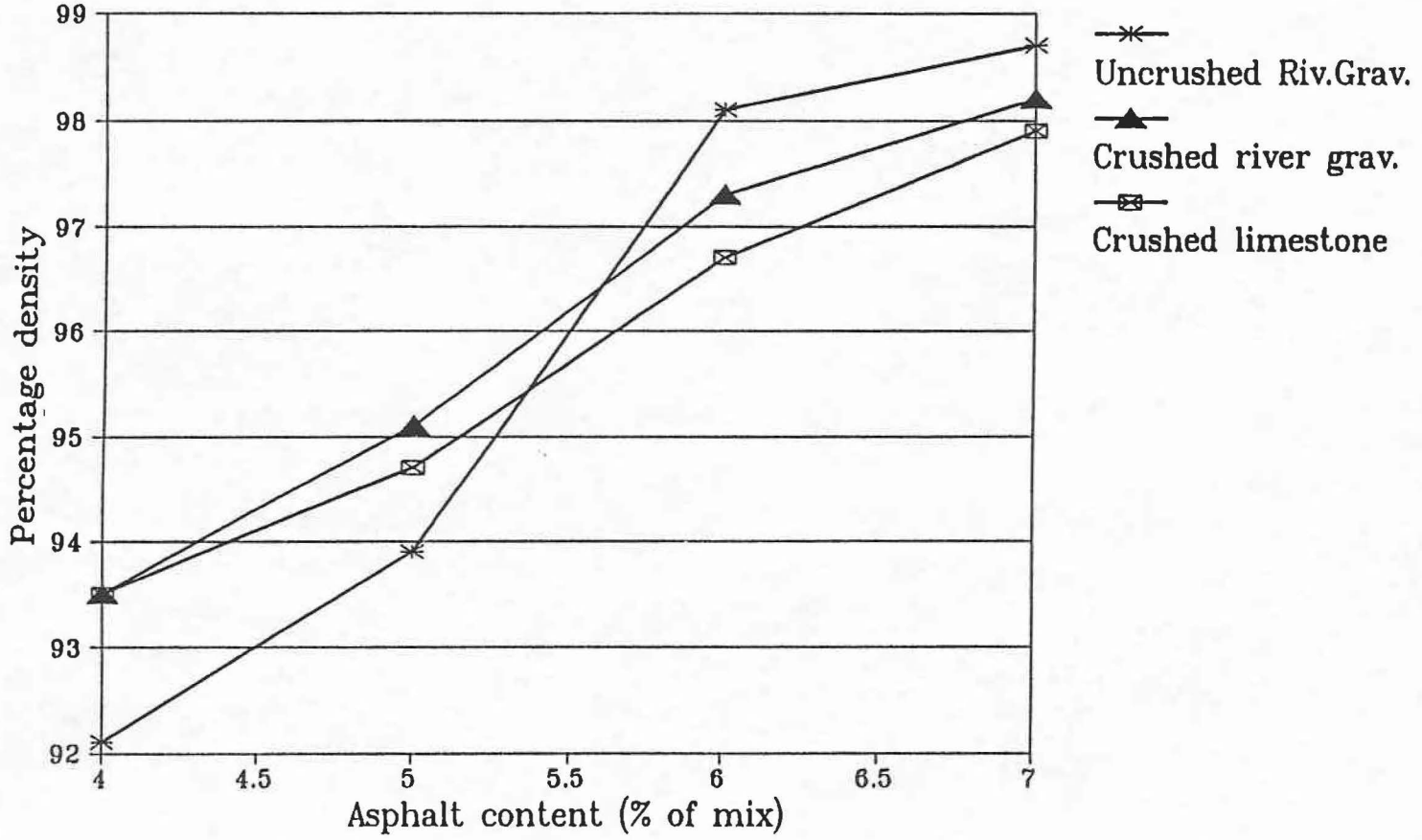

Figure 4.1. Density of Mixtures with 0 and 100 Percent Crushed Aggregate vs. Asphalt Content.

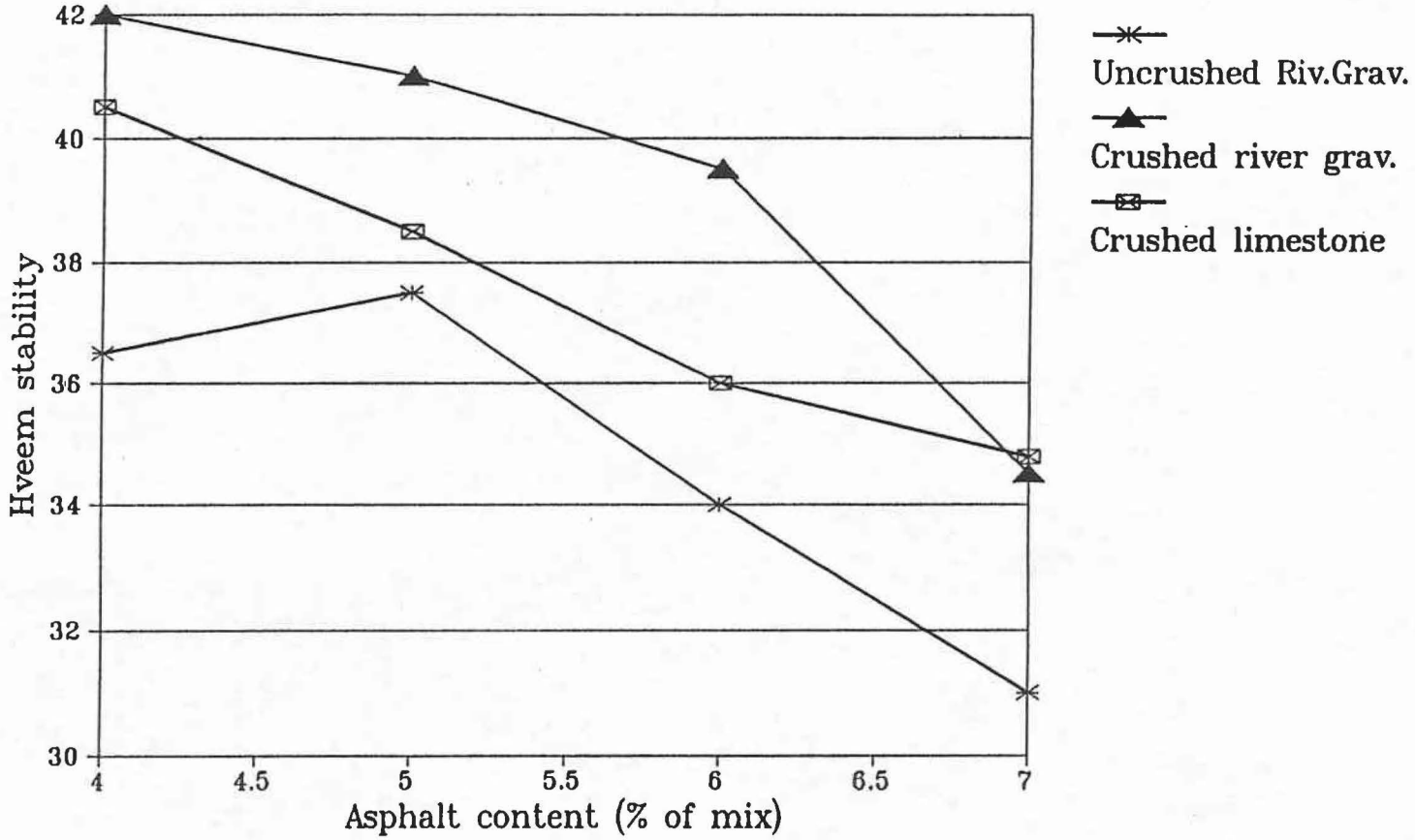

Figure 4.2. Hveem Stability of Mixtures with 0 and 100 Percent Crushed Aggregate vs. Asphalt Content.

Table 4.1. Optimum Binder Contents For Mixtures with Different Percentages of Crushed Aggregate Contents.

Percent crushed coarse river gravel	Optimum binder content (% of mix)	Percent crushed coarse limestone	Optimum binder content (% of mix)
0	5.2	0	5.2
50	5.3	50	5.35
85	5.35	85	5.45
100	5.4	100	5.5

RESILIENT MODULUS

Measurement of resilient modulus over a range of temperatures allowed the researchers to evaluate relative temperature susceptibility of the mixtures. Resilient modulus testing was performed at 0, 68, 77, and 115°F (32, 20, 25, 46°C) for the samples made with different amounts of crushed coarse aggregates. Table 4.2 summarizes the test results. In order to test the statistical significance of the change of resilient moduli of asphalt concrete mixture with the change in amount of crushed coarse aggregate, a paired t-test was performed. The combinations of data sets used in the t-test were resilient moduli of samples made with crushed coarse aggregate percentages of:

1) 0 and 50,
2) 0 and 85,
3) 0 and 100,
4) 50 and 85,
5) 50 and 100, and
6) 85 and 100.

Three samples made with each amount of coarse aggregate (0, 50, 85, and 100 percent) were tested for resilient modulus; and these modulus values were used in the statistical significance test for a confidence interval of 95 percent.

Table 4.2. The Resilient Moduli of Mixtures with All Seven Aggregate Blends and Texaco AC-20.

Percent of Crushed Aggregate	Resilient Modulus psi x 1000 (Pa x 10^6)				Air Voids (percent)
	0°F (-18°C)	68°F (20°C)	77°F (25°C)	115°F (46°C)	
Limestone					
0	1829 (12,610)	446 (3,070)	206 (1,420)	28.4 (195)	3.9
50	1772 (12,220)	382 (2,630)	215 (1,480)	29.8 (205)	4.5
85	1864 (12,850)	556 (3,830)	316 (2,180)	36.2 (250)	4.6
100	1803 (12,430)	436 (3,010)	349 (2,406)	42.8 (295)	4.9
River Gravel					
0	1829 (12,610)	446 (3,070)	209 (1,440)	28.4 (196)	3.9
50	1841 (12,690)	368 (2,540)	226 (1,558)	32.6 (225)	4.6
85	1824 (12,570)	381 (2,630)	233 (1,606)	33.6 (232)	4.8
100	1889 (13,020)	481 (3,320)	251 (1,730)	37.2 (256)	4.9

At 0°F (-18°C), no direct correlation was observed between resilient moduli and the crushed aggregate percentage (Figures 4.3, 4.4, A1-A3). Change in the resilient moduli of asphalt samples with an increase in crushed aggregate amount was not significant at 0°F (Table 4.3). The hard nature of asphalt at 0°F surpassed the influence of crushed aggregate.

At 68°F (20°C), no direct correlation between the amount of crushed aggregate and

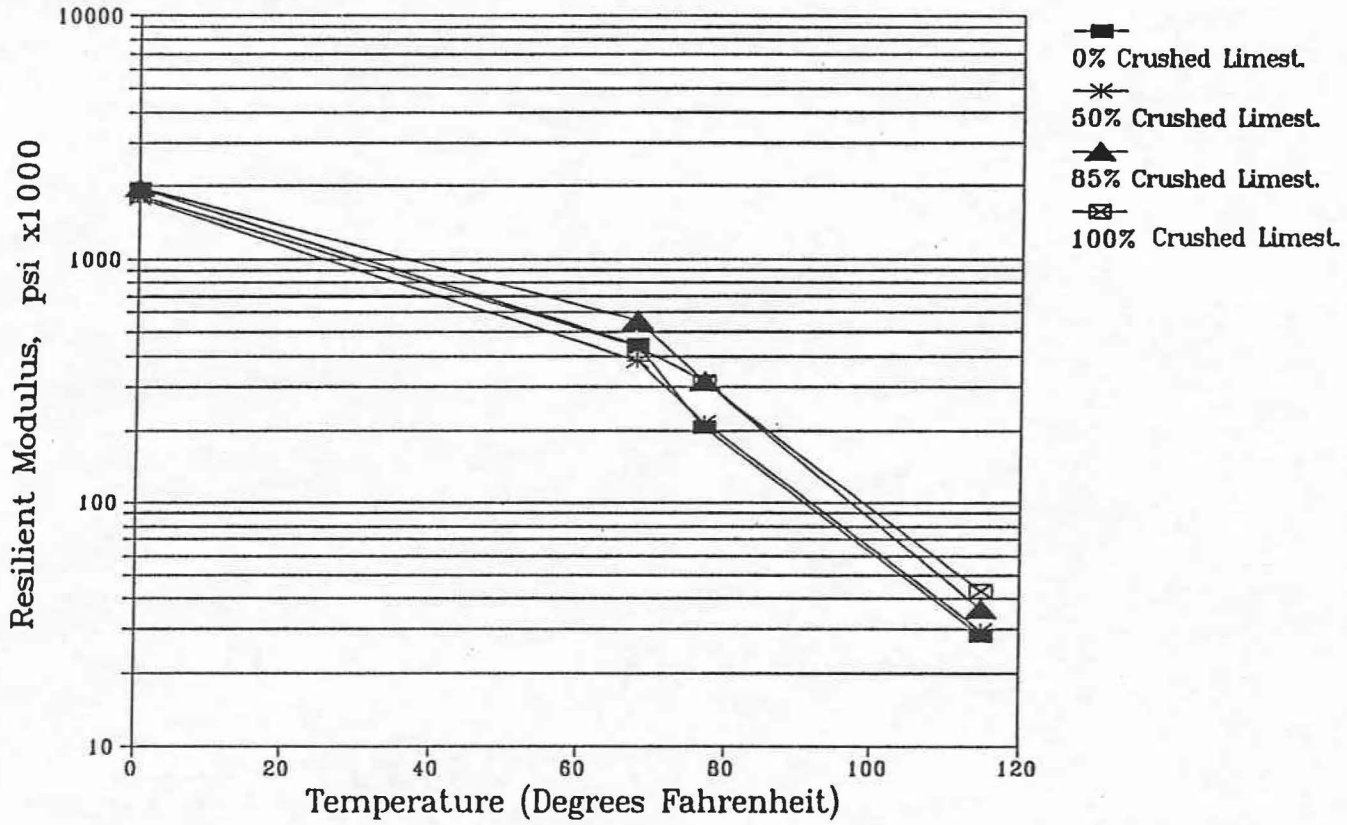

Figure 4.3. Resilient Moduli as a Function of Temperature for Mixtures with 0, 50, 85, and 100 Percent Crushed Coarse Limestone.

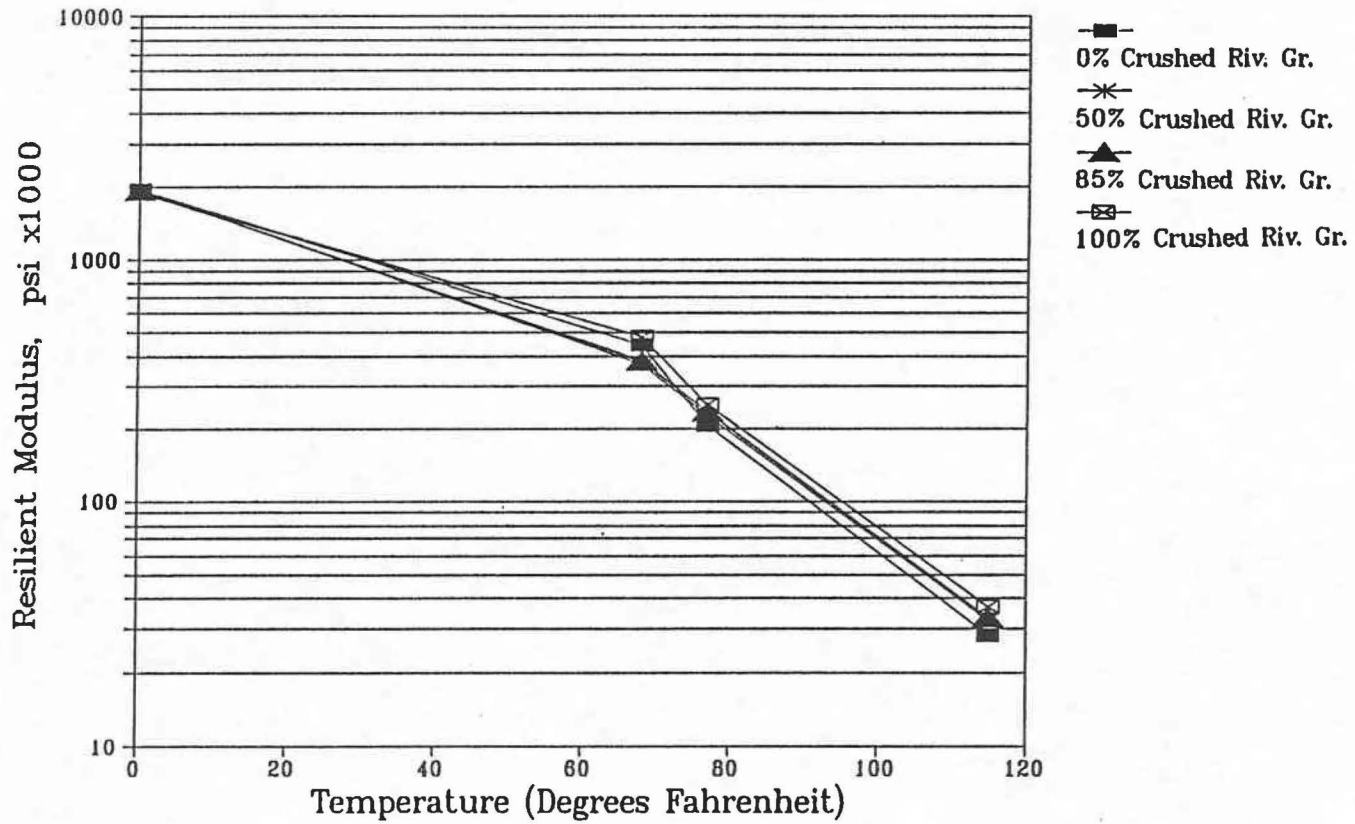

Figure 4.4. Resilient Moduli as a Function of Temperature for Mixtures with 0, 50, 85, and 100 Percent Crushed Coarse River Gravel.

Table 4.3. Summary of Statistical Significance Test Results for Difference in Resilient Moduli of Samples Made with Different Amounts of Crushed Coarse Aggregate.

HYPOTHESIS: Difference in resilient moduli is significant for the samples prepared with crushed coarse aggregate amounts of:	Result of Statistical Significance Test (paired t-test)			
	0°F (-18°C)	68°F (20°C)	77°F (25°C)	115°F (46°C)
Limestone				
0-50%	Reject	Accept	Accept	Accept
0-85%	Reject	Reject	Accept	Accept
0-100%	Reject	Reject	Accept	Accept
50-85%	Reject	Reject	Accept	Accept
50-100%	Reject	Reject	Accept	Accept
85-100%	Reject	Reject	Reject	Accept
River gravel				
0-50%	Reject	Accept	Accept	Accept
0-85%	Reject	Accept	Accept	Accept
0-100%	Reject	Reject	Accept	Accept
50-85%	Reject	Reject	Accept	Accept
50-100%	Reject	Accept	Reject	Accept
85-100%	Reject	Accept	Reject	Reject

resilient moduli was observed (Figures 4.3, 4.4, and A4-A6). Differences in resilient moduli at 68°F (20°C) of specimens prepared with different amounts of crushed coarse limestone were not statistically significant, except for the samples prepared with zero and those with 50 percent crushed limestone (Table 4.3). Although there is no direct correlation between amounts of crushed coarse river gravel in the mix and resilient moduli, the differences in resilient modulus values of samples prepared with different amounts of crushed coarse river gravel were statistically significant except for the samples made with 0 and 100 percent crushed coarse aggregate and those containing 50 and 85 percent crushed coarse aggregate.

The amount of crushed coarse aggregate has more influence on resilient modulus at higher temperatures (77 and 115°F [25 and 46°C]) than at lower temperatures. It was observed that the resilient modulus consistently increased with an increase in the percent of crushed coarse aggregate at 77°F (25°C) (Figures 4.3, 4.4, and A7-A9 and Table 4.2). Significance tests at 77°F (25°C) show that the difference in resilient moduli with the change of crushed coarse aggregate was significant for all the combinations except the following three combinations:

1) 85 and 100 percent limestone,
2) 50 and 100 crushed river gravel, and
3) 85 and 100 percent crushed river gravel (Table 4.3).

Resilient moduli at 115°F (46°C) increased consistently with an increase in the amount of crushed coarse aggregate amount (Figures 4.3, 4.4, and A10-A12 and Table 4.2). There is a significant difference in resilient moduli of all combinations except the samples prepared with 85 and 100 percent crushed river gravel.

Figures 4.3 and 4.4 show a trend of decline in resilient modulus with an increase in temperature for different percentages of crushed coarse limestone and river gravel. These figures demonstrate that temperature susceptibility of a mix decreases with an increase in crushed aggregate content. Although diametral resilient modulus is a binder sensitive property of asphalt concrete, the amount of crushed aggregate in the mix has a significant influence on resilient modulus at high temperatures.

HVEEM STABILITY

Results show a consistent increase in Hveem stability with an increase in crushed coarse aggregate fraction in the mix. This trend can be observed in Figures 4.5, A13, and A14. Table 4.4 gives a summary of Hveem stability of the samples made with different amounts of crushed coarse aggregates. A statistical test (paired t-test) was performed to test the significance of change in Hveem stability with change in crushed coarse aggregate content. Table 4.5 contains results of the statistical significance tests for six different combinations of aggregate amounts.

MARSHALL STABILITY

Marshall stability of mixes increased consistently with an increase in the amount of crushed coarse limestone and river gravel (Figures 4.6, A15, and A16). A direct correlation can be observed between the amount of crushed aggregate and Marshall stability values from Figure 4.6. Table 4.6 summarizes the Marshall test results. Table 4.7 gives the significance of change in Marshall stability with change in crushed coarse aggregate from the paired t-test on six different combinations of crushed aggregate amounts. A significant influence of crushed aggregate on Marshall stability value was observed, which infers that the crushed coarse aggregate provides significant resistance to plastic flow of an asphalt concrete mixture.

CREEP AND PERMANENT DEFORMATION

As explained in the previous chapter, two types of creep tests were performed: 1) static and 2) dynamic.

Static Creep

Accumulated deformation was recorded throughout 1000 seconds of loading and about 700 seconds with no load. This deformation is plotted with time in Figures 4.7 and 4.8. Figure 4.9 gives creep compliance at 1000 seconds and 104°F (40°C) for samples with different amounts of crushed coarse aggregate. Creep compliance decreased with an increase in crushed coarse aggregate content. Continuous deformation and recovery data

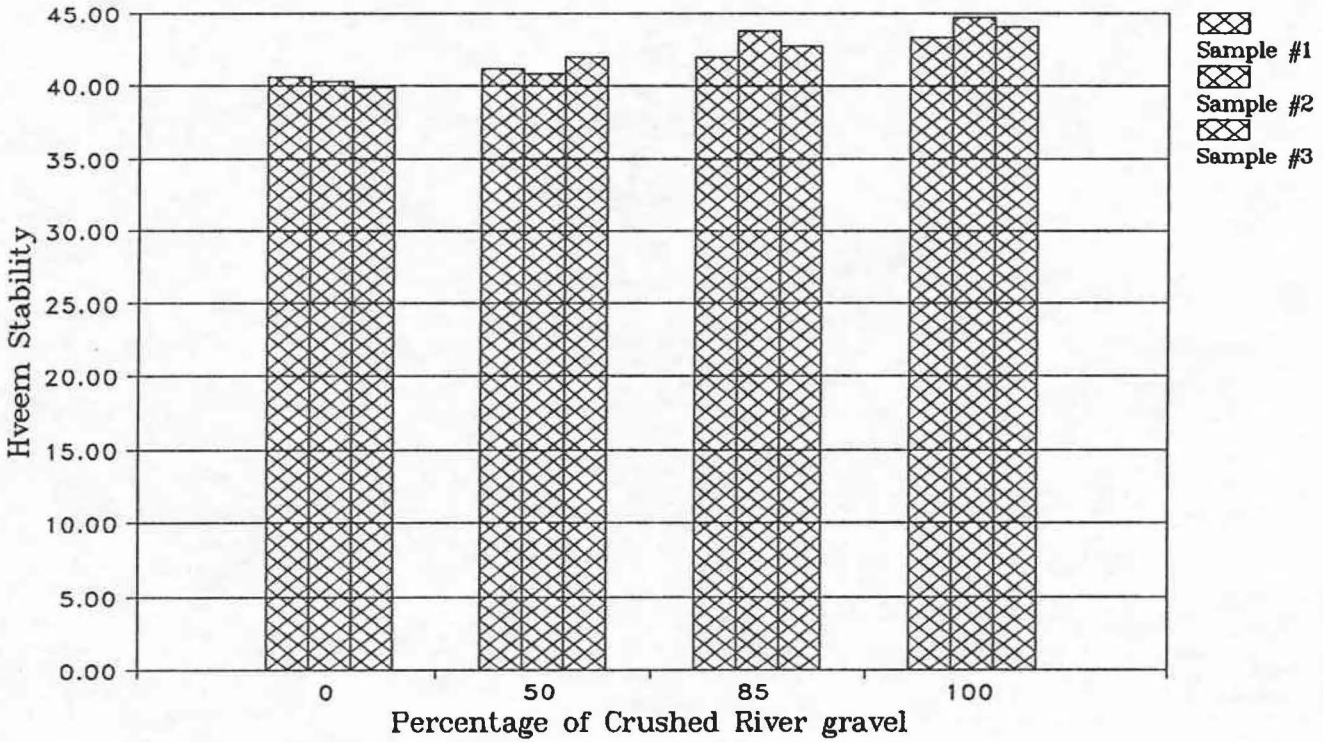

Figure 4.5. Hveem Stability vs. Percentage Crushed Coarse Aggregate.

Table 4.4. Hveem Stability Values for Mixes with All Seven Aggregate Blends.

Percent Crushed Aggregate	Hveem Stability (percent)	Air Voids (percent)
River Gravel		
0	40.3	3.9
50	41.3	4.5
85	42.8	4.6
100	44.0	4.9
Limestone		
0	40.3	3.9
50	41.2	4.6
85	42.8	4.8
100	44.8	4.9

Table 4.5. Summary of Statistical Significance Test Results for Difference in Hveem Stability of Samples Made with Different Amounts of Crushed Coarse Aggregate.

HYPOTHESIS: Difference in Hveem stability is significant for the specimens prepared with crushed coarse aggregate amounts of:	Result of Statistical Significance Test (Paired t-test)	
	Limestone	River Gravel
0 and 50%	Reject	Reject
0 and 85%	Reject	Reject
0 and 100%	Accept	Accept
50 and 85%	Reject	Reject
50 and 100%	Accept	Accept
85 and 100%	Accept	Accept

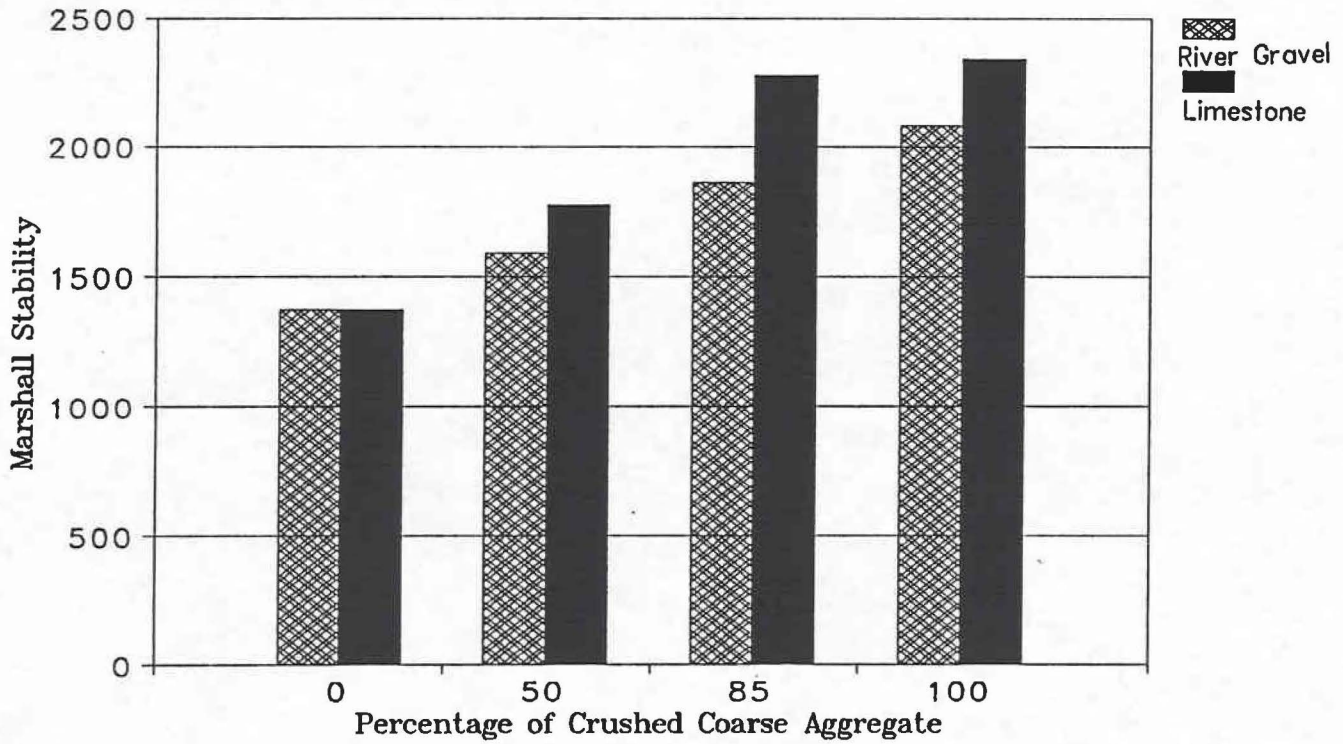

Figure 4.6. Marshall Stability vs. Percentage Crushed Aggregate.

Table 4.6. Summary of Marshall Stability of Test Specimens.

Percent Crushed Aggregate	Marshall Stability (pounds) (kgs)	Air Void (percent)
Limestone		
0	1370 (623)	3.92
50	1780 (809)	4.47
85	2280 (1036)	4.64
100	2340 (1064)	4.85
River Gravel		
0	1370 (623)	3.92
50	1590 (723)	4.63
85	1870 (850)	4.78
100	2080 (945)	4.89

Table 4.7. Summary of Statistical Significance Test Results of Difference in Marshall Stability of Samples Made with Different Amounts of Crushed Coarse Aggregates.

HYPOTHESIS: Difference in Marshall stability is significant for the samples prepared with crushed coarse aggregate amounts of:	Result of Statistical Significance Test (Paired t-test)	
	Limestone	River Gravel
0 and 50%	Accept	Accept
0 and 85%	Accept	Accept
0 and 100%	Accept	Accept
50 and 85%	Accept	Accept
50 and 100%	Accept	Accept
85 and 100%	Reject	Accept

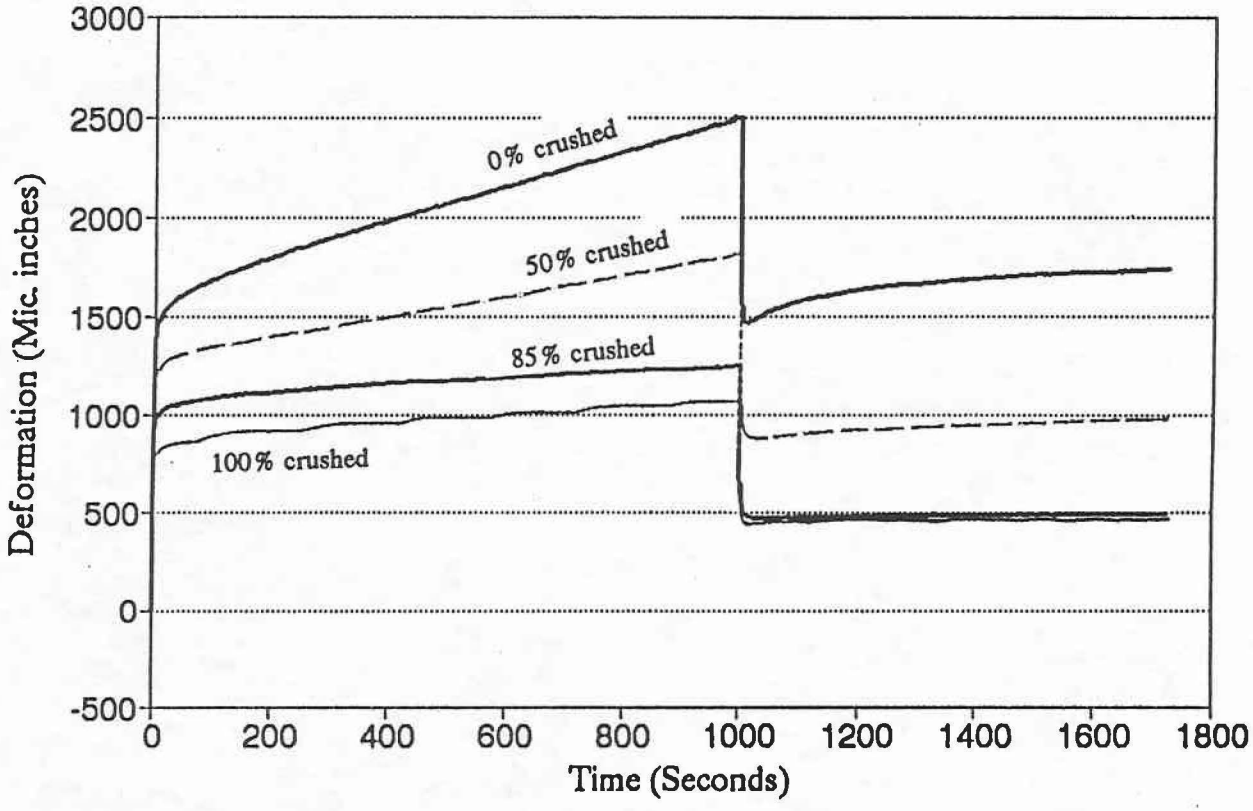

Figure 4.7. Static Creep at 104°F (40°C) During 1000 Second Loading (6 psi [41 kPa]) for Mixes with 0, 50, 85, and 100 Percent Crushed Coarse Limestone.

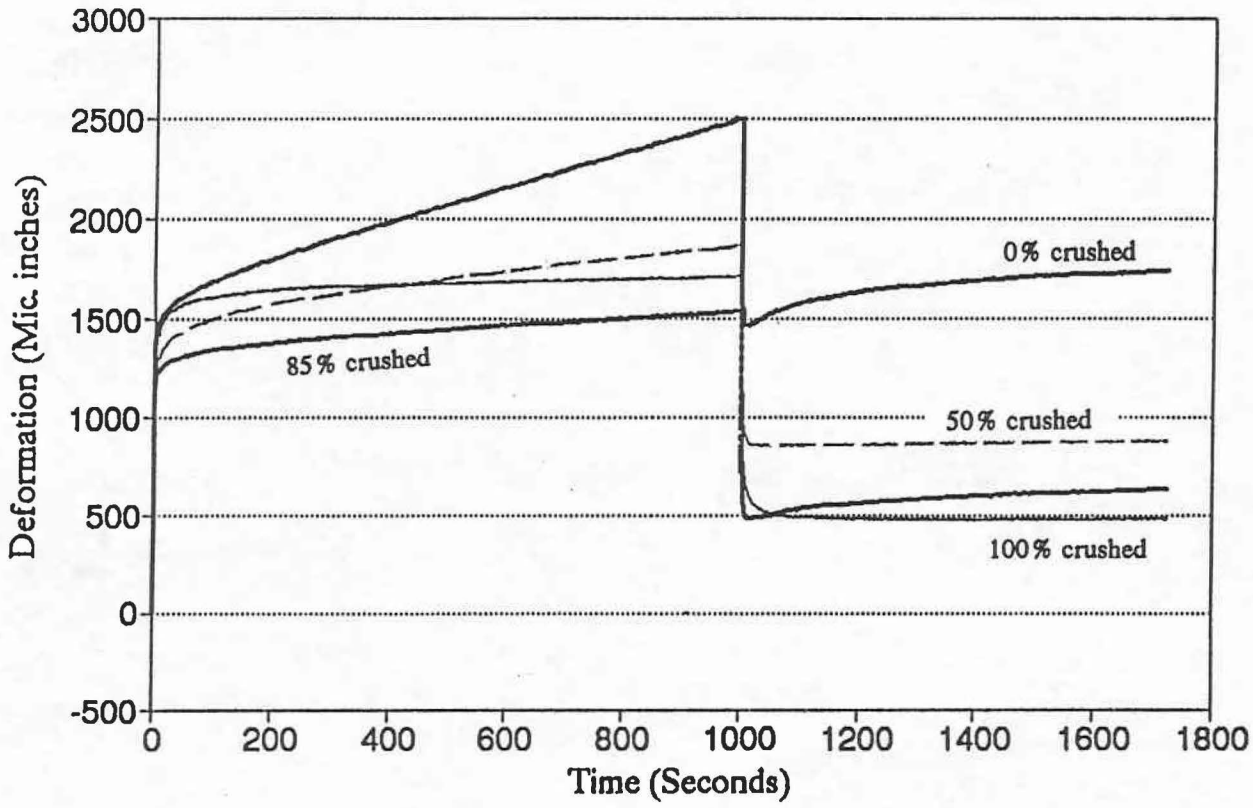

Figure 4.8. Static Creep at 104°F (40°C) During 1000 Second Loading (6 psi [41 kPa]) for Mixes with 0, 50, 85, and 100 Percent Crushed Coarse River Gravel.

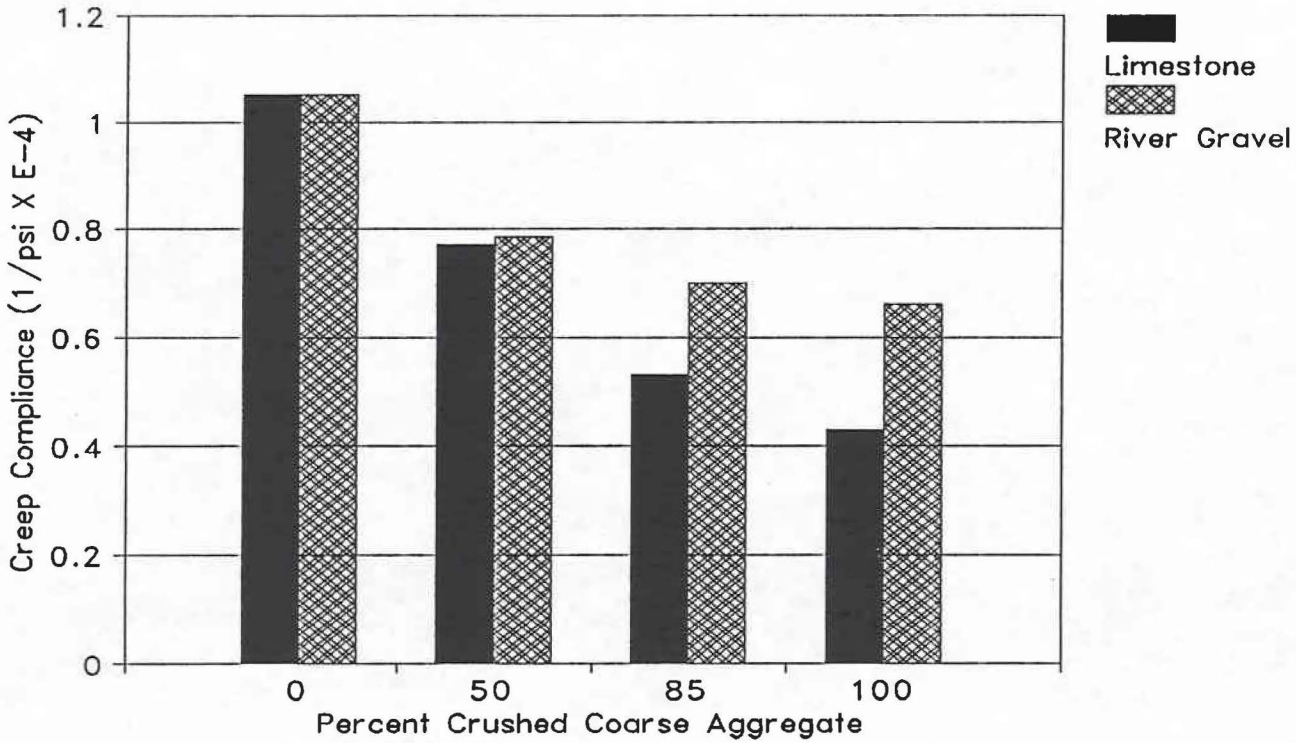

Figure 4.9. Creep Compliance at 1000 Seconds (Static Creep Test) as a Function of Percentage Crushed Coarse Aggregate. Tested at 104°F (40°C).

recorded during static creep tests are given in Appendix B (Figures B1-B7). The static creep test results show that the addition of angular aggregate increased the resistance to creep flow by increasing the stability of the mix through aggregate interlocking or interparticle friction.

Dynamic Creep

Continuous deformation and recovery data were recorded during 10,000 seconds of loading and 2,000 seconds with no load at 104°F (40°C). Deformations recorded throughout the test for the samples with 0, 50, 85, and 100 percent crushed limestone and river gravel are plotted against time in Figures 4.10 and 4.11, respectively. Deformation decreased with an increase in concentration of crushed coarse aggregate. Creep compliance calculated for the deformation at 3600 seconds decreased with increasing amounts of crushed coarse aggregate (Figure 4.12).

Angular coarse aggregate is shown to play a major role in increasing the resistance to plastic deformation of an asphalt concrete mixture.

CHARACTERIZATION OF AGGREGATE SHAPE AND TEXTURE

The objective of the second phase of this program was to quantify the shape and surface texture of aggregates used in the mixture analysis and relate these physical properties to mixture characteristics. As explained in the previous chapter, shape and surface texture of aggregate particles were quantified using fractal dimension analysis. This was a minor part of the overall study.

Shape

Fractal dimension is a measure of angularity or irregularity of the shape of an aggregate particle. The fractal dimension number for shape increases with an increase in the irregularity. Fractal dimension values for shape were determined for uncrushed river gravel, crushed limestone, and crushed river gravel particles ranging in size from 3/8 to 5/8 inch (9.5 to 16 mm). For instance, the fractal dimension number of rectangular particles was determined to be higher than that of triangular particles. These values are listed in Table 4.8.

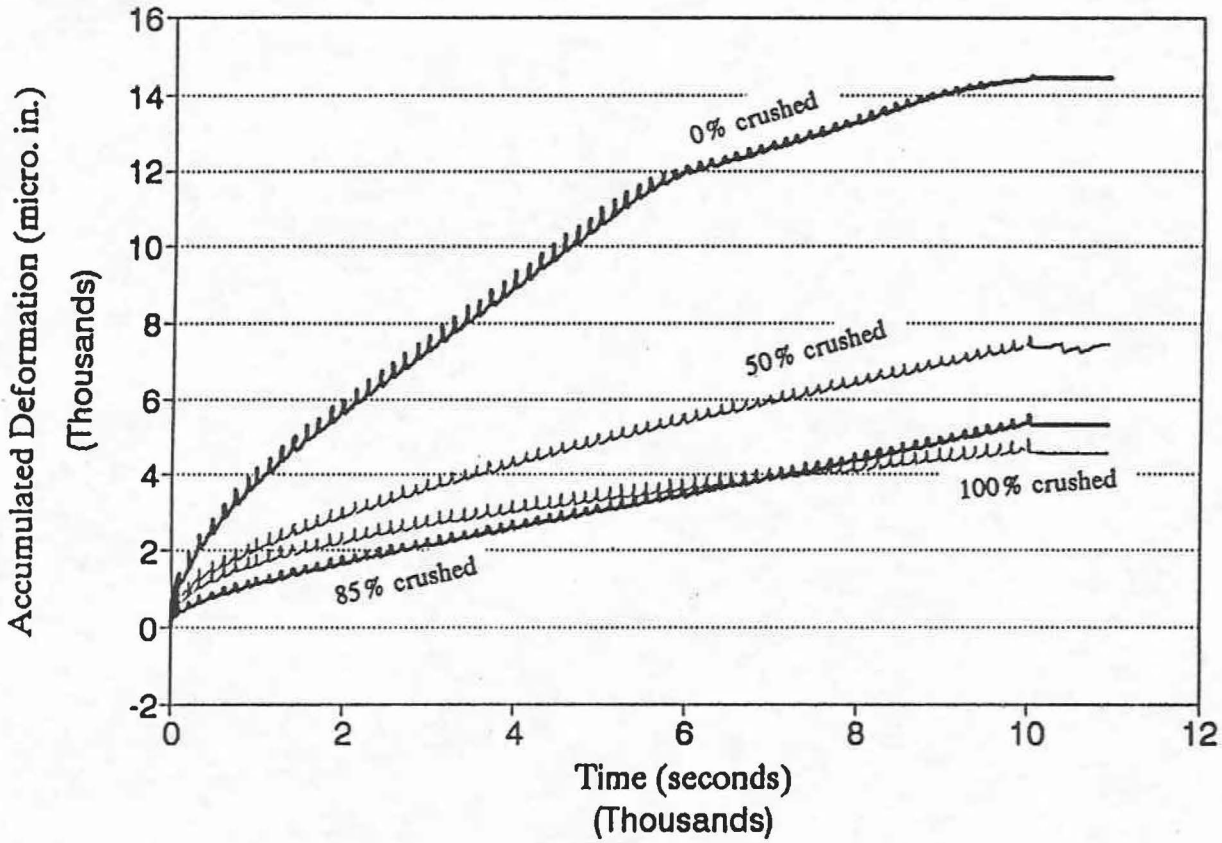

Figure 4.10. Deformation During 10,000 Seconds Dynamic Loading (6 psi [41 kPa]) and 2000 Seconds Recovery for Mixes with 0, 50, 85, and 100 Percent Crushed Coarse Limestone. Tested at 104°F (40°C).

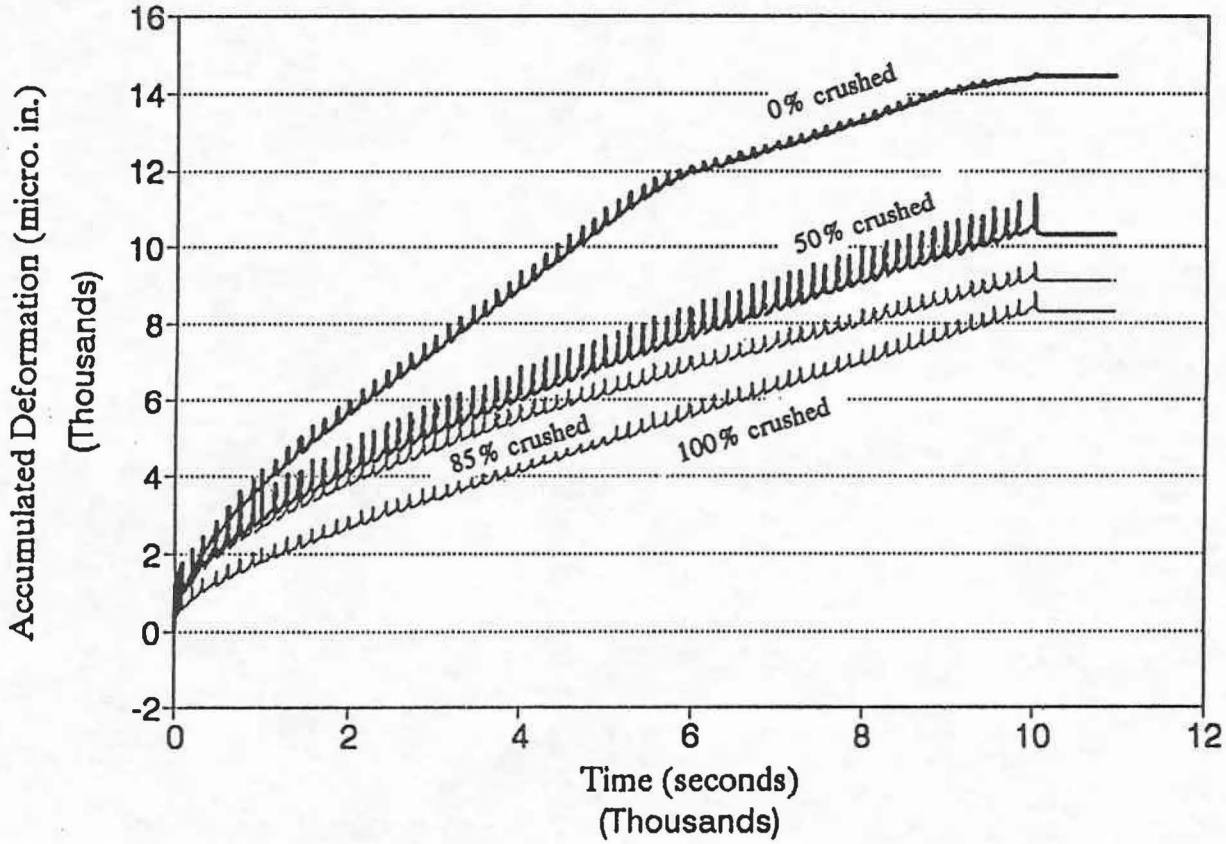

Figure 4.11. Deformation During 10,000 Seconds Dynamic Loading (6 psi [41 kPa]) and 2000 Seconds Recovery for Mixes with 0, 50, 85, and 100 Percent Crushed Coarse River Gravel. Tested at 104°F (40°C).

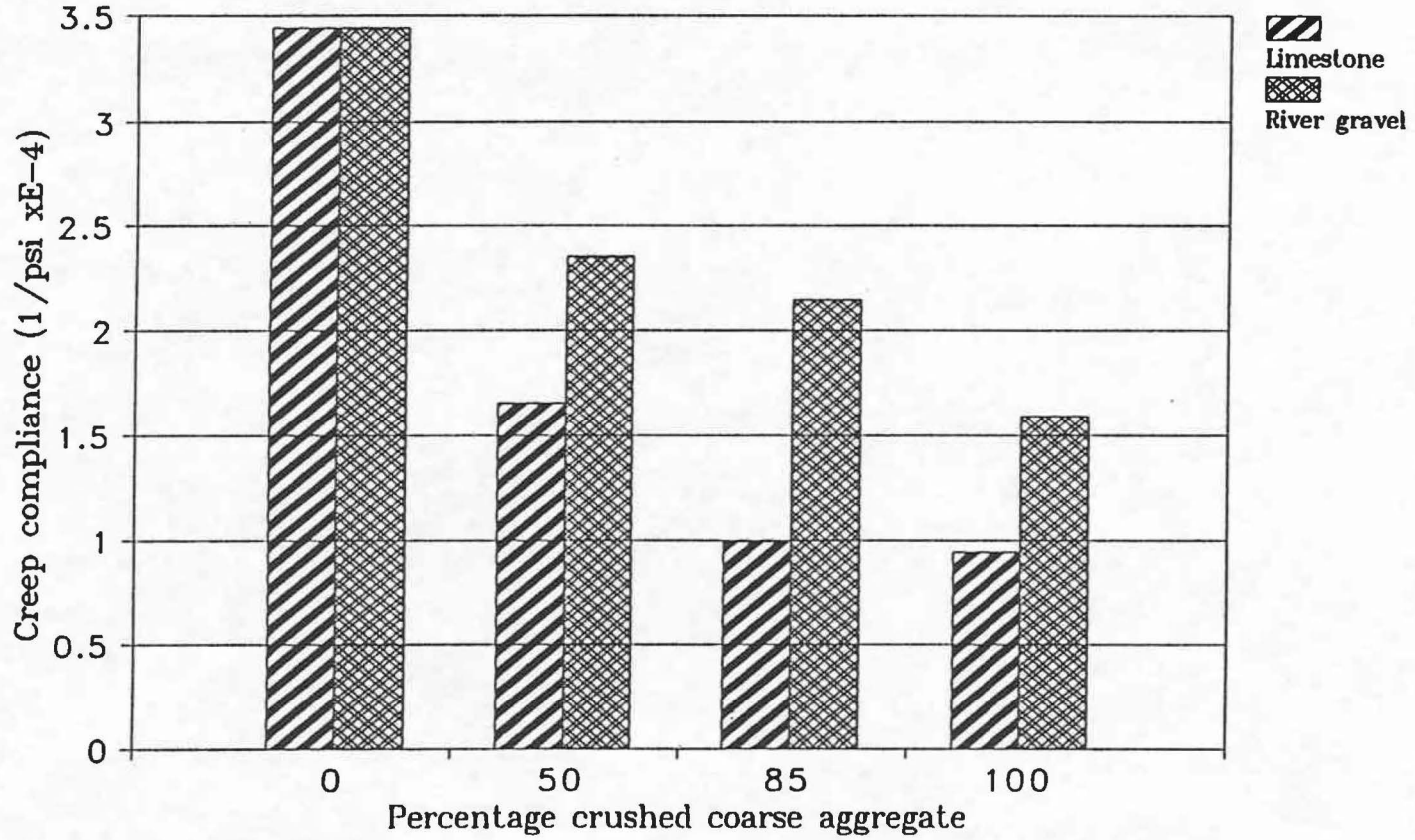

Figure 4.12. Creep Compliance at 3600 Seconds (Dynamic Creep) as a Function of Crushed Coarse Aggregate.

Table 4.8. Summary of Fractal Numbers for Shape of Three Individual Aggregate Particles of Different Shapes.

Shape of Aggregate	Fractal Dimension	Average Fractal Dimension
circle1 circle2 circle3	1.02 1.01 1.04	1.02
triangle1 triangle2 triangle3	1.08 1.09 1.07	1.07
rectangle1 rectangle2 rectangle3	1.12 1.12 1.13	1.13
pentagon1 pentagon2 pentagon3	1.05 1.07 1.06	1.06
elongated1 elongated2 elongated3	1.17 1.19 1.16	1.17

An important point noticed in this testing program was that the fractal dimension changed with a change in shape, but has been found to be similar for two particles of the same shape and with different degrees of roughness. For example, the fractal dimension for shape of triangular crushed and uncrushed river gravel particles were found to be very similar. This is due to the low resolution of video images, and the smallest box used in box counting was not small enough to take into account the irregularity of the edge shown by SDF. This problem can be rectified by using high resolution video cameras and smaller size boxes on a magnified SDF curve to get a better fractal dimension number for shape.

Differences in fractal dimension values for different shapes were statistically tested using the paired t-test at a 95 percent confidence interval. Findings of the significance tests are recorded in Table 4.9. The difference in fractal dimension for shape of circular and triangular aggregates is not significant. There is a significant difference in fractal dimension values of circular, rectangular, and elongated aggregates.

Table 4.9. Summary of Statistical Significance Test Results for Shape of the Individual Aggregate Particles.

HYPOTHESIS: Difference in fractal dimension number for shape is significant for the aggregate particles of shape:	Result of significant test at 95 percent confidence interval.
Circular and Triangular	Reject
Circular and Rectangular	Accept
Circular and Pentagon	Reject
Circular and Elongated	Accept

Surface Texture

Fractal dimension for surface texture was determined in two ways: 1) for a group of particles and 2) for a single particle. Surface texture values were determined for all the aggregate blends used in the mixture analysis and for individual particles of crushed limestone, river gravel, and uncrushed river gravel. Images for fractal analysis were obtained from the aggregate blends prepared for asphalt concrete specimens. These samples contained coarse aggregate (+ No.4 sieve) with varying amounts of crushed particles. Appendix C (Figures C5a-g) illustrates images of the aggregate blends. Table 4.10 includes the fractal dimension number for texture of all the aggregate blends tested.

It can be observed from these values that there is no reasonable correlation between the fractal number and crushed aggregate content. This is due to the shadows that form along the edges of the particles in the images of groups of aggregate particles. Dark shades or shadows between particles can be observed in the images given in Figures C5a-g in Appendix C. These dark shadows are considered by the algorithm to be low spots on a surface and, thus, increase the fractal dimension value. These shadows can be eliminated through proper lighting equipment; then, better fractal dimension values for texture can be calculated.

Degree of roughness of a surface is identified by the change in the grey levels of the pixels on the images. Since the fractal dimension value for texture is influenced by the color changes on the image, the color of aggregates affect the value. In order to make a

Table 4.10. Mean Fractal Dimension Numbers (2 samples) for Texture of Aggregate Blends Used for Asphalt Concrete Samples.

Amount of crushed coarse aggregate (%)	Fractal Dimensional Number	
	River Gravel	Limestone
0	0.46	0.46
50	0.41	0.43
85	0.41	0.34
100	0.38	0.36

valid comparison of fractal dimension numbers of two different aggregate types, they must have the same surface color.

Images of crushed river gravel, limestone, and uncrushed river gravel particles with their natural colors were taken. Table 4.10 gives the fractal dimension numbers for these surfaces. It can be observed that the fractal dimension number for uncrushed aggregate particles is higher than that for crushed particles. This is because raw limestone particles contained white dust on their surfaces which made the surface appear bright and smooth on a video image. Color variations in uncrushed river gravel particles produced a video image with much contrast which was accounted for as changes in the profile of the surface.

After observing these drawbacks in imaging of the natural aggregate surfaces, these particles were treated before taking images for the determination of surface texture. Three sets of particles with different treatments were used to determine the fractal number:

1) Unwashed (untreated) particles,
2) Washed particles, and
3) Particles coated with white spray paint.

Table 4.11 shows fractal dimension values for images of single particles. Appendix C (Figures C6-C14b) gives images of washed and white painted single particles. Differences in fractal dimension for texture of smooth river gravel, crushed river gravel, and crushed

Table 4.11. Summary of Fractal Numbers for Texture of Individual Aggregate Particles.

Aggregate type	Fractal Dimension	Average Fractal Dimension (h)
Unwashed		
Limestone1 Limestone2	0.15 0.15	0.15
Crushed river gravel1 Crushed river gravel2	0.10 0.09	0.10
Uncrushed river gravel1 Uncrushed river gravel2	0.07 0.12	0.10
Washed		
Limestone1 Limestone2	0.26 0.26	0.26
Crushed river gravel1 Crushed river gravel2	0.23 0.23	0.23
Uncrushed river gravel1 Uncrushed river gravel2	0.10 0.12	0.12
White painted		
Limestone1 Limestone2 Limestone3	0.22 0.19 0.21	0.21
Crushed river gravel1 Crushed river gravel2 Crushed river gravel3	0.18 0.16 0.19	0.17
Uncrushed river gravel1 Uncrushed river gravel2 Uncrushed river gravel3	0.09 0.10 0.09	0.10

limestone were statistically tested using the paired t-test at 95 percent confidence level. Findings from the statistical significance test show that there is a significant difference in fractal dimension of uncrushed river gravel and crushed river gravel as well as uncrushed river gravel and crushed limestone. The mean (of 3 samples) fractal dimension value of

crushed limestone is higher than that of crushed river gravel; but, the difference was not found to be statistically significant at 95 percent confidence interval.

When the effect of color is eliminated, fractal dimension value for texture increases with an increase in the degree of roughness or with an increase in the amount of crushed particles. Fractal dimension can be related to the permanent deformation characteristics of an asphalt concrete mixture as there is a direct correlation between amount of crushed aggregate and the creep test results. Figures 4.13 and 4.14 illustrate that the creep compliance decreased with an increase in the fractal number for texture. Fractal numbers for the mixtures with 50 and 85 percent crushed particles were estimated, assuming a linear relationship between the fractal number and the percentage of crushed aggregate.

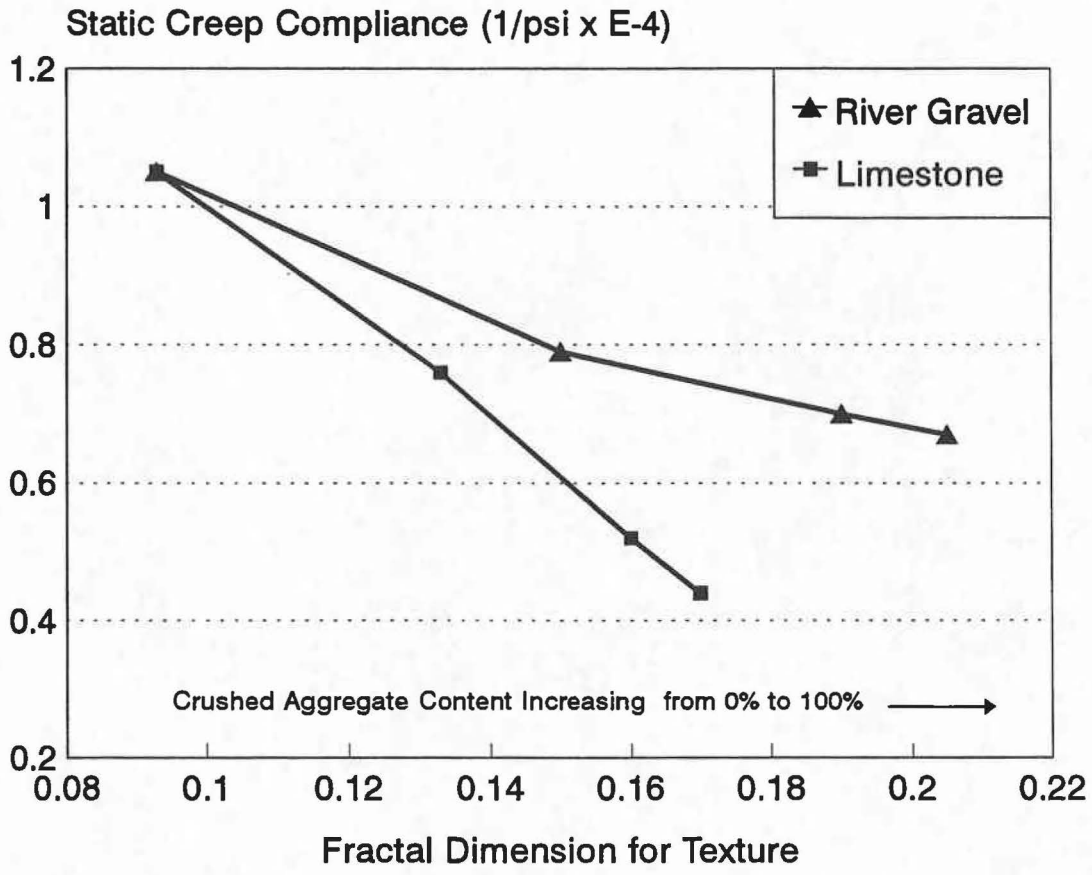

Figure 4.13. Static Creep Compliance vs. Texture of Aggregate Particles Used in the Mixes.

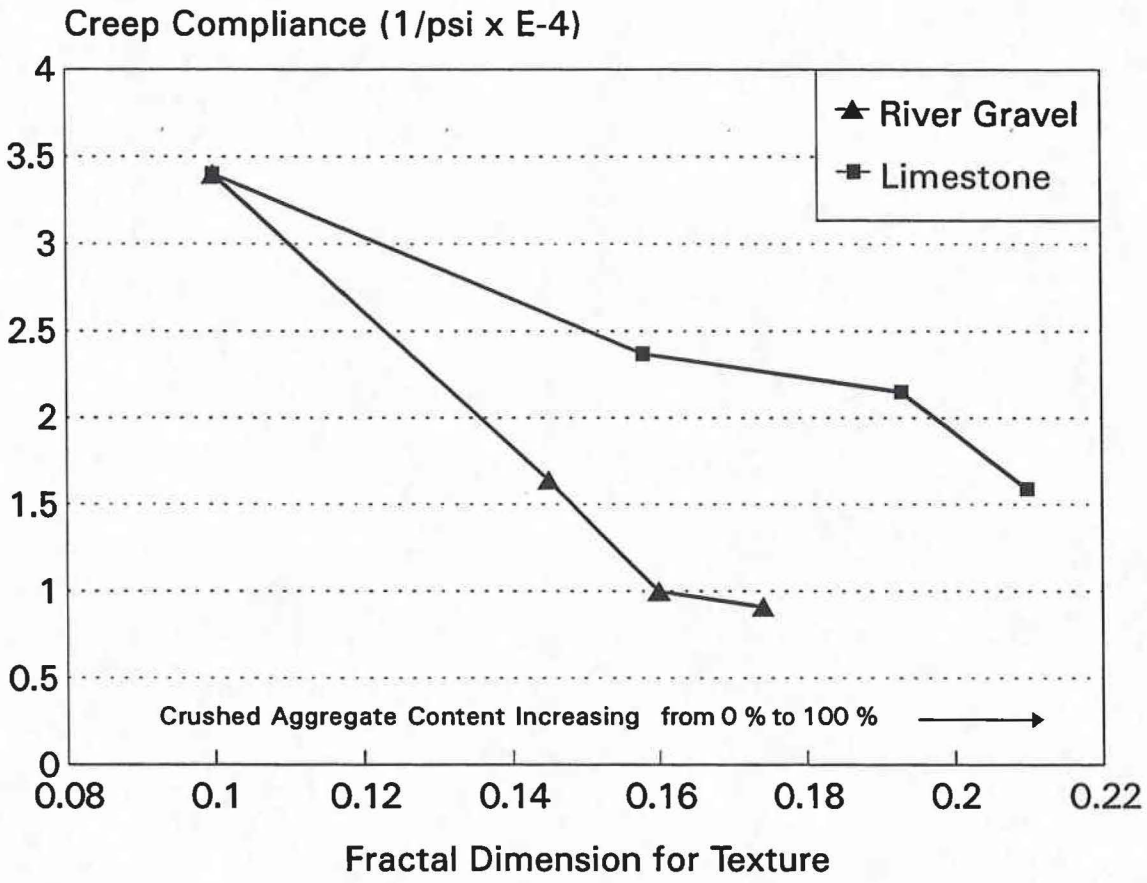

Figure 4.14. Dynamic Creep Compliance vs. Texture of Aggregate Particles Used in the Mixes.

CHAPTER 5
THEORETICAL MODELS FOR RUTTING PREDICTION

A theoretical model for rutting prediction developed by Button et al. (6) is reviewed in this chapter. The model is applied to creep and recovery tests performed on mixtures containing different amounts of crushed coarse aggregate. Results from the rutting model are correlated with fractal dimension analysis.

THEORETICAL MODELS

Based on a study of creep and recovery behavior of asphalt concrete and through philosophical approach, two hyperbolic equations were developed to estimate creep and recovery of asphalt concrete under loading. The model for creep compliance is:

$$D(t) = \frac{D_o + D_m a t^m}{1 + a t^m} \tag{5.1}$$

where

D_o = initial creep compliance (1/psi),
D_m = maximum creep compliance (1/psi),
a = regression constant,
t = time (seconds), and
m = slope factor.

and the model for recovery is:

$$R(t) = \frac{R_o + R_m b t^{mp}}{1 + b t^{mp}} \tag{5.2}$$

where

R_o = initial (elastic) recovery compliance (1/psi),
R_m = maximum recovery compliance (1/psi),

b = regression constant,

t = time (seconds), and

p = slope factor modifier.

An optimization technique known as "pattern search" was used to compute the unknown parameters in equations 5.1 (D_o, D_m, a, m) and 5.2, (R_o, R_m, b, p). This pattern search method was developed based on the optimization technique developed by Hooke and Jeeves (48). From Figures 5.1 and 5.2, it can be stated that Equations 5.1 and 5.2 represent creep and recovery behavior of asphalt concrete very well.

From Equations 5.1 and 5.2, Button et al. (6) derived a permanent deformation model. For N repeated applications of a load pulse of duration Δt, both creep and recovery equations can be used to obtain the total deformation and recovery:

$$D(N) = \frac{D_o + D_m r N^m}{1 + r N^m} \tag{5.3}$$

$$R(N) = \frac{R_o + R_m r_p N^{mp}}{1 + r_p N^{mp}} \tag{5.4}$$

where

N = Number of cycles,

r = $a\,(\Delta t)^m\,\rho$,

r_p = $b\,(\Delta t)^{mp}\,\rho_p$,

t = $N\,(\Delta t)$, and

ρ, ρ_p = load pulse factors.

For N load pulse repetitions with a constant stress, σ_o, the total accumulated strain, ϵ_a , can be calculated using:

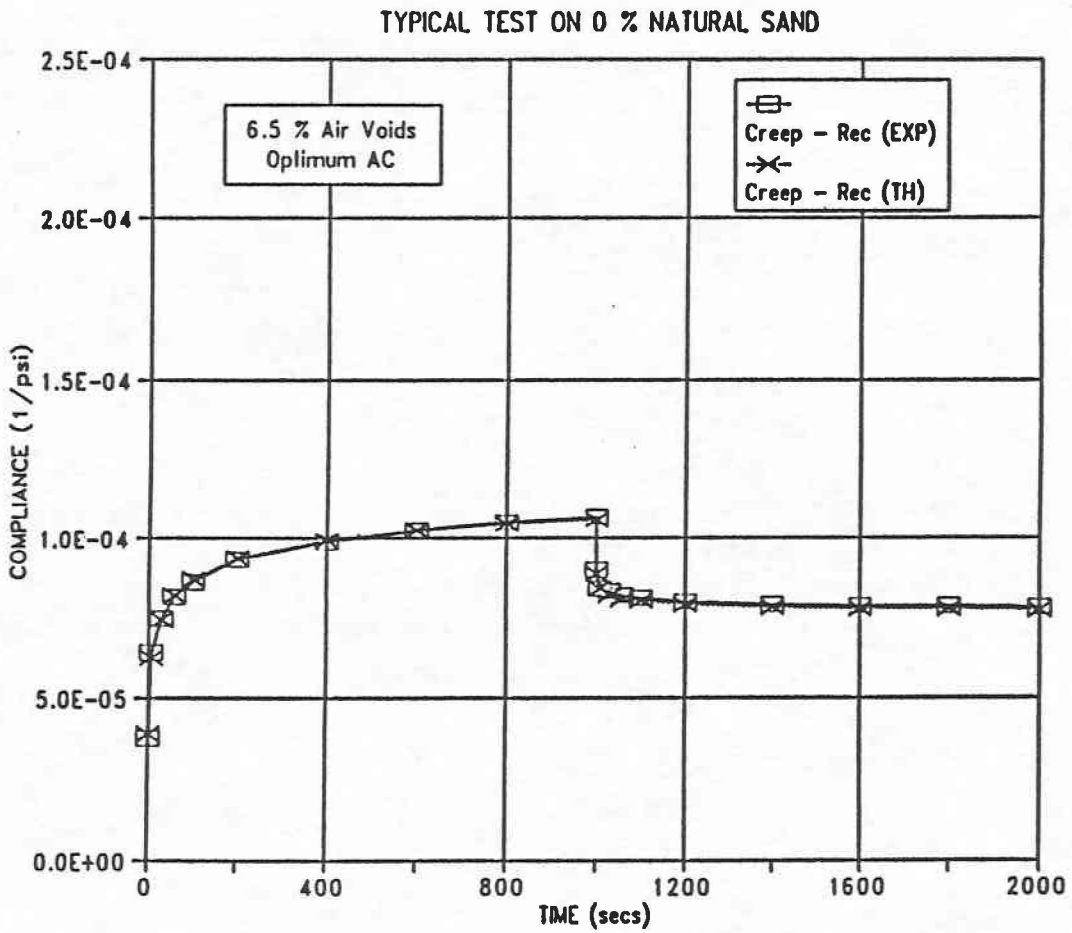

Figure 5.1. Creep and Recovery Curve of a Mix with 0 Percent Natural Sand.

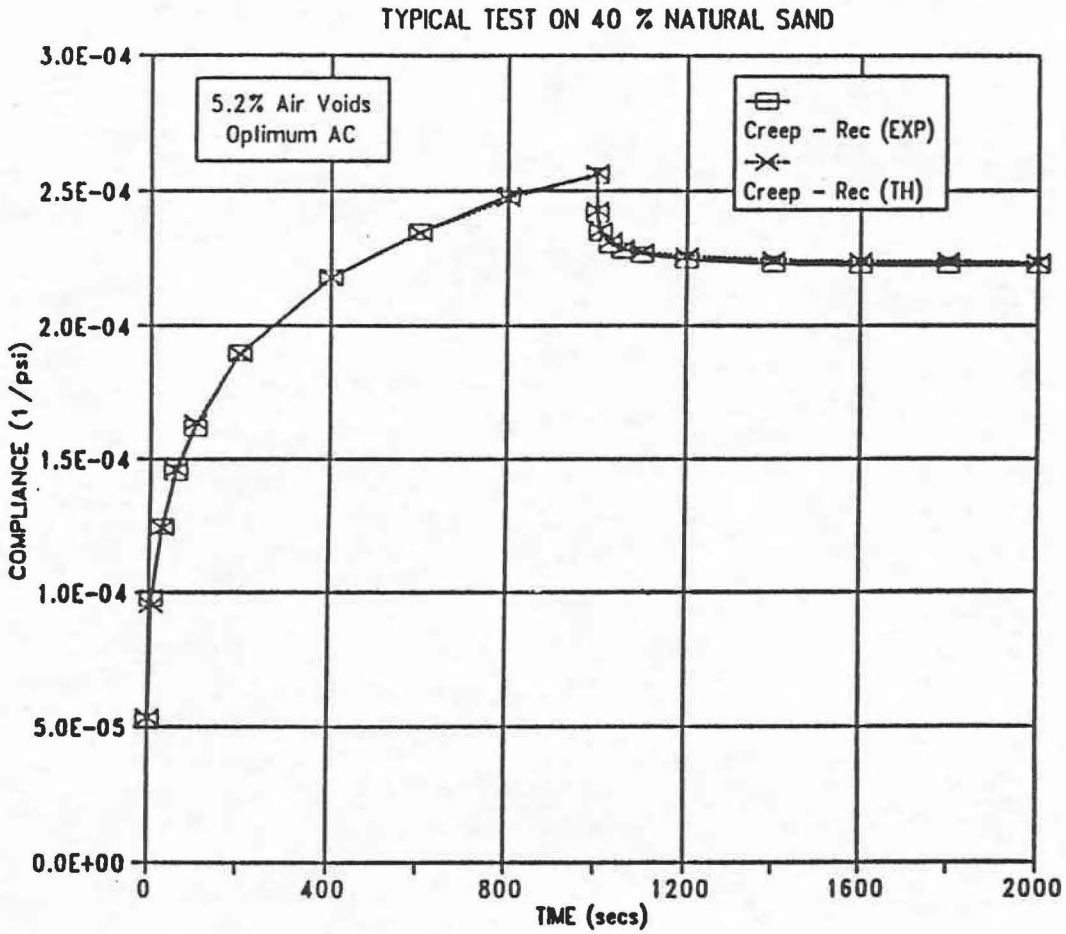

Figure 5.2. Creep and Recovery Curve of a Mix with 40 Percent Natural Sand.

$$\epsilon_a = \epsilon(N) - \epsilon_r(N) = \sigma_0[D(N) - R(N)] \quad (5.5)$$

where

ϵ_r = recoverable or resilient strain.

The rate of change of permanent strain can be obtained from:

$$\frac{\partial \epsilon_a(N)}{\partial N} = \sigma_o \left[\frac{\partial D(N)}{\partial N} - \frac{\partial R(N)}{\partial N}\right] \quad (5.6)$$

The following equation can be derived by substituting Equations 5.3 and 5.4 in Equation 5.6, and dividing by the resilient strain, ε_r:

$$\frac{1}{\epsilon_r}\frac{\partial \epsilon_a(N)}{\partial N} = E_r D_m m N^{m-1} q(1 - qN^m)[(D_m - D_o) - (R_m - R_o)ps] \quad (5.7)$$

where

$$q = \frac{r}{1+rN^m} \quad (5.8)$$

$$s = \frac{q_p(1-q_pN^m)}{q(1-qN^m)} \quad (5.9)$$

$$q_p = \frac{r_pN^{m(p-1)}}{1+r_pN^{mp}} \quad (5.10)$$

E_r = resilient modulus

The VESYS (32) permanent strain response model is:

$$\frac{\partial \epsilon_p}{\partial N} = \epsilon_r . \mu . N^{-\alpha} \quad (5.11)$$

where

μ, α = Parameters determined from Equation (5.7),

N = Number of cycles,

ϵ_r = Elastic or resilient strain, and

$\frac{\partial \epsilon_p}{\partial N}$ = Rate of change of permanent strain with load repetitions

Replacing permanent strain, ϵ_p , in Equation 5.11 by the accumulated strain, ϵ_a , Equation 5.11 can be written as:

$$\mu N^{-\alpha} = \frac{1}{\epsilon_r} \left[\frac{\partial \epsilon_a}{\partial N} \right]$$

Comparing the above equation with Equation 5.7, it can be shown that

$$\alpha = 1\text{-}m \tag{5.12}$$

and

$$\mu = E_r D_m mq(1 - qN^m) [(D_m - D_o) - (R_m - R_o)ps] \tag{5.13}$$

where

$$s = \frac{q_p(1 - q_p N^m)}{q(1 - qN_m)} \tag{5.14}$$

The α and μ, permanent deformation characteristics, shown in Equations 5.12 and 5.13 can be incorporated into the Texas Flexible Pavement System (TFPS) (49), which was developed at the Texas Transportation Institute for prediction of rutting. In TFPS, the strain response of the pavement was divided into two components, elastic strain and permanent strain, as shown in Figure 5.3. The total strain, ϵ_t , is the sum of elastic strain, ϵ_e , and the permanent strain, ϵ_p .

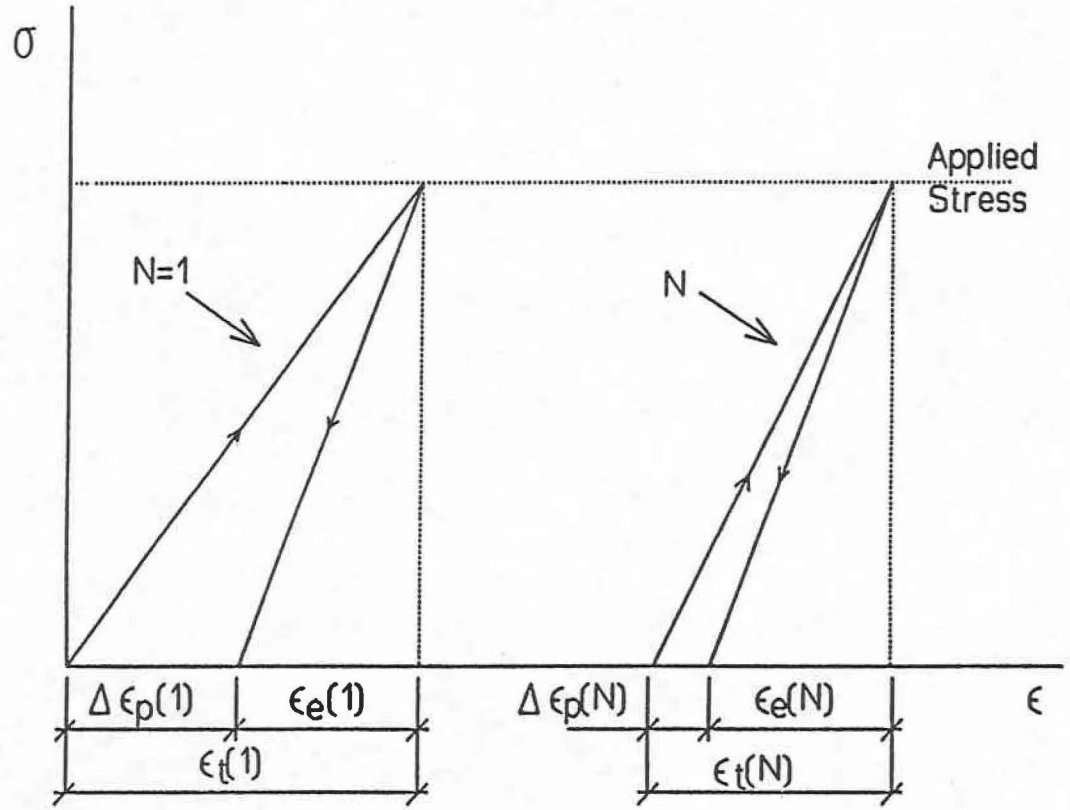

Figure 5.3. Typical Strain Response to Loading - Unloading for an Asphalt Pavement Material.

From Figure 5.3, the modulus during loading and unloading can be given as:

$$E_{lo} = \frac{\sigma}{\epsilon_t(N)} = \text{Modulus during loading} \quad (5.15)$$

$$E_{un} = \frac{\sigma}{\epsilon_e} = \text{Modulus during unloading} \quad (5.16)$$

By rewriting Equation 5.15, using Equation 5.11, modulus during loading can be written as:

$$E_{lo}(N) = \frac{E_{un}}{1 + \mu N^{-\alpha}} \quad (5.17)$$

Equation 5.17 gives a relation between loading modus, $E_{lo}(N)$, and unloading moduli, $E_{un}(N)$, as a function of permanent deformation characteristics of asphalt concrete mix, α and μ, and the number of load applications. The permanent deformation in pavement can be calculated by subtracting the recovery during unloading from deflection during loading. Deflection during loading can be calculated by assigning the loading moduli to all the pavement layers, and recovery during unloading can be calculated by assigning the unloading moduli to all the layers.

CORRELATION BETWEEN P-VALUE AND FRACTAL DIMENSION

Creep and recovery compliance can be represented by two theoretical models as shown in Equations 5.1 and 5.2. The recovery model has the parameter "p" which is a slope modifier of the creep and recovery compliance curve. Button et al. (6) showed that this parameter accounts for aggregate shape and texture. From the creep and permanent deformation test data, "p" values were calculated and are listed in Table 5.1. It can be observed from the data given in Table 5.1 that the "p" value decreased with an increase in the amount of crushed aggregate in the mix. The "p" value increased with an increase in

Table 5.1. Mean "p" Values for Mixes with 0, 50, 85 and 100 Percent Crushed Coarse Aggregate.

Percent Crushed Aggregate	Mean "p" value for 2 samples
Crushed coarse river gravel	
0	2.42
50	1.96
85	1.64
100	1.60
Crushed coarse limestone	
0	2.42
50	1.78
85	1.41
100	1.19

creep compliance (Figures 5.4 and 5.5). The fractal dimension (fd) number for texture of coarse aggregate in the asphalt concrete mixture gives an inverse relationship with the "p" value (Figure 5.6). These findings demonstrate that the "p" value represents creep and recovery behavior of asphalt concrete regarding aggregate physical properties.

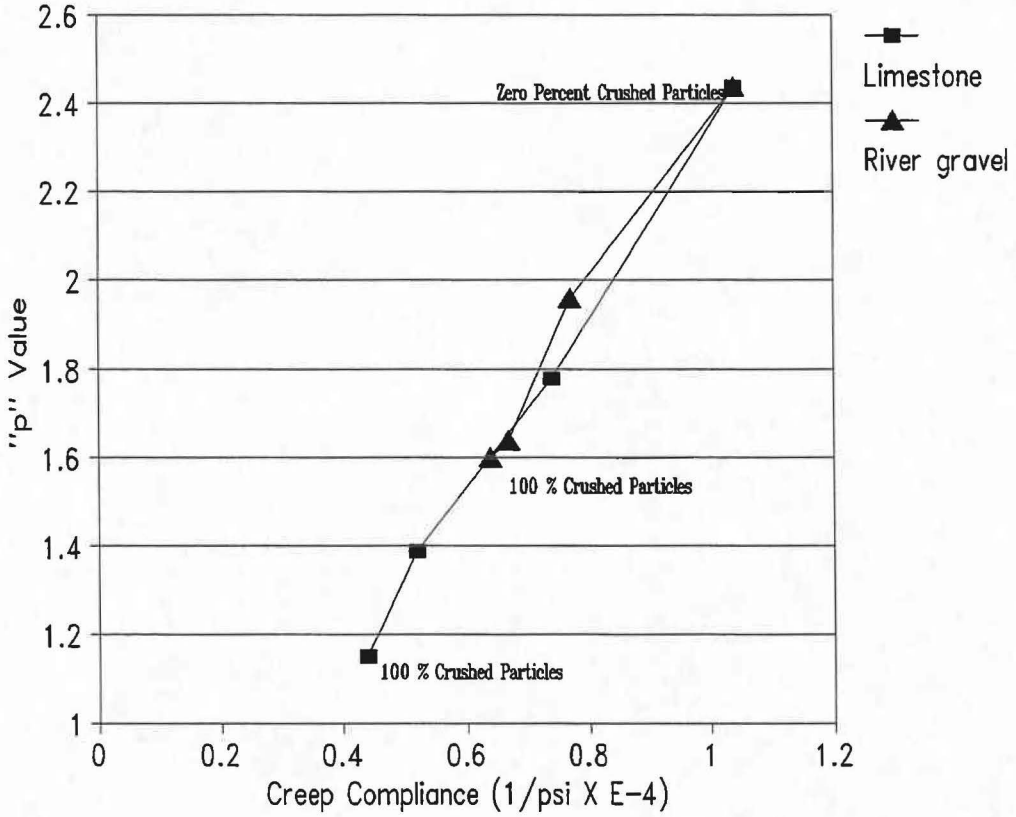

Figure 5.4. "p" Value vs. Creep Compliance at 1000 Seconds (Static Creep Test).

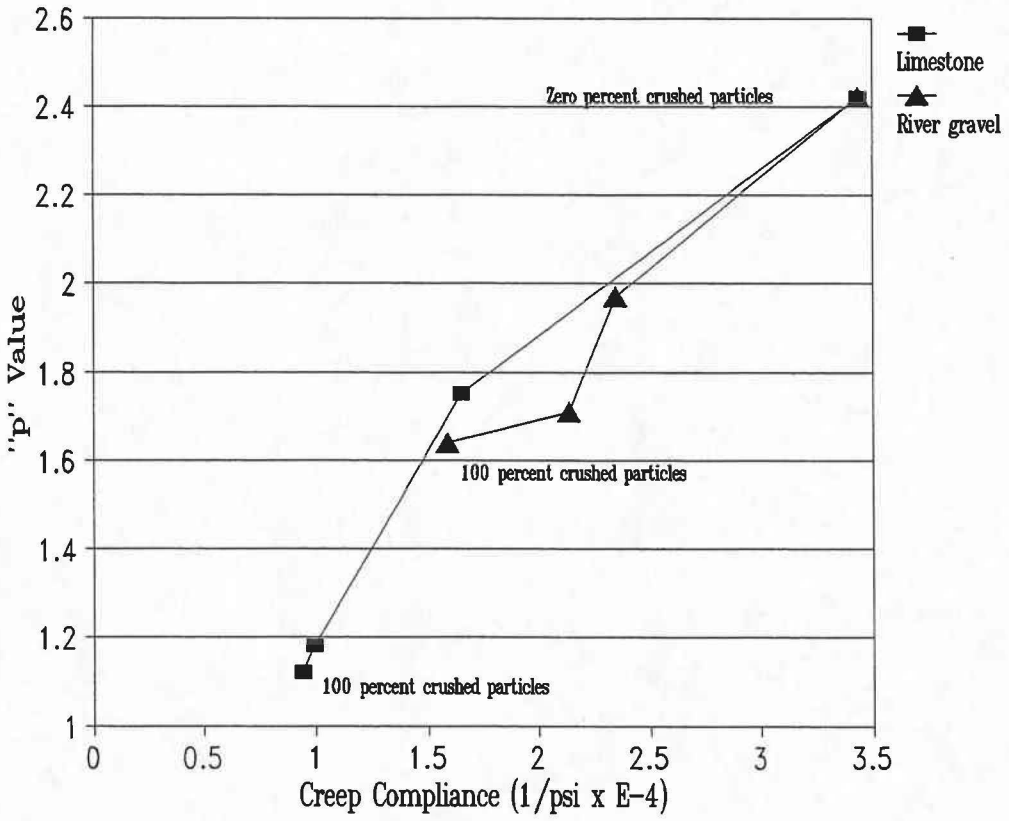

Figure 5.5. "p" Value vs. Creep Compliance at 3600 Seconds (Dynamic Creep Test).

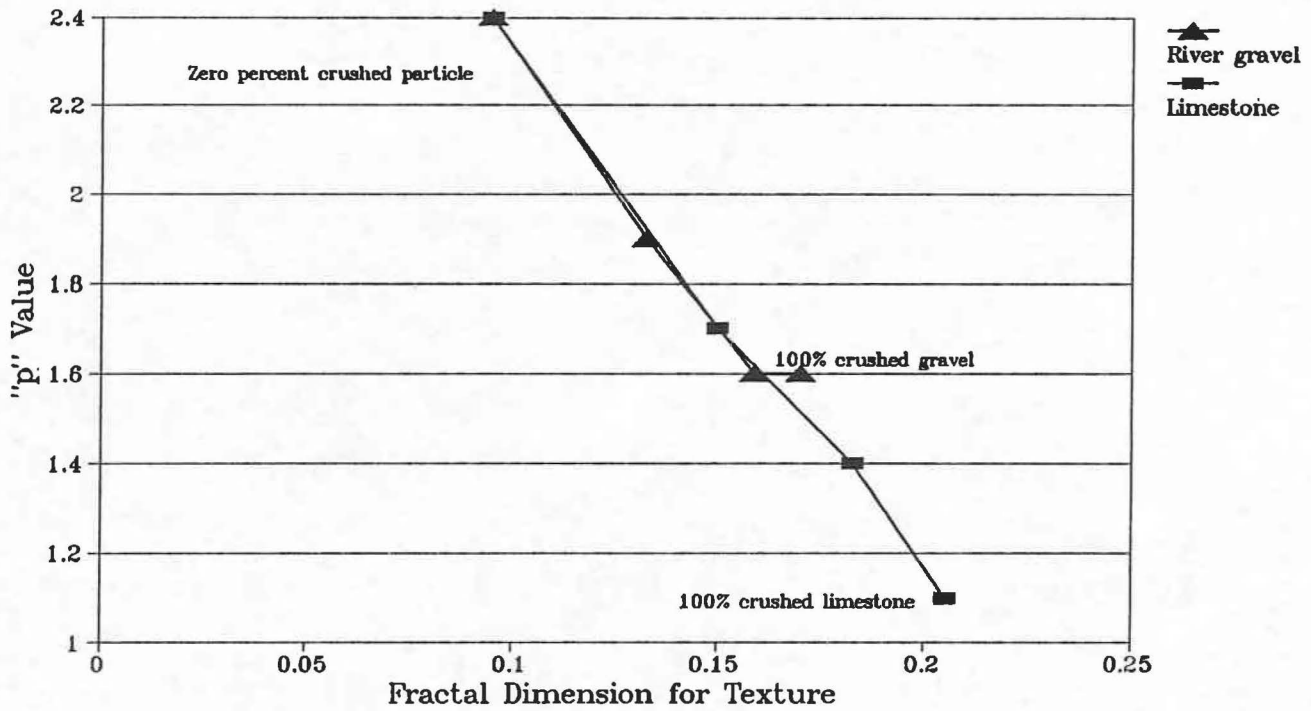

Figure 5.6. "p" Value vs. Fractal Dimension Number of Texture for Asphalt Concrete Mixtures Made of Different Amounts of Crushed Coarse Aggregates.

CHAPTER 6
CONCLUSIONS AND RECOMMENDATIONS

Based on laboratory evaluation of asphalt mixtures prepared using different amounts of crushed and uncrushed coarse aggregates, and an objective measurement of aggregate shape and surface texture, the researchers submit the following conclusions and recommendations.

CONCLUSIONS

1. Long-term static and cyclic creep (unconfined compression) tests were sensitive to changes in coarse aggregate surface characteristics. Both static and dynamic tests showed a decrease in creep and permanent deformation with an increase in the amount of crushed coarse aggregate in asphalt mixtures of the same gradation.
2. Hveem stability increased consistently with an increase in the percentage of crushed coarse aggregate.
3. At high pavement service temperatures, an increase in the percentage of crushed coarse aggregate increased resilient modulus. At low service temperatures, aggregate type had little effect on resilient modulus.
4. Marshall stability increased with an increase in the amount of crushed coarse aggregate in the mixture.
5. Fractal dimension analysis has potential to be a practical, objective measure of shape and texture of aggregate particles. The fractal number for aggregate particles correlated with creep and permanent deformation behavior of asphalt mixtures.
6. The "p" value, as defined herein, decreased with an increase in percentage of crushed coarse aggregate. The "p" value correlates with creep compliance of the mixture and accounts for the influence of aggregate shape and texture on permanent deformation of asphalt concrete.

7. Fractal dimension for texture and "p" value show an inverse linear correlation. The "p" value increased with a decrease in the fractal number which indicates that rutting susceptibility increases with a decrease in the fractal dimension number.
8. The amount of angular coarse aggregate is a major factor that should be considered when designing rut-resistant hot mix asphalt concrete.
9. TxDOT standard specification for Item 340, hot mix asphalt concrete requires that 85 percent of the particles retained on the No. 4 sieve must have two or more crushed faces. This research provides evidence that this requirement is about optimum for rut resistance and economy.

RECOMMENDATIONS

1. Since the findings of the experimental work show that angular coarse aggregate improves Hveem stability, Marshall stability, resilient modulus (at higher temperature), and resistance to creep and permanent deformation, it follows that the use of angular coarse aggregate to the extent possible will reduce rutting potential of asphalt concrete.
2. Use of subrounded, smooth surfaced coarse aggregates (retained on the No. 4 sieve) should be limited to 15% in order to develop asphalt concrete mixtures that can withstand heavy traffic and higher wheel loads and tire pressures.
3. Fractal numbers for shape and texture can be correlated with permanent deformation characteristics of asphalt concrete mixtures. Minimum fractal dimension values could be used in an aggregate specification to minimize the probability of rutting. Fractal dimension could provide an objective measure of aggregate shape and texture in a revised aggregate classification system. More research using fractal dimension analysis on a wide variety of aggregate types and under different conditions of lighting and aggregate particle surface preparation is needed.

REFERENCES

1. V. J. Marks, R. W. Monroe, and J. F. Adam. *Effects of Crushed Particles in Asphalt Mixtures.* Transportation Research Record 1259, March 1989.

2. I. V. Kalcheff and D. G. Tunnicliff. *Effects of Crushed Stone Aggregate Size and Shape on Properties of Asphalt Concrete*. Proceedings of the Association of Asphalt Paving Technologists, Vol. 51, 1982.

3. E. R. Hargett. *Effects of Size, Surface Texture, and Shape of Aggregate Particles on the Properties of Bituminous Mixtures*. Highway Research Board, Special Report 109, 1968.

4. C. L. Monismith. *Influence of Shape, Size, and Surface Texture on the Stiffness and Fatigue Response of Asphalt Mixtures*. Highway Research Board, Special Report 109, 1968.

5. F. J. Benson. *Effects of Aggregate Size, Shape, and Surface Texture on the Properties of Bituminous Mixtures-A Literature Survey*. Highway Research Board, Special Report 109, 1968.

6. J. W. Button, D. Perdomo, and R. L. Lytton. *Influence of Aggregate on Rutting in Asphalt Concrete Pavements*. Transportation Research Record 1259, March 1989.

7. S. P. Kandhal. *Design of Large-Stone Asphalt Mixes To Minimize Rutting.* Transportation Research Record 1259, March 1989.

8. A. K. Sharma and L. L. Larson. *Rut-Resistant Asphalt Concrete Overlays in Wisconsin*. Transportation Research Record 1259, March 1989.

9. Western Association of State Highway and Transportation Officials. *Asphalt Pavement Rutting, Western States*. WASHTO Executive Committee, May 1984.

10. W. S. Mendenhall, Jr., R. G. Fairbrother, L. M. Papet, R. Scott, C. J. Kliethermes, D. Wilken, and F. M. Mayer. *Asphalt Pavement Rutting and Stripping*. Ad hoc task force report, 1987.

11. K. Mahboub and D. L. Allen. *Characterization of Rutting Potential Of Large-Stone Asphalt Mixes (LSAM) In Kentucky*. Transportation Research Board, 69th annual meeting, 1990.

REFERENCES (Continued)

12. N. C. Krutz and M. Stroup-Gardiner. *Relationship Between Permanent Deformation of Asphalt Concrete and Moisture Sensitivity*. Transportation Research Record 1259, March 1989.

13. M. Herrin and W. H. Goetz. *Effect of Aggregate Shape on Stability of Bituminous Mixes*. Proceedings, Highway Research Board, Vol. 33, 1954.

14. G.A. Huber and G.H. Heiman. *Effect of Asphalt Concrete Parameters on Rutting Performance: A Field Investigation.* Proceedings, Association of Asphalt Paving Technologists, Vol. 56, 1987, pp. 33-61.

15. R. B. Moore and R. A. Welke. *Effect of Fine Aggregate on Stability of Bituminous Mixes.* Michigan Transportation Commission, Research Report No. 78 TB-34-79F, December 1979.

16. *Rutting Investigation.* Materials Laboratory, Wyoming State Highway Department, Cheyenne, Wyoming, April 1982.

17. Warburton, R. G., W. B. Bentenson, D. I. Hanson, W. C. Jones, J. J. Maykuth, R. T. Rask, and R. D. Tea. *Asphalt Pavement Rutting in the Western States.* A workshop report WASHTO Executive Committee, Western Association of State Highway and Transportation Officials, May, 1984.

18. R. P. Lottman. *NCHRP Report 246: Predicting Moisture-Induced Damage to Asphaltic Concrete*. Transportation Research Board, National Research Council. Washington, D.C., May 1982.

19. F. N. Finn, C. L. Monismith, and N. J. Markevich. *Pavement Performance and Asphalt Concrete Mix Design.* Proceedings, The Association of Asphalt Paving Technologists, Vol. 52, 1983, pp. 121-150.

20. J. S. Lai. *Evaluation of Rutting Characteristics of Asphalt Mixes Using Loaded Wheel Tester*. Georgia Department of Transportation, Research Project No. 8609, December 1986.

21. F. L. Roberts, J. T. Tielking, D. Middleton, R. L. Lytton, and K. Tseng. *Effects of Tire Pressures on Flexible Pavement.* Report No. FHWA-TX-85-372-1 (TTI 372-IF), Texas Transportation Institute, Texas A&M University, College Station, Texas, December 1985.

REFERENCES (Continued)

22. M. Huhtala, J. Pihlajamaki, and M. Pienimaki. *The Effects of Tires and Tire Pressures on Road Pavements*. Transportation Research Board, 68th Annual Meeting, Washington, D.C., January 1989.

23. *Mix Design Methods for Asphalt Concrete and Other Hot-Mix Types*. Asphalt Institute, College Park, Maryland, May 1984.

24. M. Acott. *Today's Traffic Calls for Heavy Duty Asphalt Mixes*. Roads and Bridges, Vol. 26, No.1, January 1988, pp.39-45.

25. J. Miller, H. Monroney, and M. Traylor. *Illinois Develops Stable Mixes*. Engineering and Research Division, Illinois Asphalt Pavement Association, Springfield, Illinois, 1987.

26. F. M. S. Bayomy and H. R. Guirguis. *An Upgrading Technique for AC Pavement Materials*. Roads and Developments, Vol. 2, Roads and Development Center, Kuwait, May 1984.

27. J. W. Button and V. Jagadam. *Cement Coating Marginal Aggregates for Use in Asphalt Pavements*. FHWA/TX-93/1253-IF, Research Report 1253-1F, Texas Transportation Institute, Texas A&M University, College Station, Texas, November 1992.

28. *Construction Bulletin C-14*. State Department of Highways and Public Transportation, Construction Division, Austin, Texas, 1984.

29. *Manual Testing Procedures*. 200-F Series, Texas State Department of Highways and Public Transportation, Austin, Texas, 1985.

30. *ASTM D-1559-89 Resistance to Plastic Flow of Bituminous Mixtures Using Marshall Procedure*. Annual Book of ASTM Standards. Vol. 04.03, American Society of Testing and Materials, Philadelphia, Pennsylvania, 1991.

31. *ASTM D-4123-82 Indirect Tension Test for Resilient Modulus of Bituminous Mixtures*. Annual Book of ASTM standards, Vol. 04.03, American Society of Testing and Materials, Philadelphia, Pennsylvania, 1991.

32. W. J. Kenis. *Predictive Design Procedures, VESYS User's Manual*. FHWA Report 77-154, 1978.

REFERENCES (Continued)

33. L. Li, P. Chan, D. G. Zollinger, and R. L. Lytton. *Aggregate Shape Quantitative Analysis from Fractals.* ACI Materials Journal, Vol. 90, No. 4, July-August 1993.

34. The Asphalt Institute, *The Asphalt Hand Book.* Manual series no. 4 (MS-4), 1989.

35. B. Mather, *Significance of Tests and Properties of Concrete and Concrete-Making Materials (Shape, Surface Texture, and Coatings).* ASTM STP 169-A, 1966, pp. 415-431.

36. *ASTM D-3398-91 Index of Aggregate Particle Shape and Texture.* Annual Book of ASTM Standards. Vol. 04.03, American Society for Testing and Materials, Philadelphia, Pennsylvania, 1991.

37. R. D. Barksdale, M. A. Kemp, W. J. Sheffield, and J. L. Hubbard. *Measurement of Aggregate Shape, Surface Area and Roughness.* Georgia Institute of Technology, Atlanta, Georgia, February 1991.

38. J. D. Wilson, J. W. Landis, and M. A. Gross. *Determination of Aggregate Angularity Using Image Processing.* Electronics and Instrumentation Department, University of Arkansas at Little Rock, Submitted for presentation at the Transportation Research Board 70th Annual Meeting, 1991.

39. J. R. Carr, G. M. Norris, and D. E. Newcomb. *Characterization of Aggregate Shape Using Fractal Dimension.* Transportation Research Board, 69th Annual Meeting, Washington, D.C., January 1990.

40. J. R. Carr, M. Misra, and J. Litchfield. *Estimating Surface Area for Aggregate in the Size Range: One Millimeter or Larger.* Transportation Research Board, 71st Annual Meeting, Washington, D.C., January 1992.

41. J. LeBlanc, M. A. Gennert, D. Gosselin, and N. Wittels. *Analysis and Generation of Pavement Distress Images Using Fractals.* Worcester Polytechnic Institute, Worcester, Massachusetts, Transportation Research Record No. 1311, pp. 158-165, 1991.

42. B. B. Mandelbrot, D. E. Passoja, and A. J. Paullay. *Fractal Character of Fracture Surfaces of Metals.* Nature, Vol. 308, April 1984.

43. B. J. West and A. L. Goldberger. *Physiology in Fractal Dimensions.* American Scientist, Vol. 75, pp. 354-365, July-August 1987.

REFERENCES (Continued)

44. C. Ribble, R. Szecsy, and D. G. Zollinger. *Aggregate Macro Shape and Micro Texture in Concrete Mix Design.* American Society of Civil Engineers, Spring meeting, Fort Worth, Texas, April 1992.

45. B. B. Mandelbrot and R. E. Smith. *The Fractal Geometry of Nature.* San Francisco, California, 1982.

46. D. Perdomo and J.W. Button. *Identifying and Correcting Rut Susceptible Asphalt Mixtures.* Research Report 1121-F, Texas Transportation Institute, Texas A&M University, College Station, Texas, February 1991.

47. B. B. Mandelbrot. *Fractals: Form, Chance and Dimension.* San Francisco, California, 1977.

48. R. Hooke and T. A. Jeeves. *Direct Search Solution of Numerical and Statistical Problems.* Journal of the Association of Composite Mechanics, 8, 2, April 1961.

49. J. Uzan, D. G. Zollinger, and R. L. Lytton. *Mechanistic/Empirical Model for the Structural Design of Flexible Pavement.* Research Report 455-1, Texas Transportation Institute, Texas A&M University, College Station, Texas, November 1991.

APPENDIX A

DATA FROM RESILIENT MODULUS, HVEEM, AND MARSHALL STABILITY TESTS

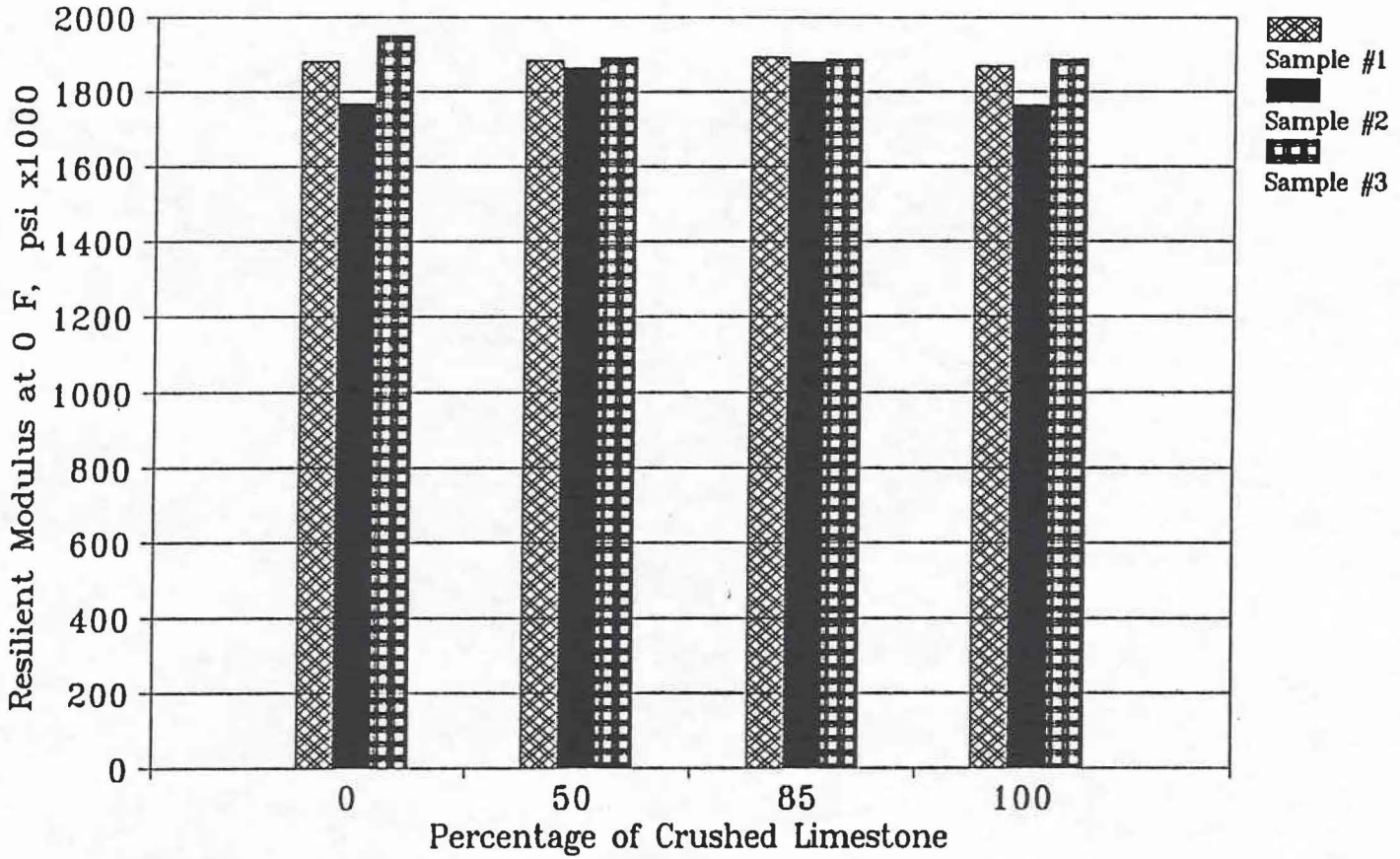

Figure A1. Resilient Modulus at 0°F (-18°C) vs. Percent Crushed Coarse Limestone.

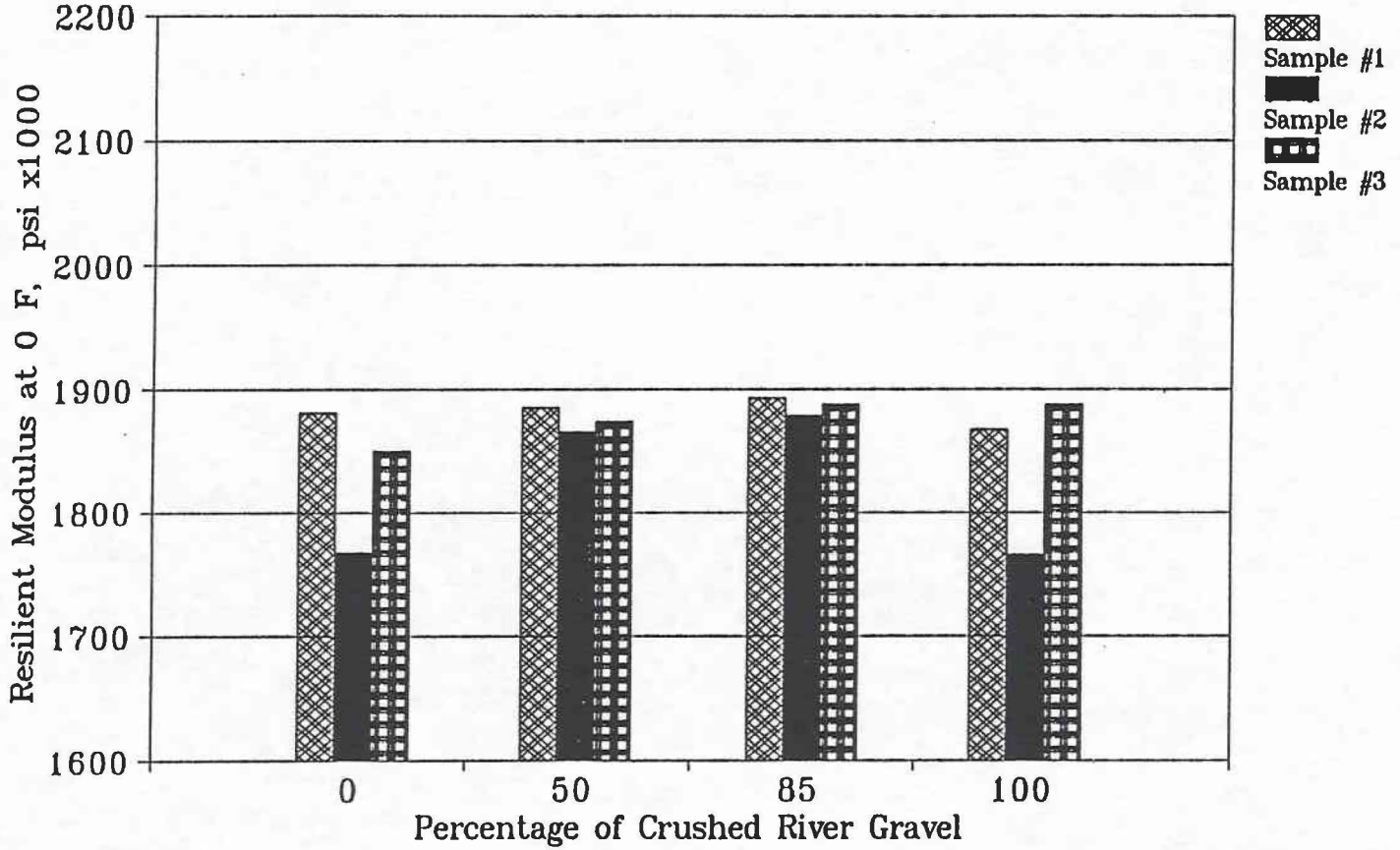

Figure A2. Resilient Modulus at 0°F (-18°C) vs. Percent Crushed Coarse River Gravel.

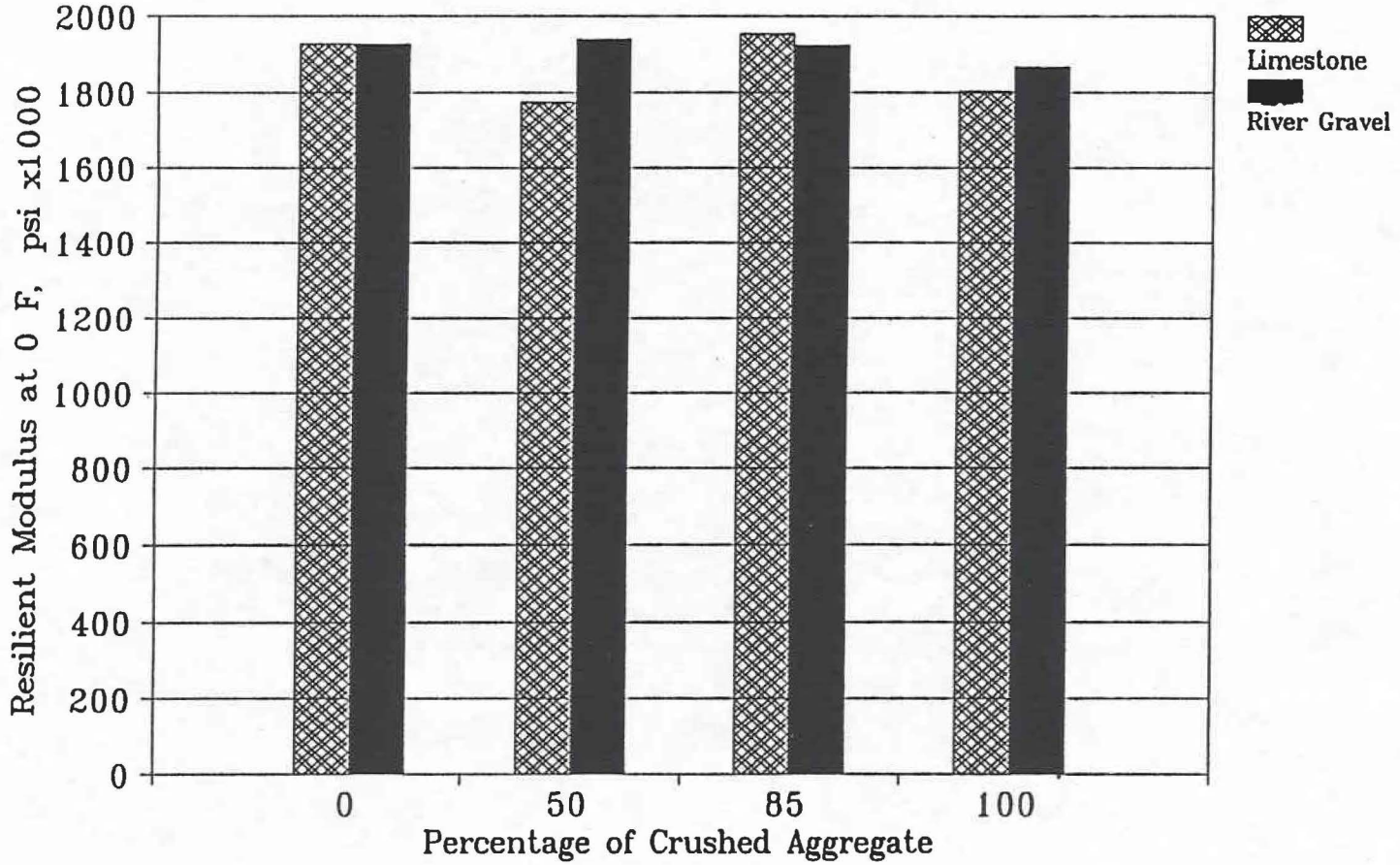

Figure A3. Resilient Moduli vs. Percentage Crushed Aggregate at 0°F (-18°C).

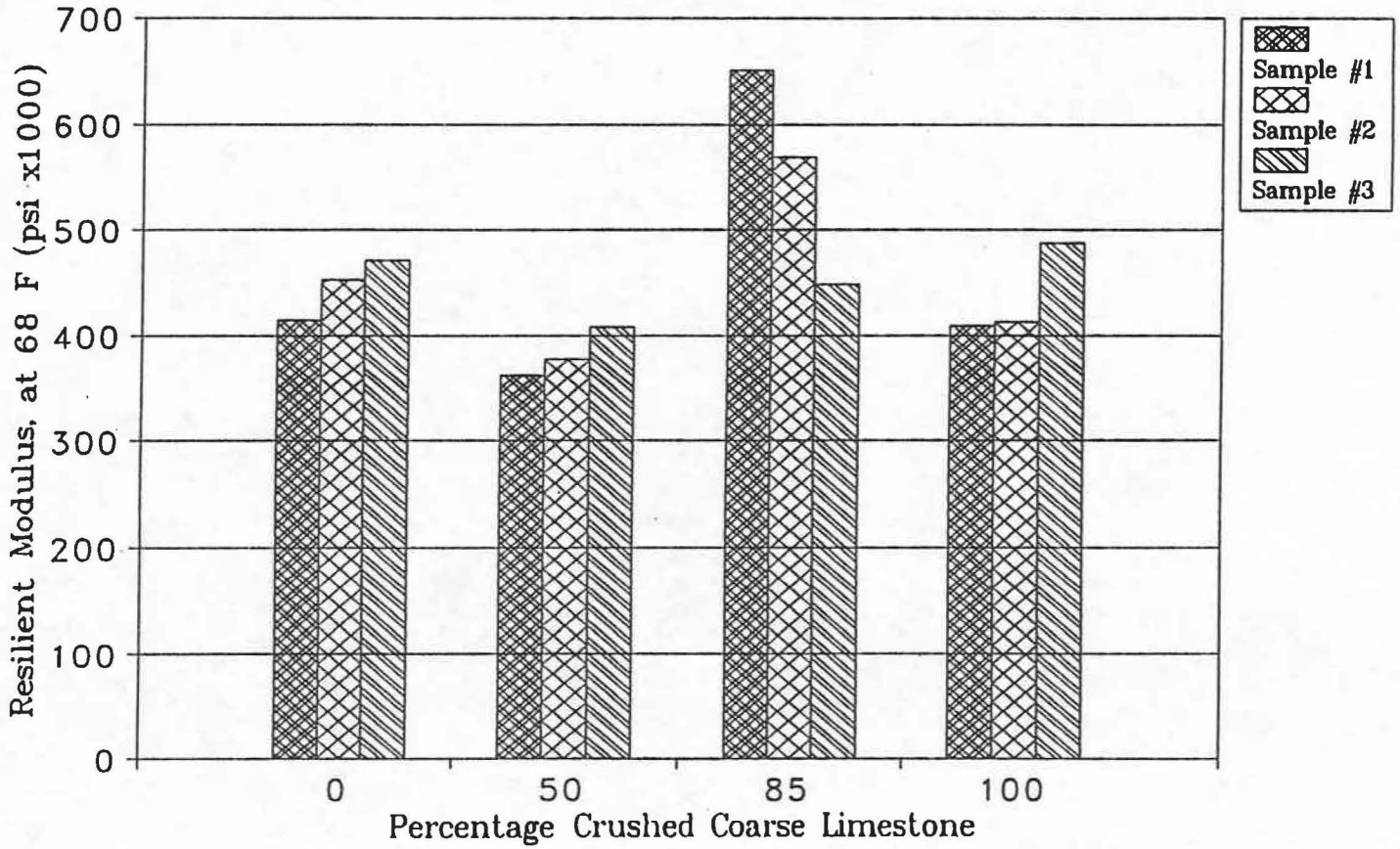

Figure A4. Resilient Modulus at 68°F (20°C) vs. Percentage Crushed Limestone.

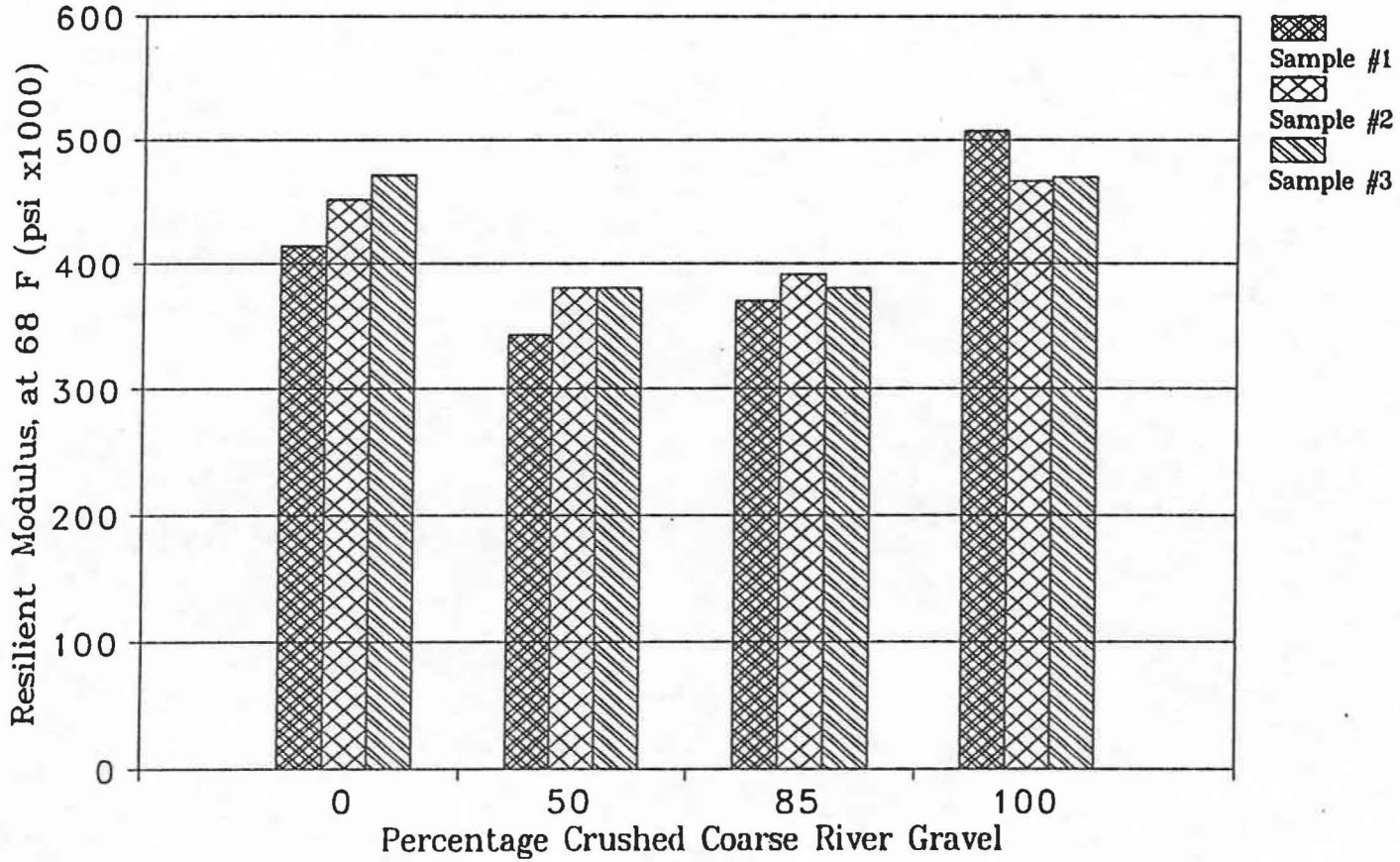

Figure A5. Resilient Modulus at 68°F (20°C) vs. Percentage Crushed River Gravel.

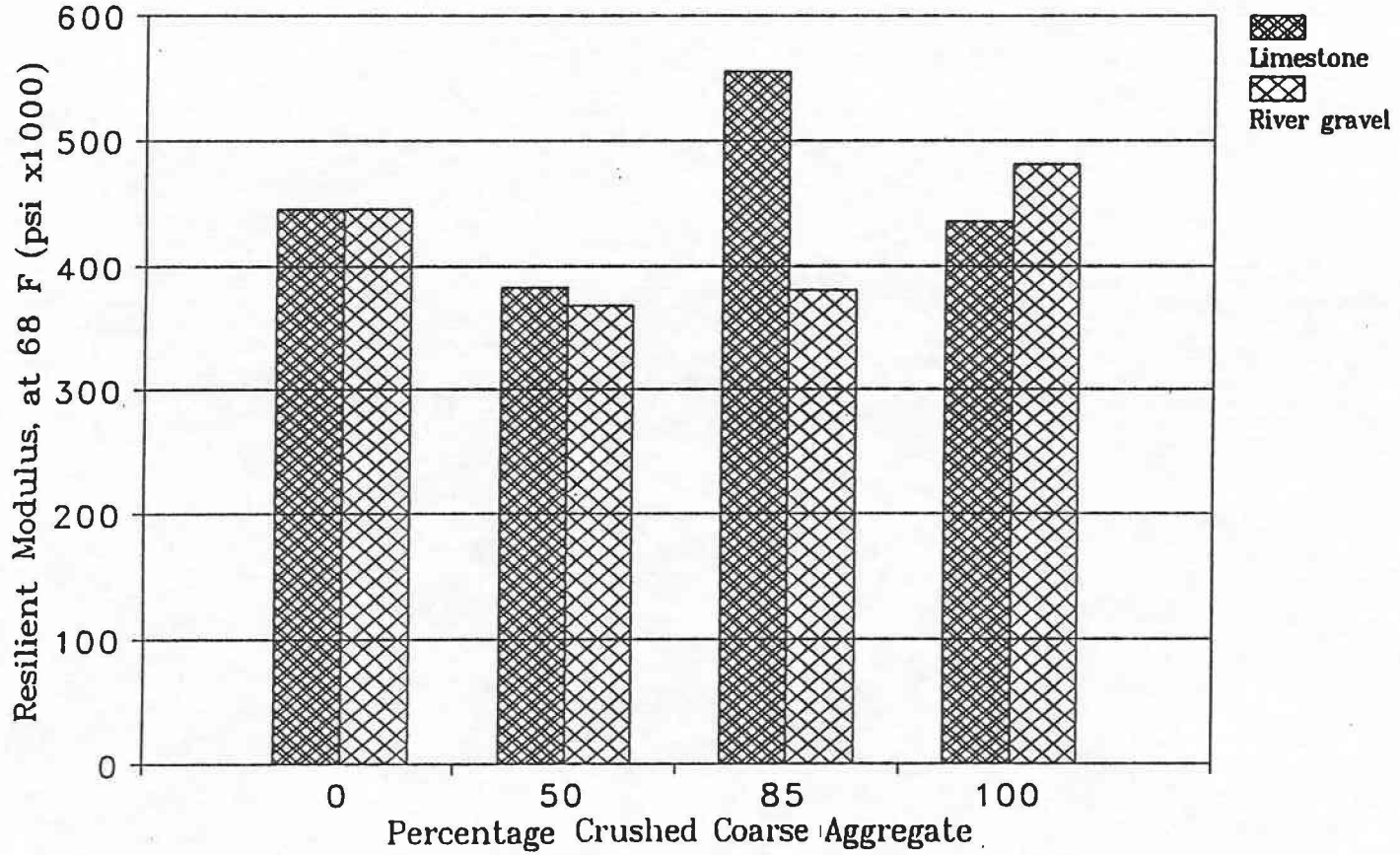

Figure A6. Resilient Moduli at 68°F (20°C) vs. Percentage Crushed Aggregate.

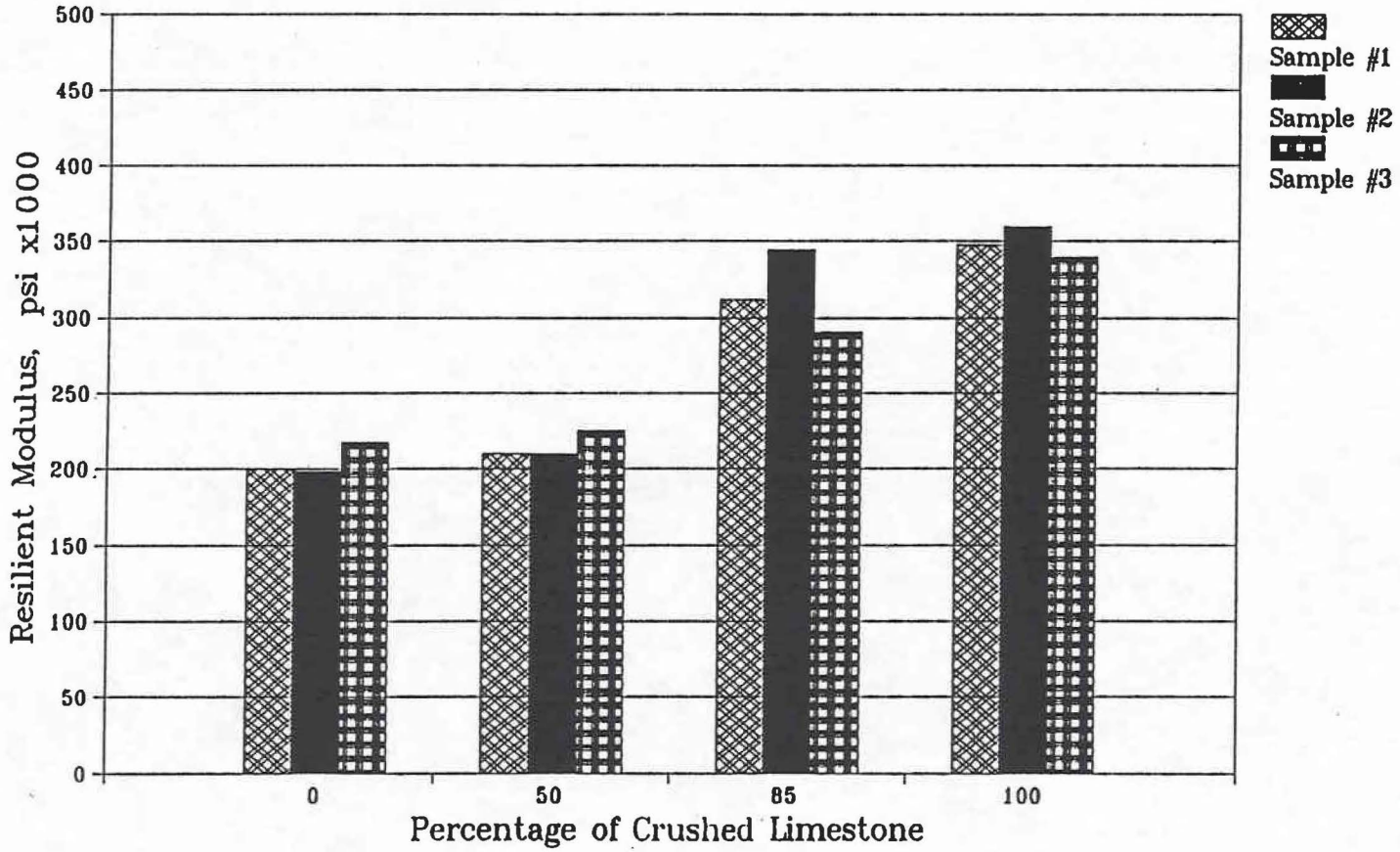

Figure A7. Resilient Modulus at 77°F (25°C) vs. Percentage Crushed Coarse Limestone.

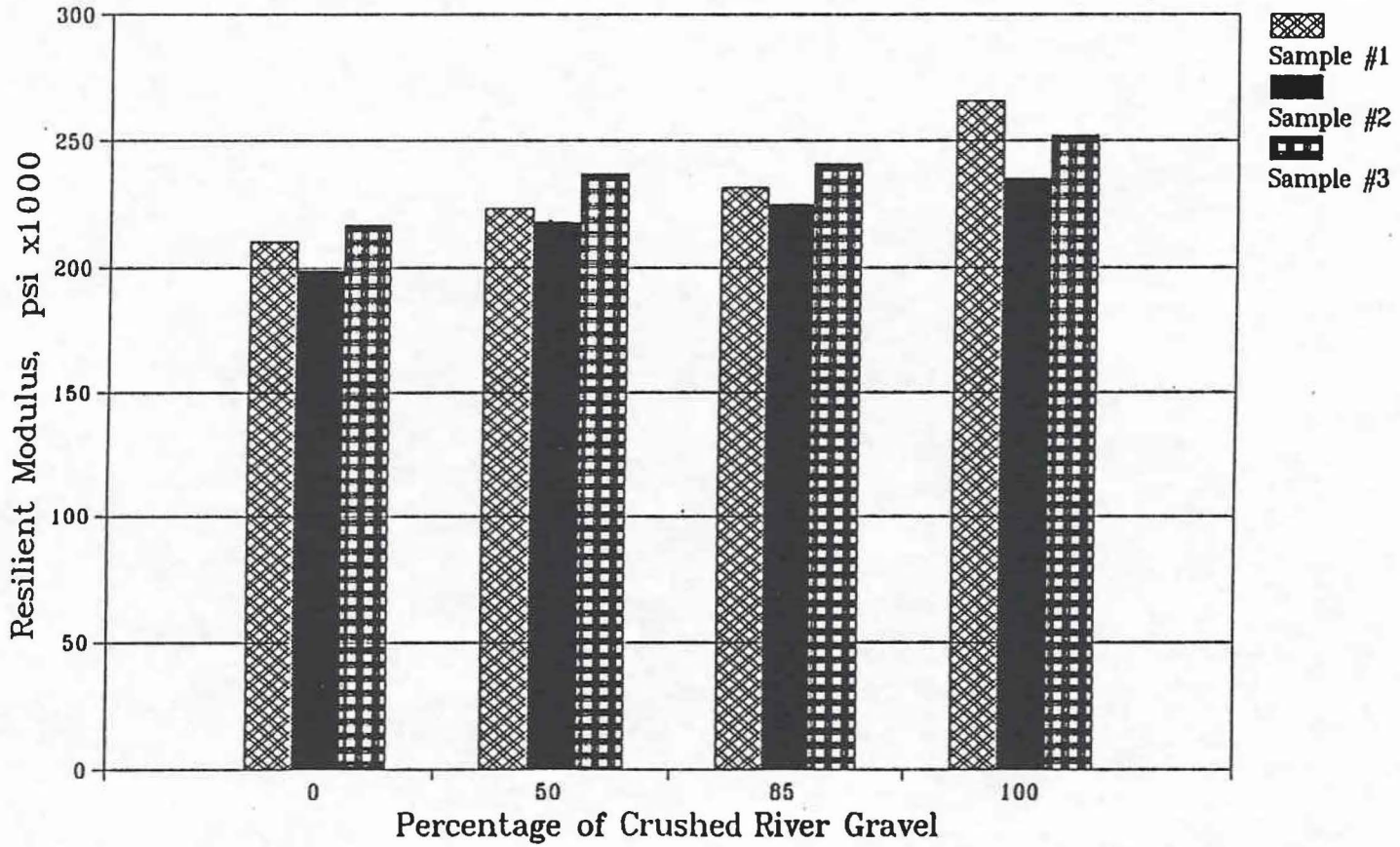

Figure A8. Resilient Modulus at 77°F (25°C) vs. Percent Crushed River Gravel.

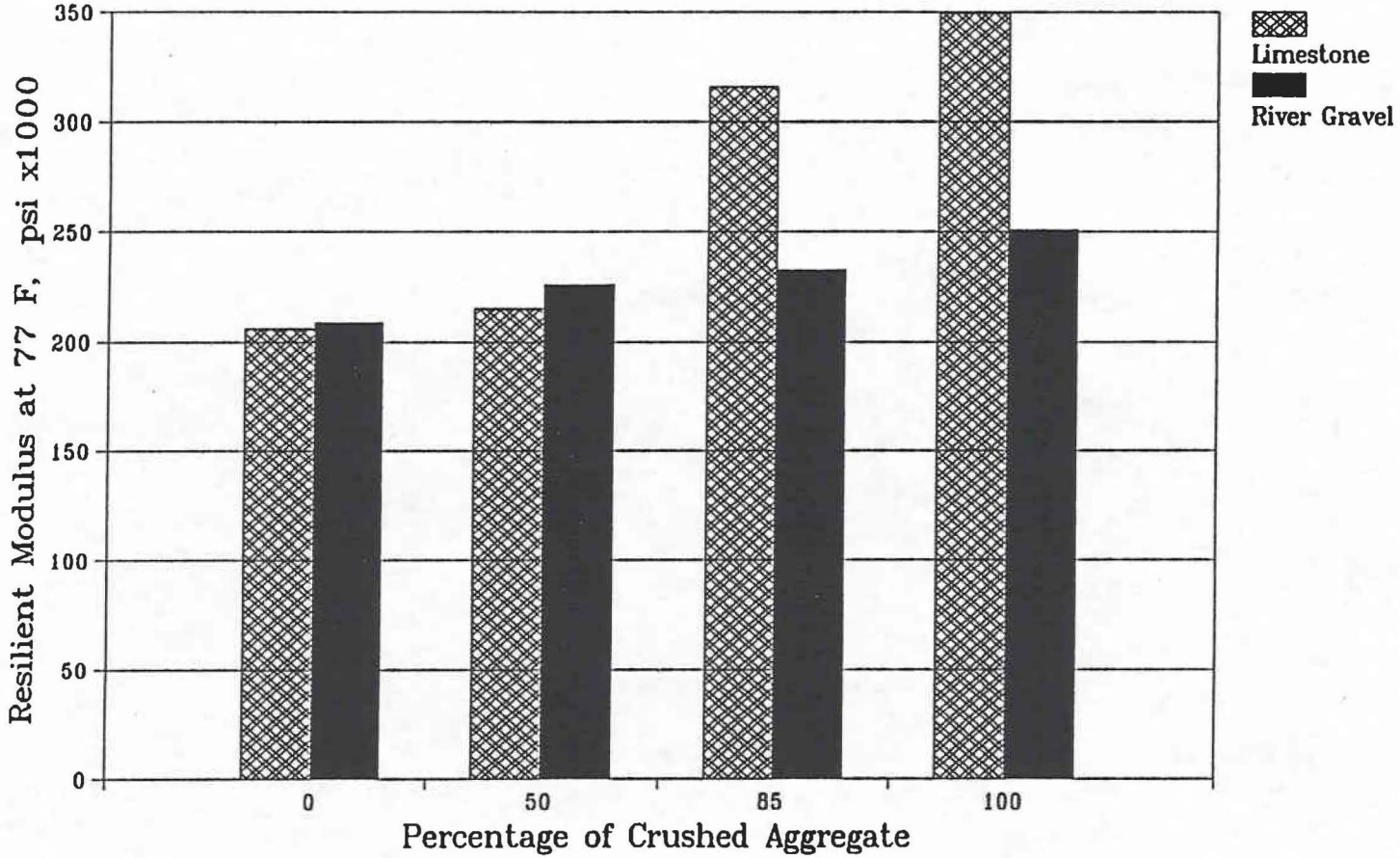

Figure A9. Resilient Moduli vs. Percentage Crushed Aggregate at 77°F (25°C).

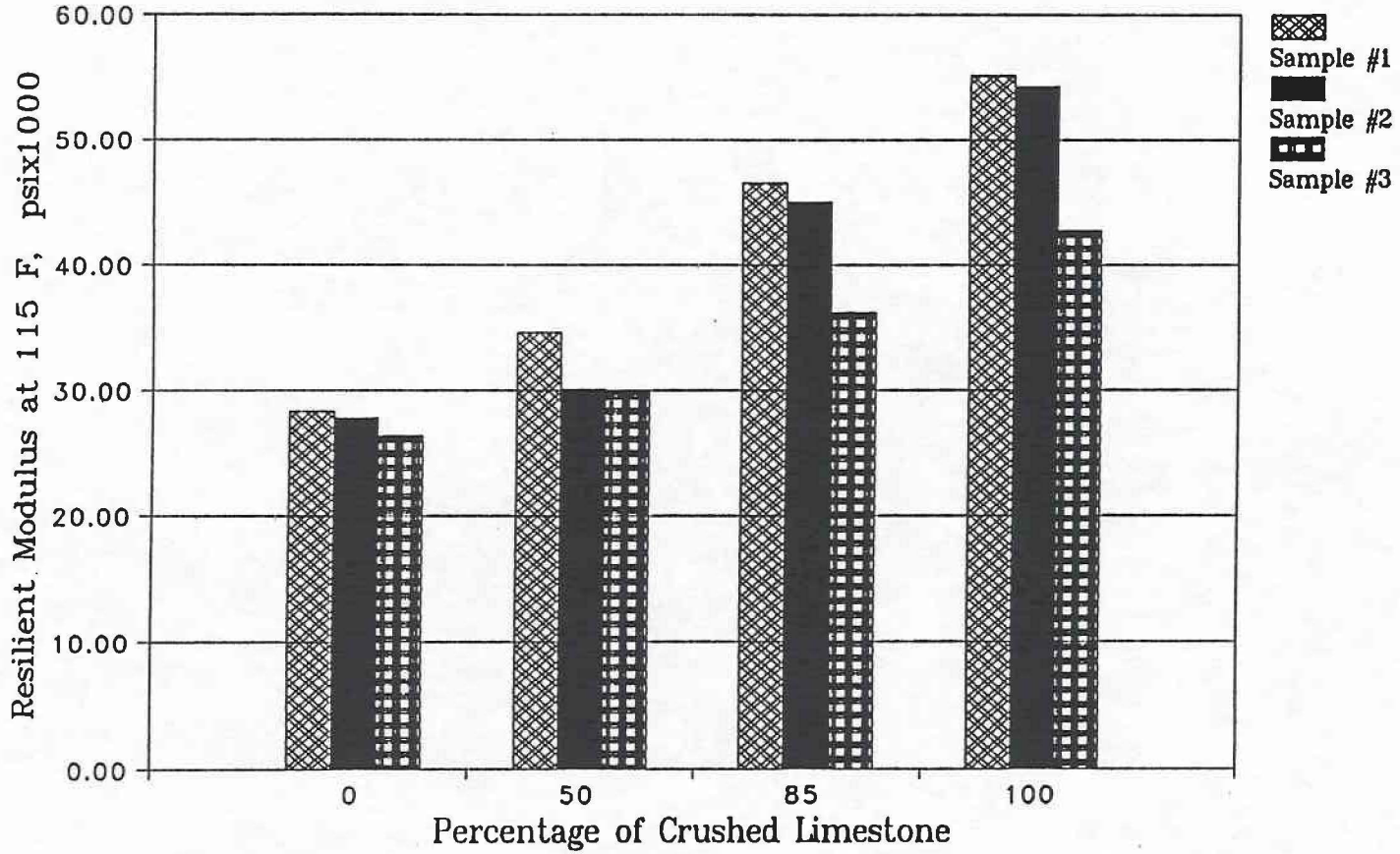

Figure A10. Resilient Modulus at 115°F (46°C) vs. Percentage Crushed Coarse Aggregate.

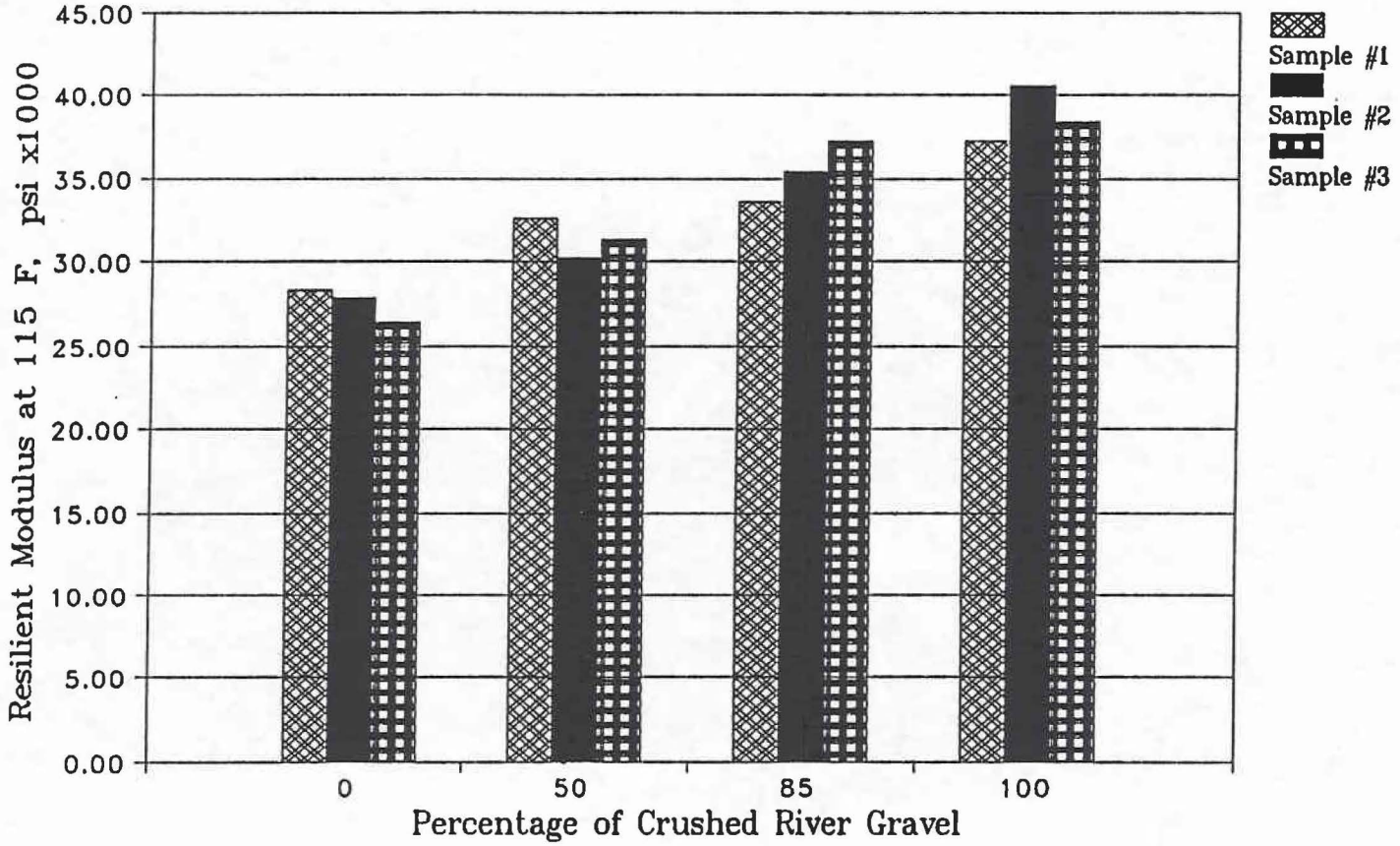

Figure A11. Resilient Modulus at 115°F (46°C) vs. Percent Crushed Coarse River Gravel.

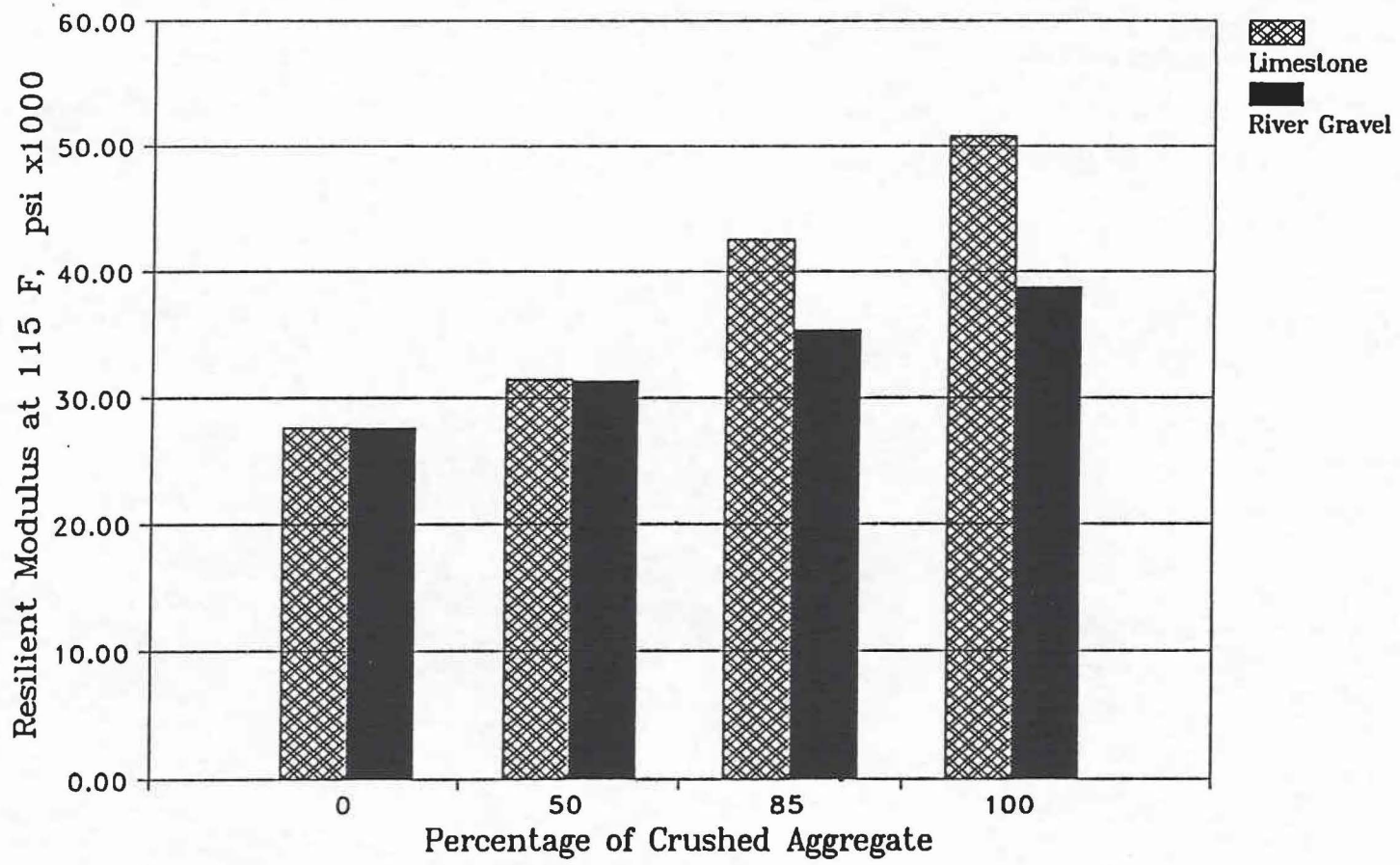

Figure A12. Resilient Moduli vs. Percentage Crushed Aggregate at 115°F (46°C).

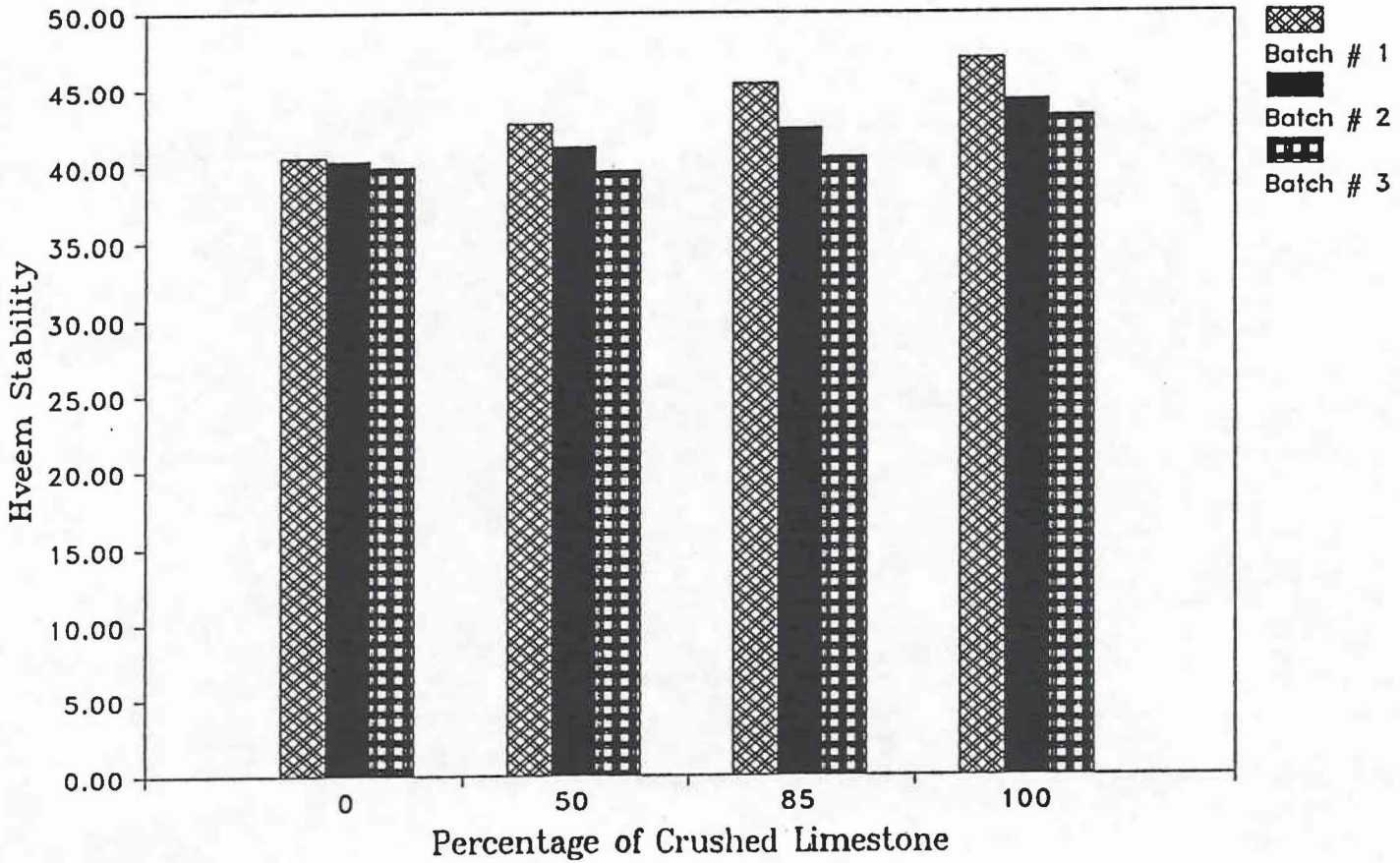

Figure A13. Hveem Stability vs. Percent Crushed Coarse Limestone.

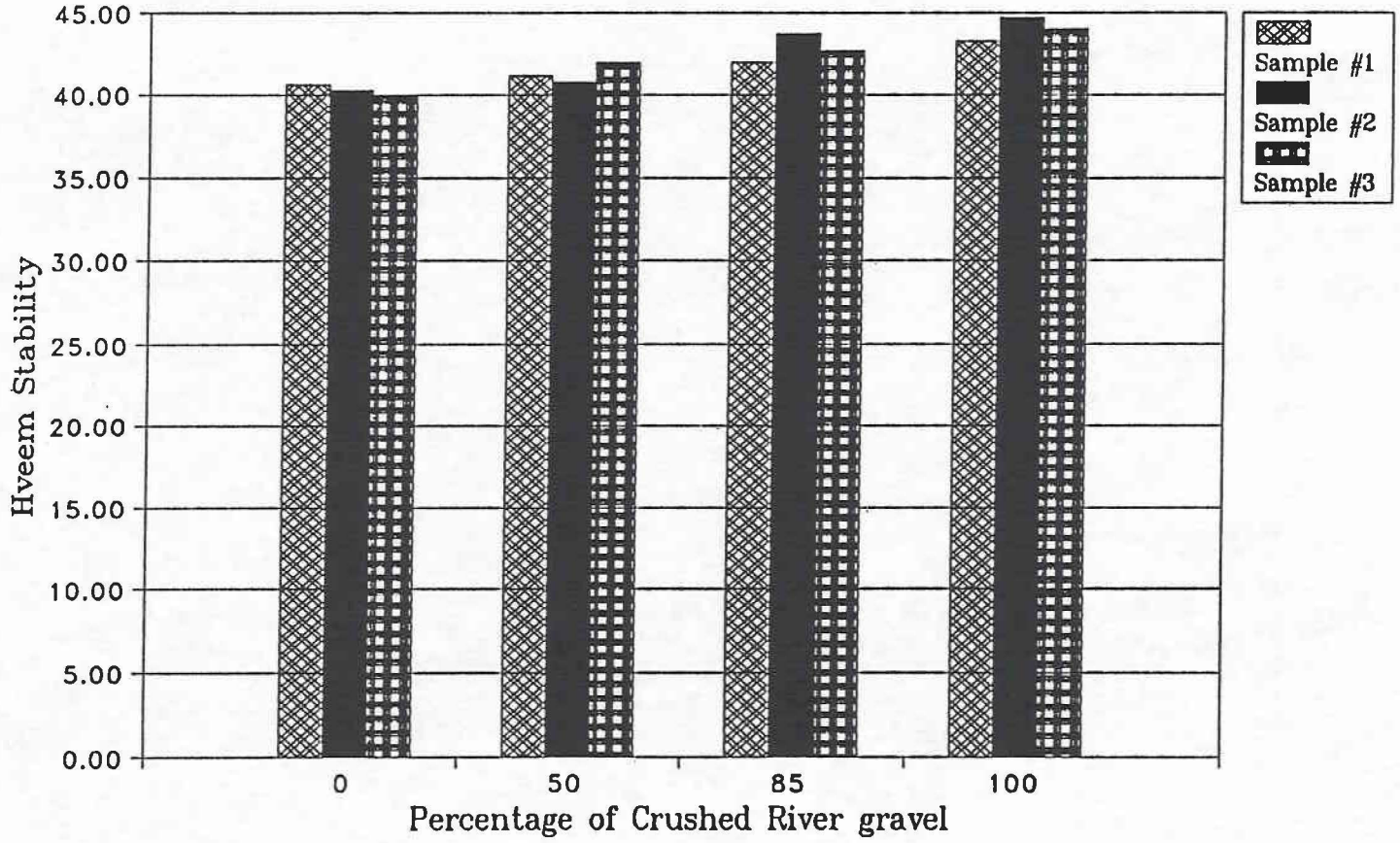

Figure A14. Hveem Stability vs. Percent Crushed Coarse River Gravel.

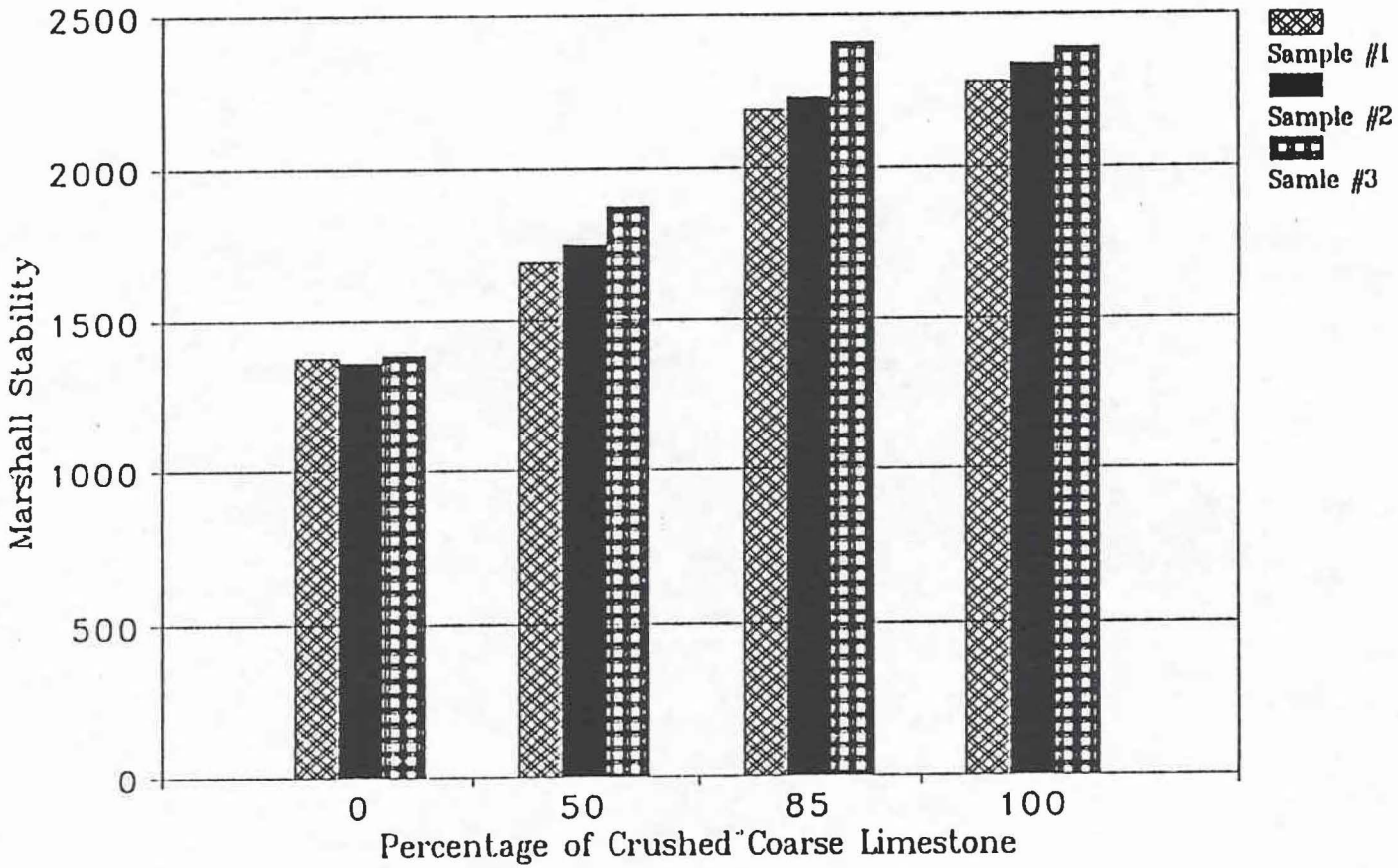

Figure A15. Marshall Stability vs. Percentage Crushed Limestone.

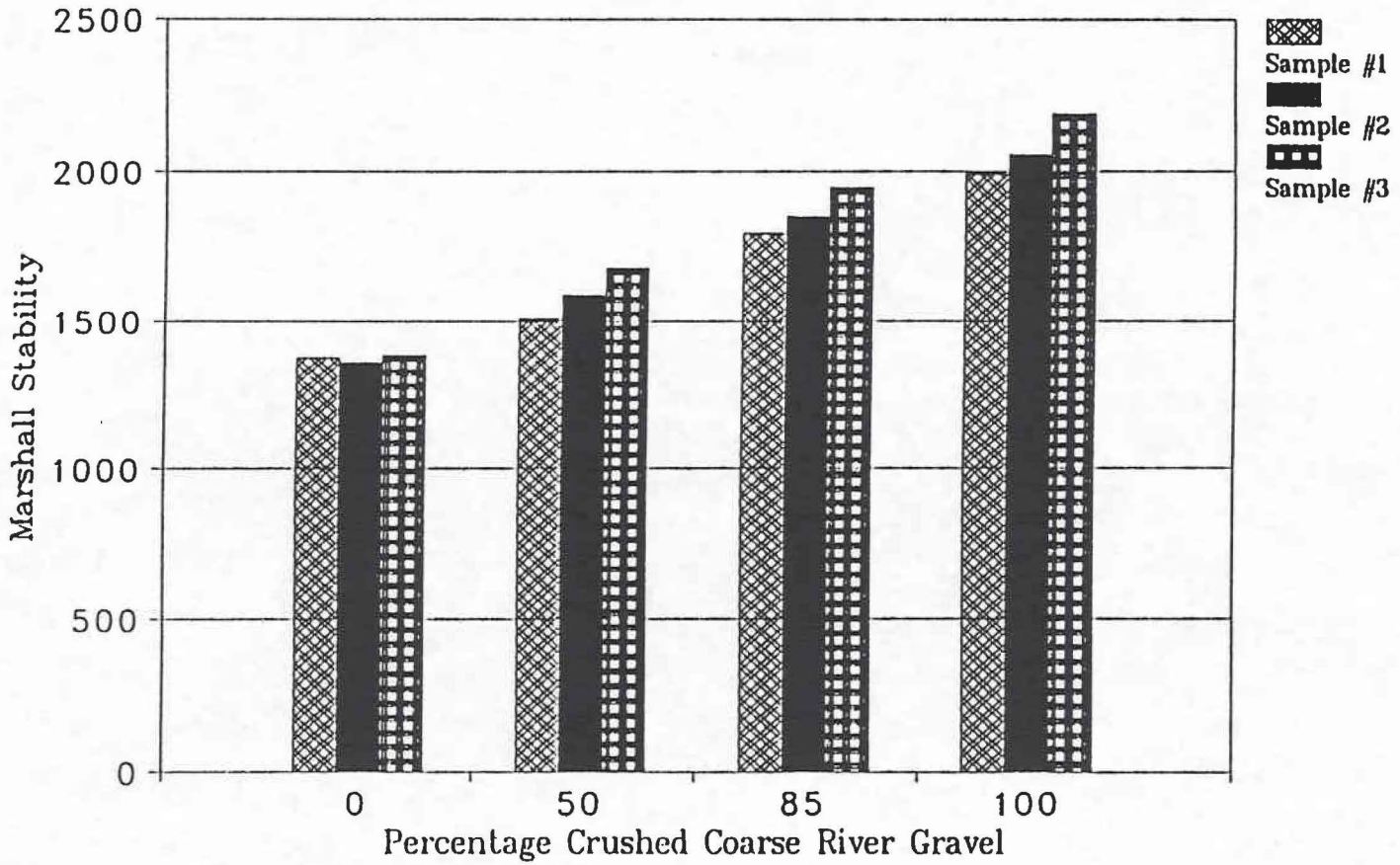

Figure A16. Marshall Stability vs. Percentage Crushed River Gravel.

APPENDIX B

DATA FROM STATIC CREEP TESTS

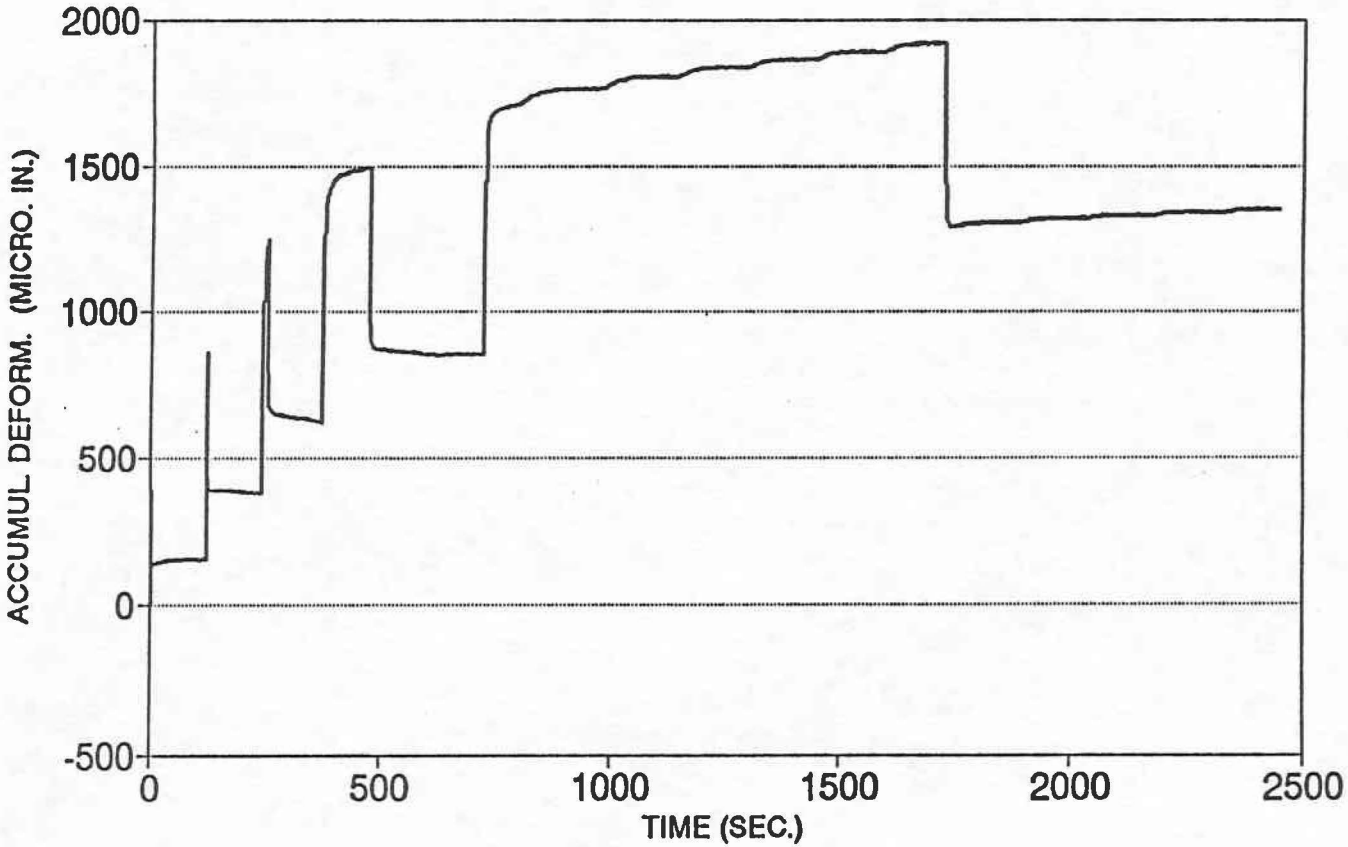

Figure B1. Static Creep Test Data for a Sample with 100 Percent Crushed Coarse Limestone.

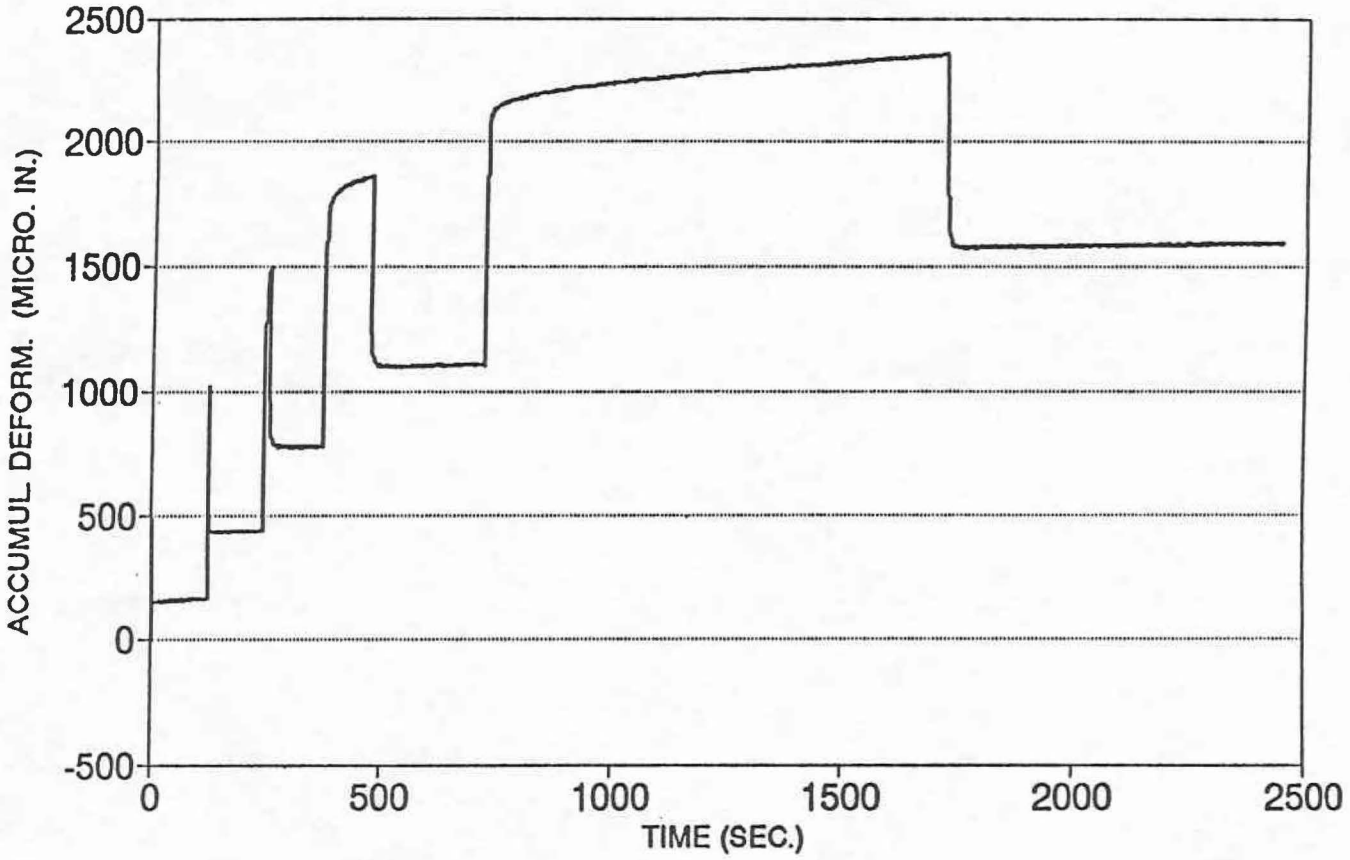

Figure B2. Static Creep Test Data for a Sample with 85 Percent Crushed Coarse Limestone.

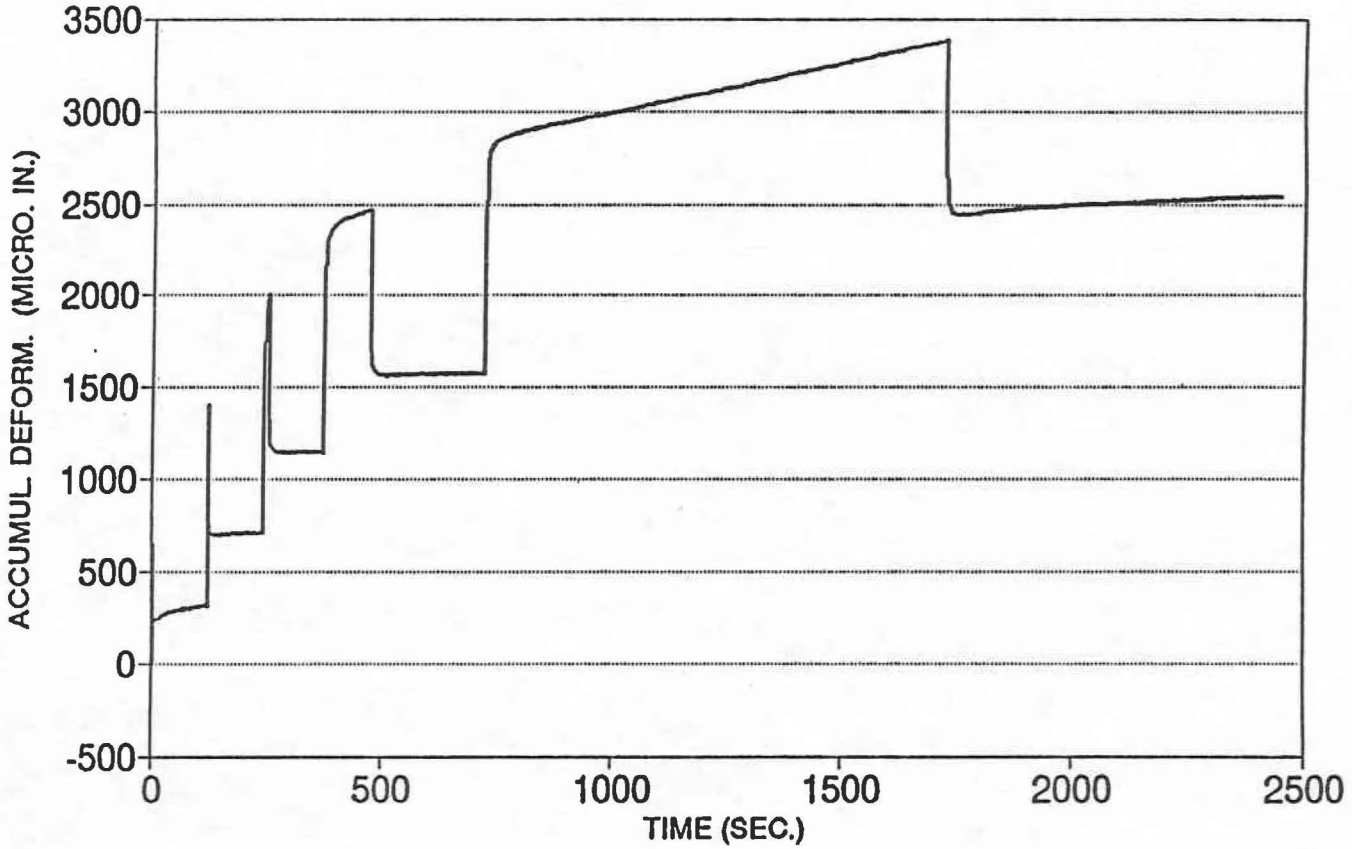

Figure B3. Static Creep Test Data for a Sample with 50 Percent Crushed Coarse Limestone.

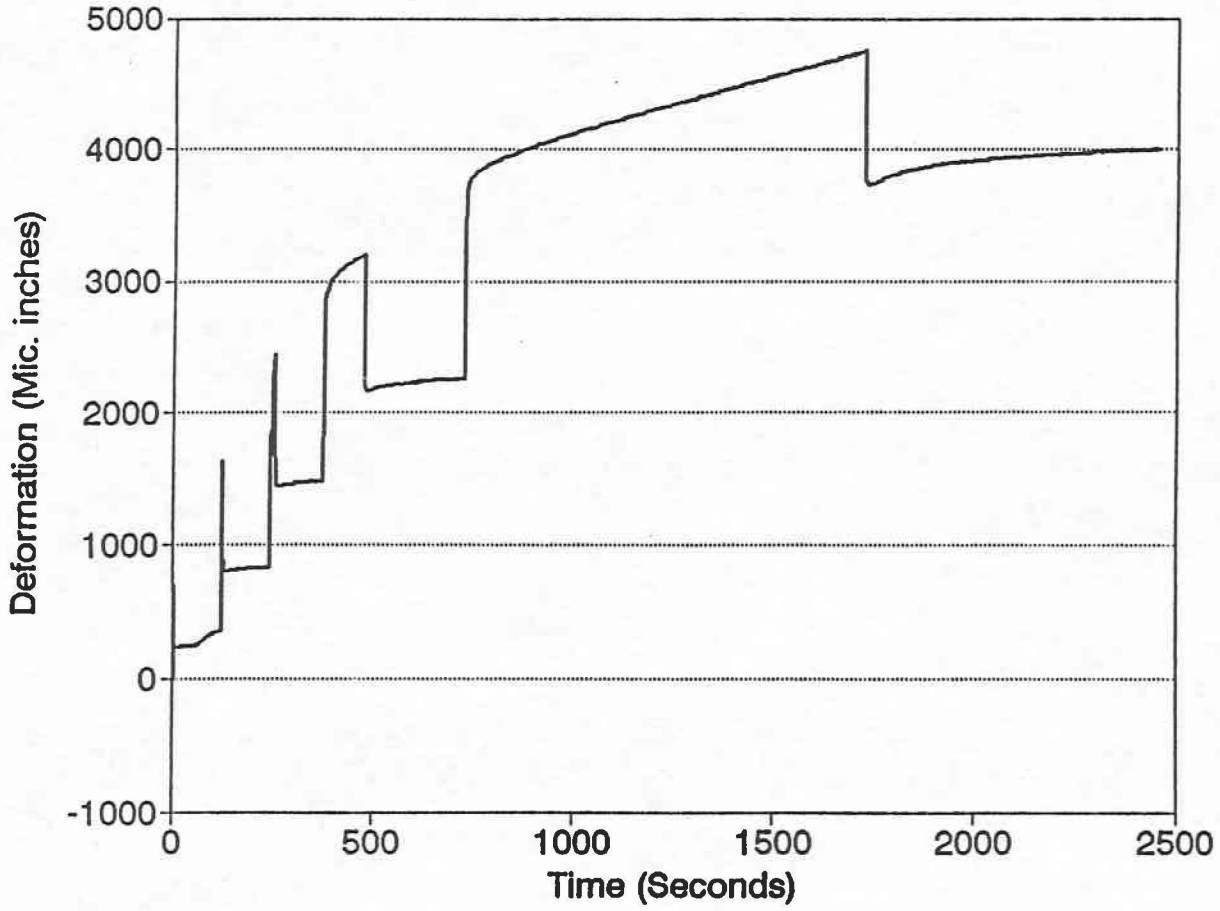

Figure B4. Static Creep Test Data for a Sample with 0 Percent Crushed Coarse Aggregate.

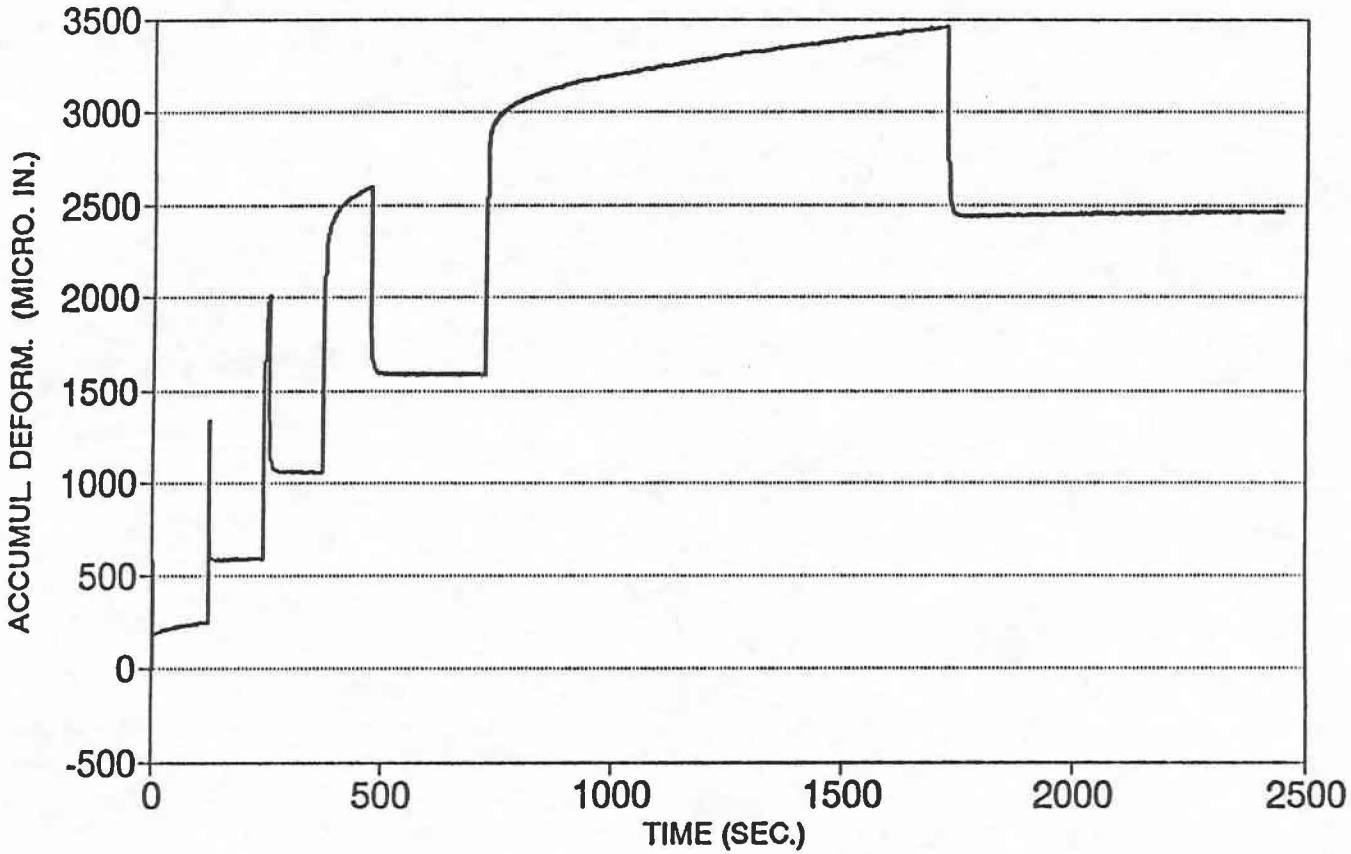

Figure B5. Static Creep Test Data for a Sample with 50 Percent Crushed River Gravel.

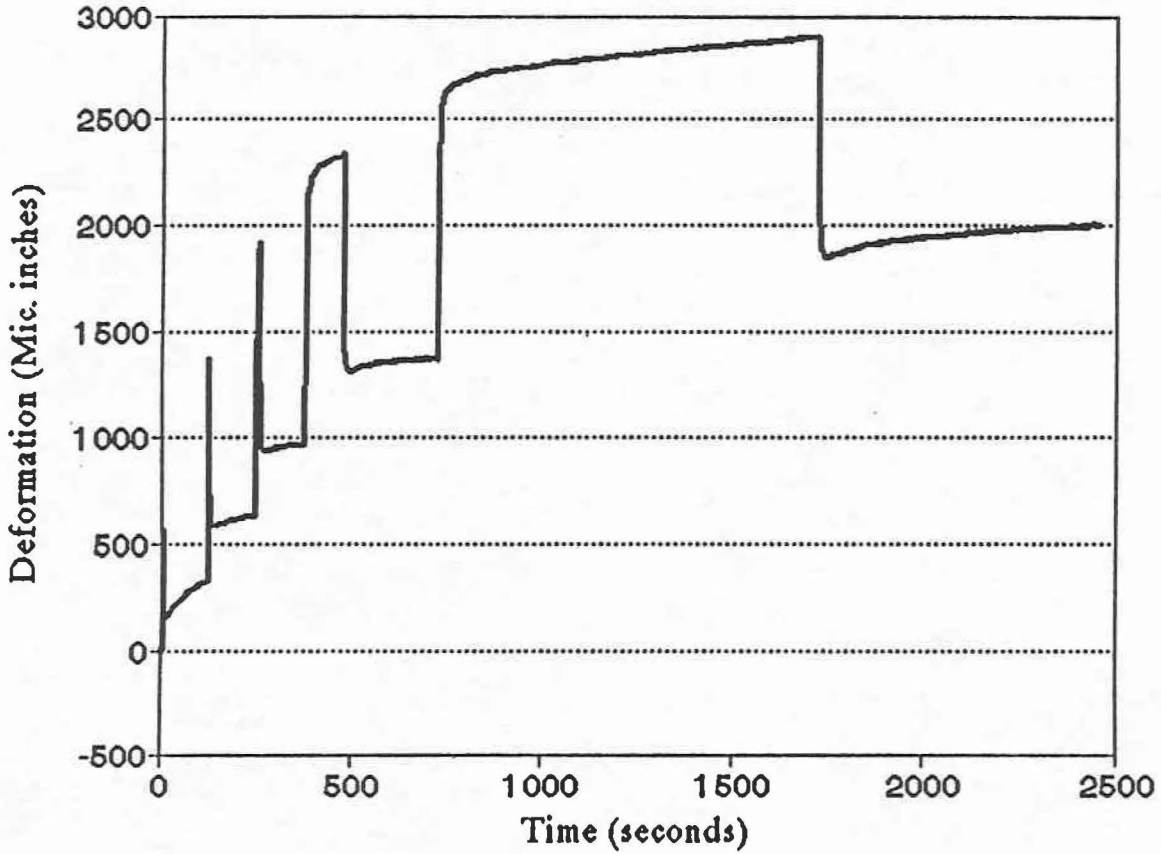

Figure B6. Static Creep Test Data for a Sample with 85 Percent Crushed Coarse River Gravel.

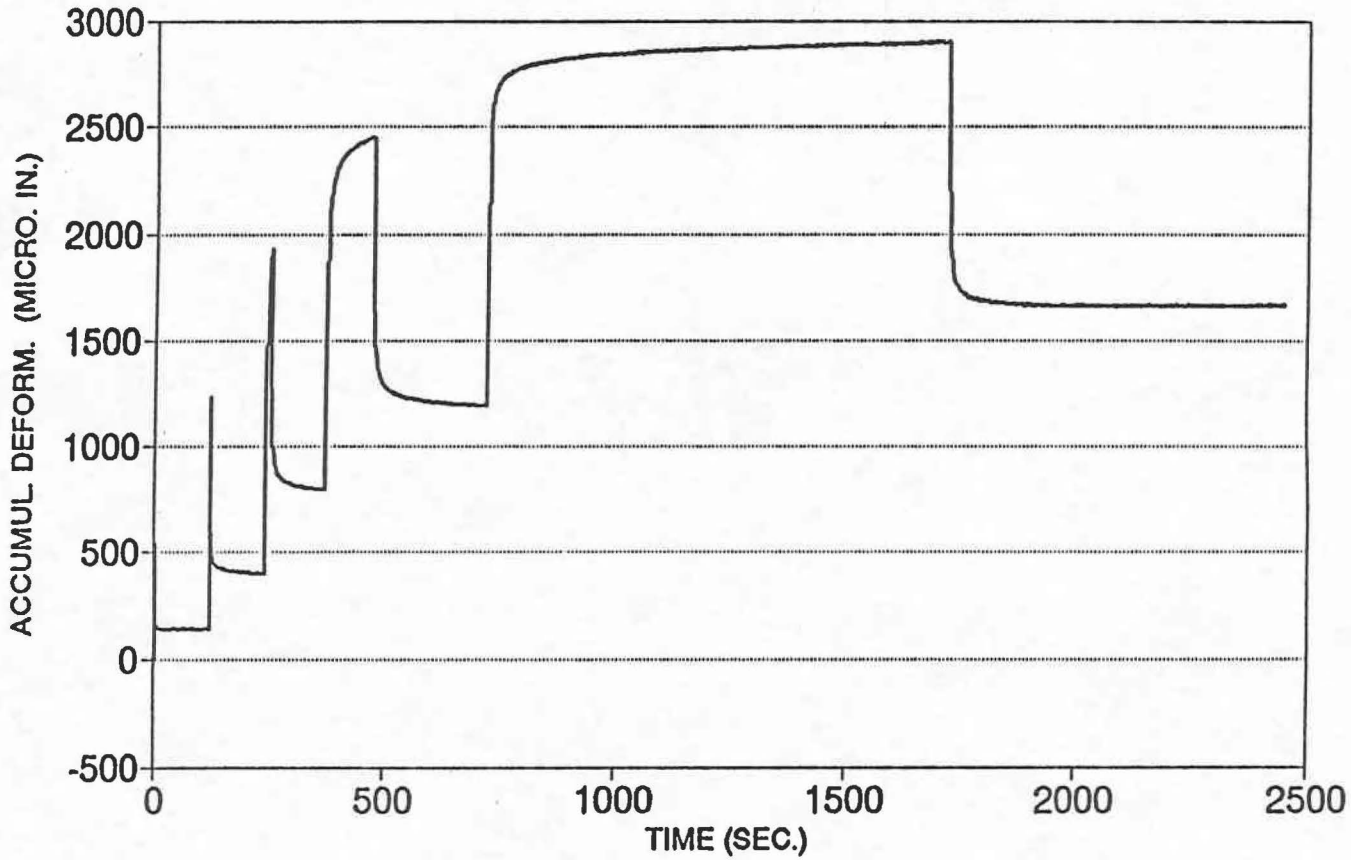

Figure B7. Static Creep Test Data for a Sample with 100 Percent Crushed Coarse River Gravel.

APPENDIX C

IMAGES FROM FRACTAL DIMENSIONAL ANALYSIS

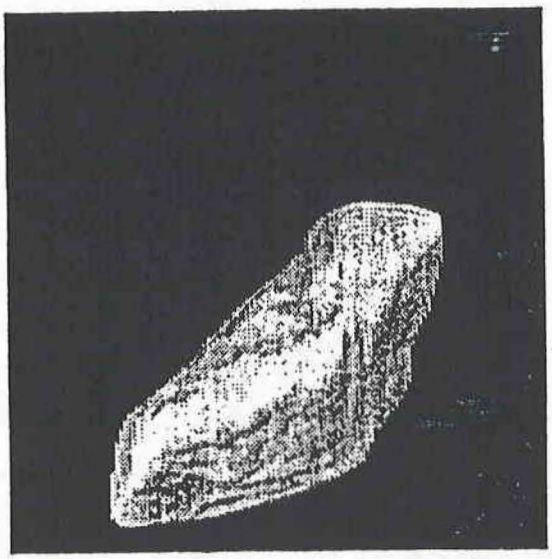

Figure C1a. Original Image of Limestone Aggregate Particle.

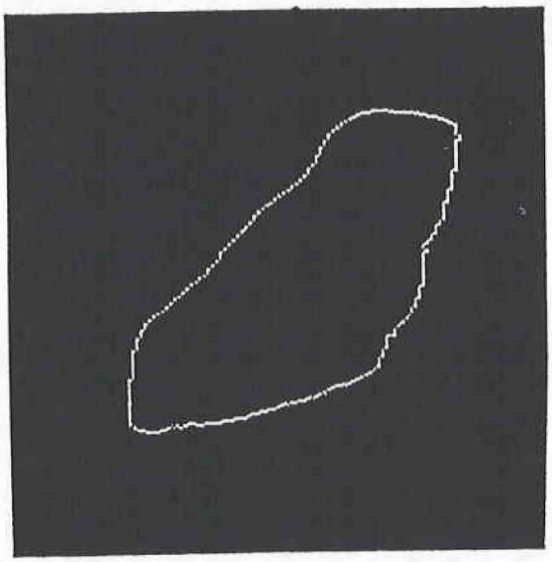

Figure C1b. Extracted Image of Limestone Aggregate Particle.

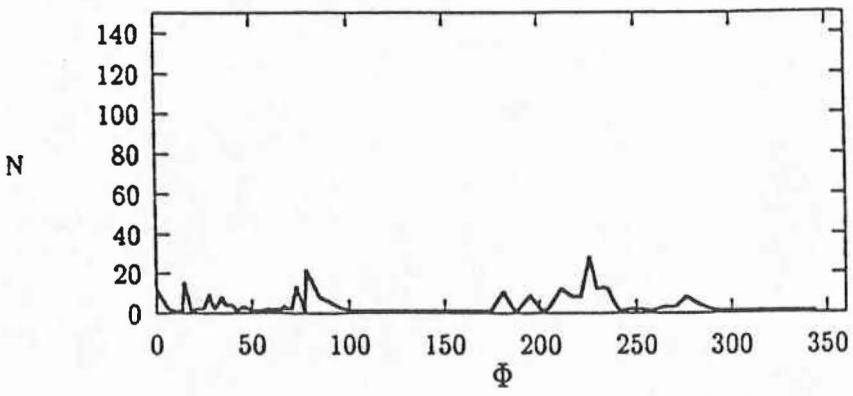

Figure C2a. SDF Plot of Crushed Limestone Particle.

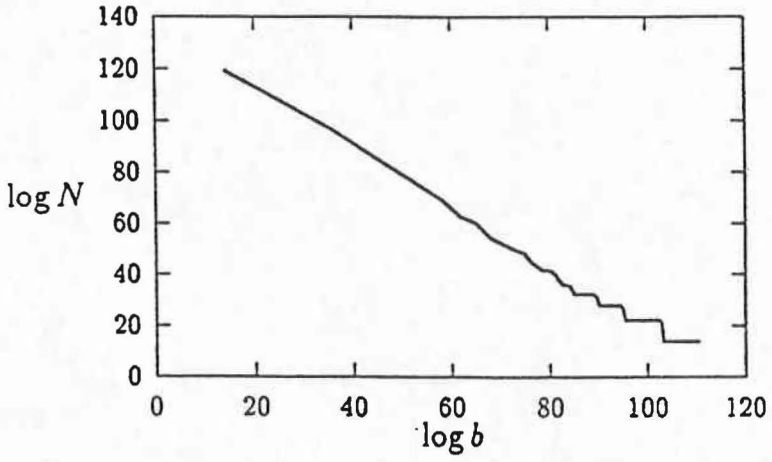

Figure C2b. Box Count Plot of Crushed Limestone Particle.

Figure C3a. Original Image of a River Gravel Aggregate Particle.

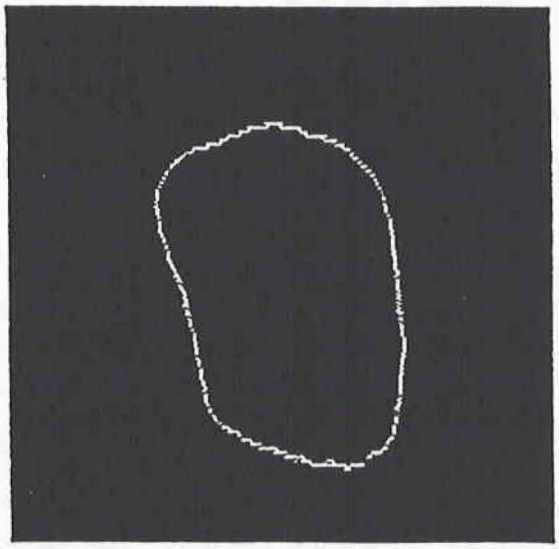

Figure C3b. Extracted Edge of River Gravel Aggregate Particle.

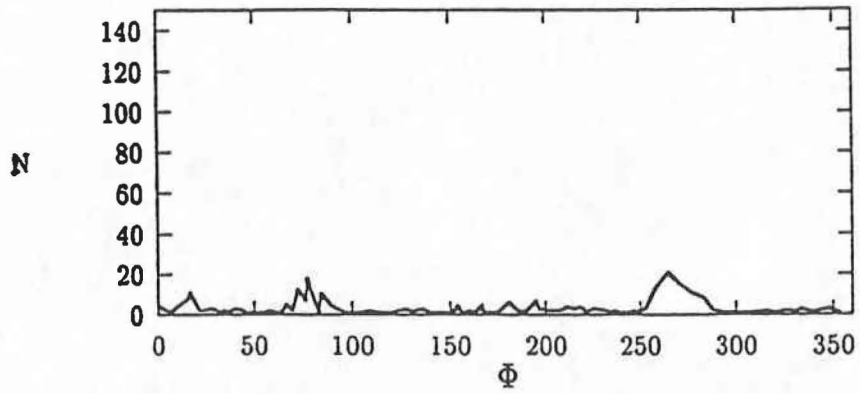

Figure C4a. SDF Plot of River Gravel Aggregate Particle.

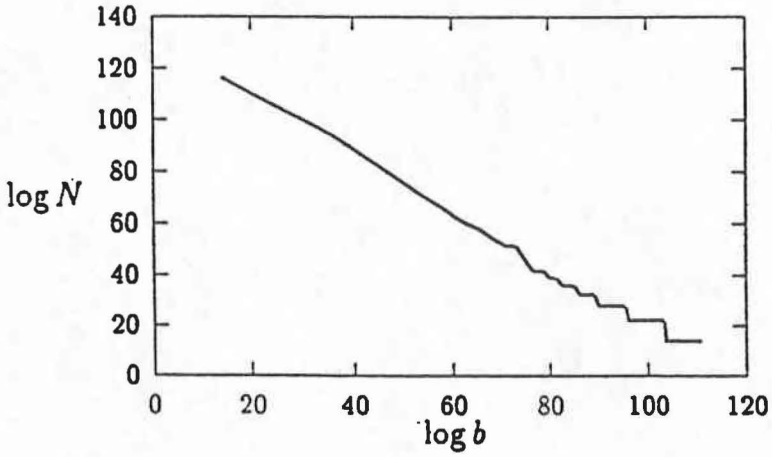

Figure C4b. Box Count Plot of River Gravel Particle.

Figure C5a. Image of 100 Percent Crushed Limestone Blend.

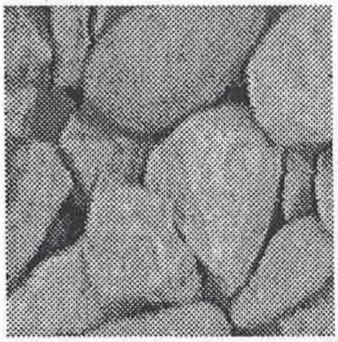

Figure C5b. Image of 85 Percent Crushed Limestone Blend.

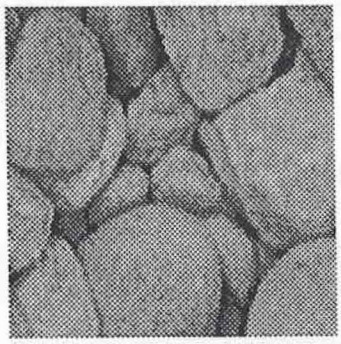

Figure C5c. Image of 50 Percent Crushed Limestone Blend.

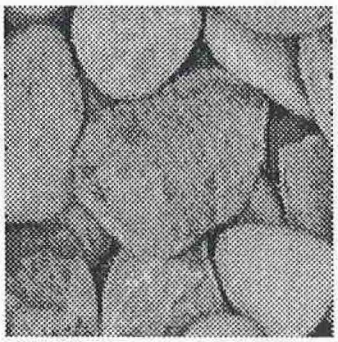

Figure C5d. Image of 100 Percent Uncrushed River Gravel Blend.

Figure C5e. Image of 50 Percent Crushed River Gravel Blend.

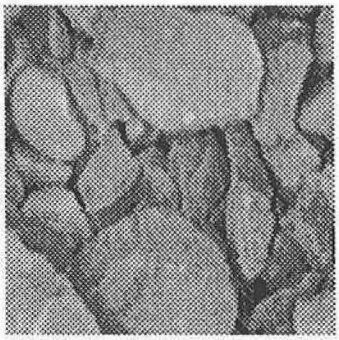

Figure C5f. Image of 85 Percent Crushed River Gravel Blend.

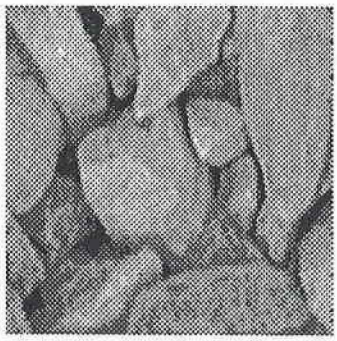

Figure C5g. Image of 100 Percent Crushed River Gravel Blend.

Figure C6. Image of White Painted Crushed Limestone Particle.

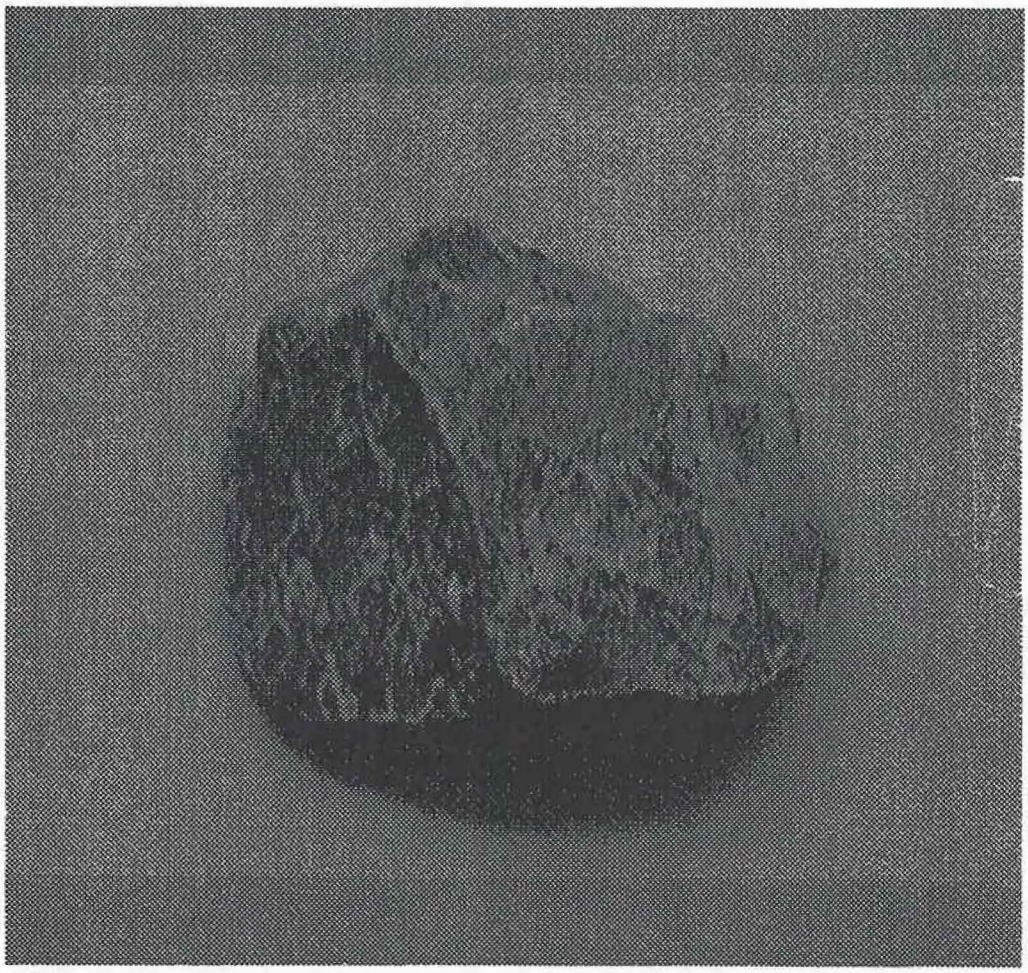

Figure C7. Image of Washed Limestone Particle.

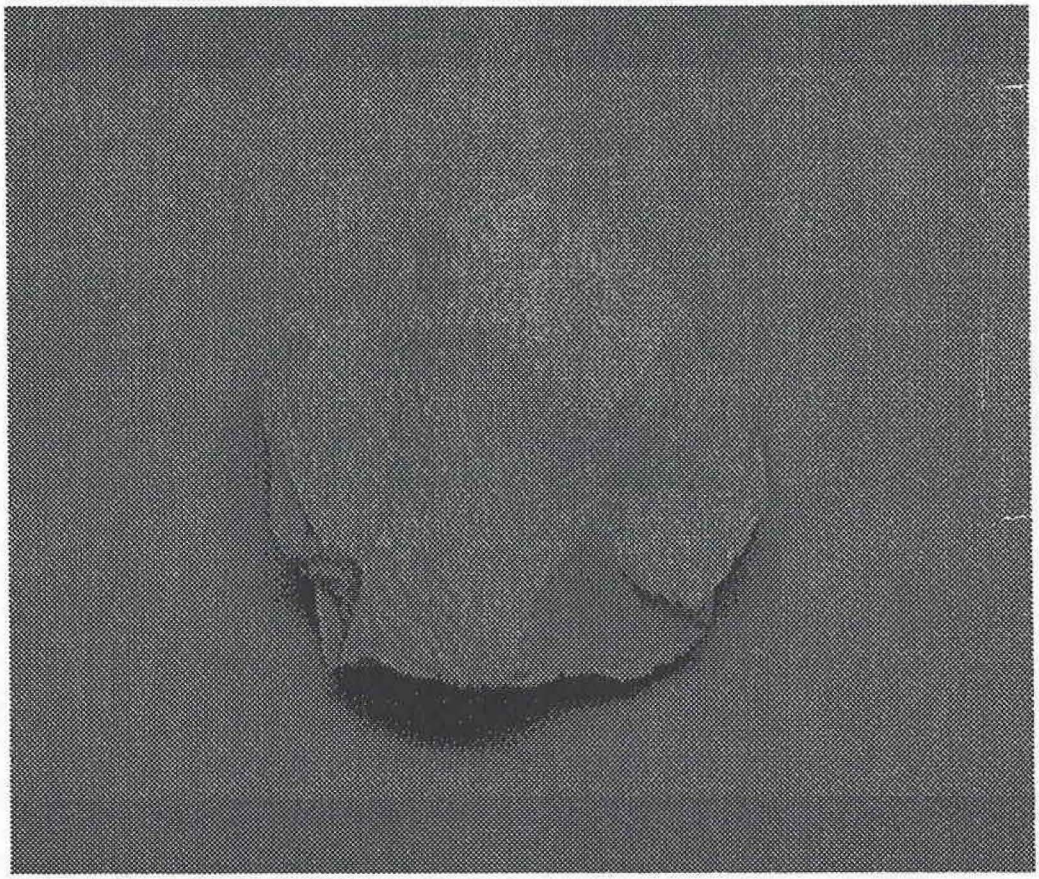

Figure C8. Image of White Painted Crushed River Gravel Particle.

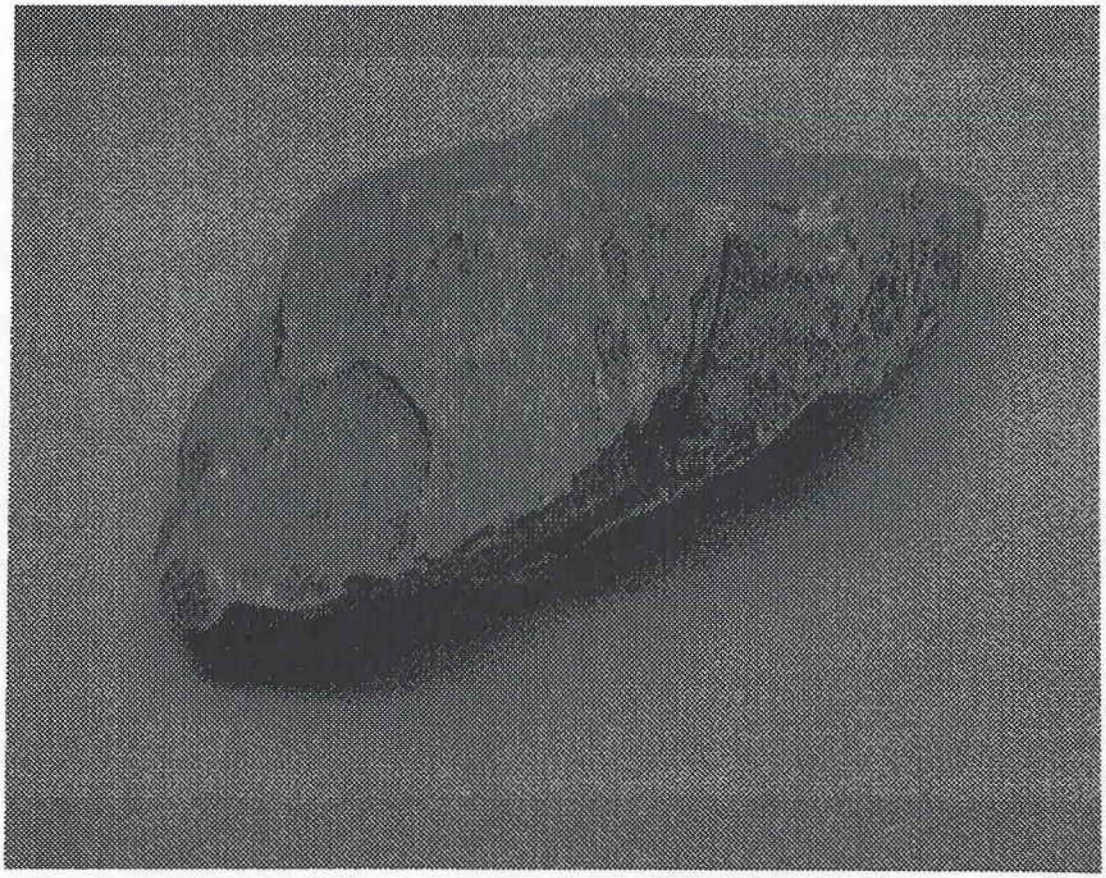

Figure C9. Image of Washed Crushed River Gravel Particle.

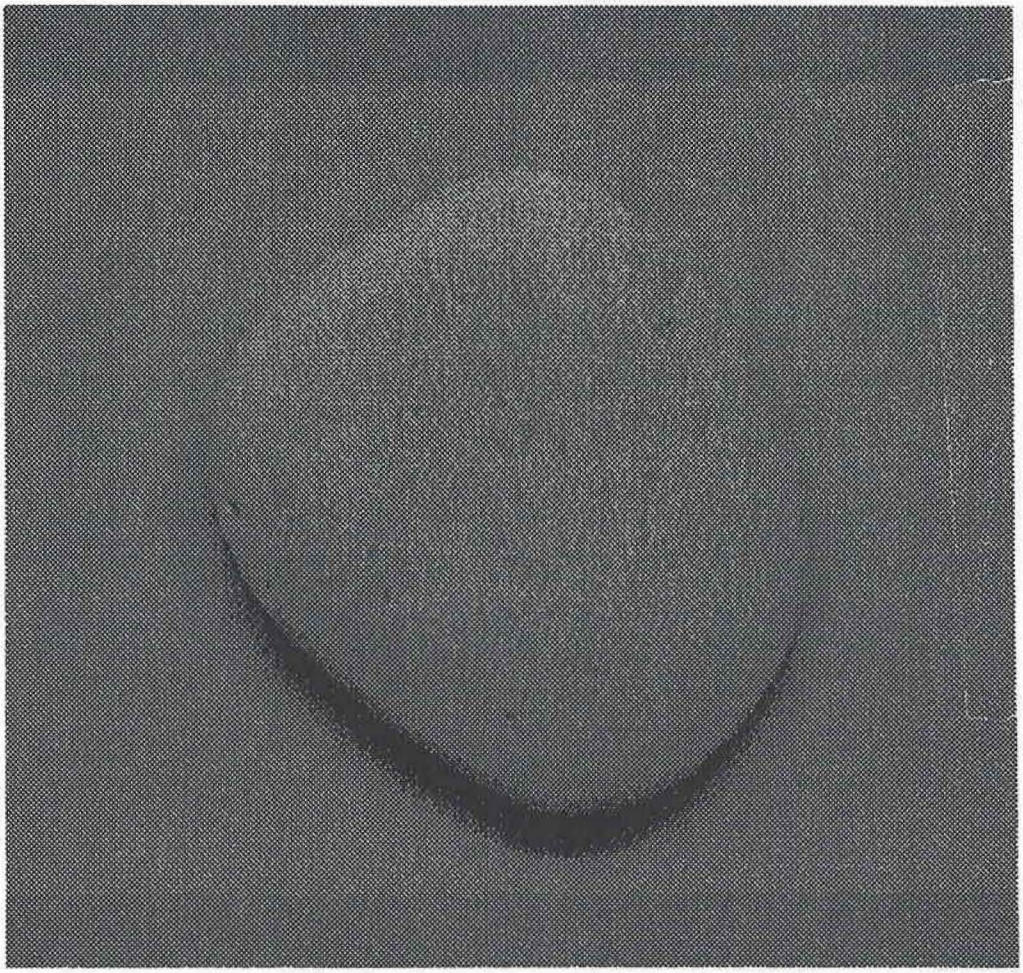

Figure C10. Image of White Painted Uncrushed River Gravel Particle.

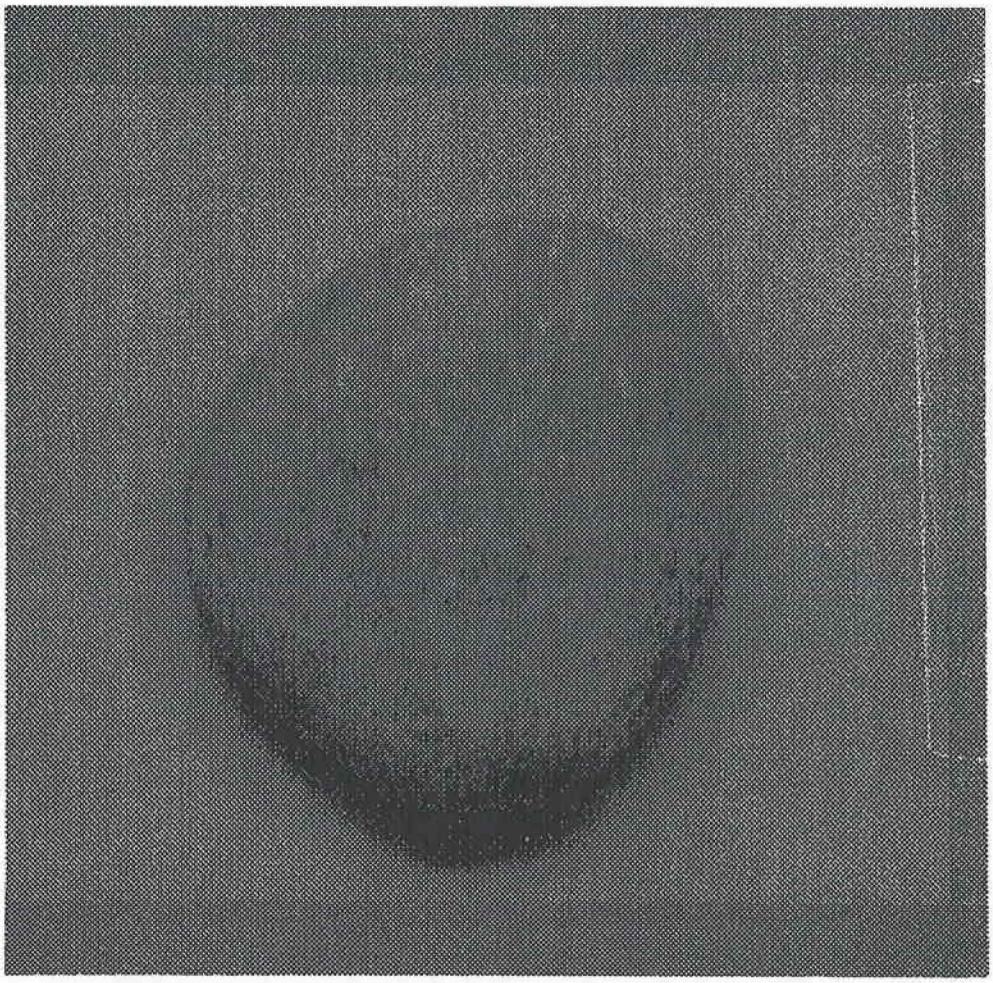

Figure C11. Image of Washed Uncrushed River Gravel Particle.

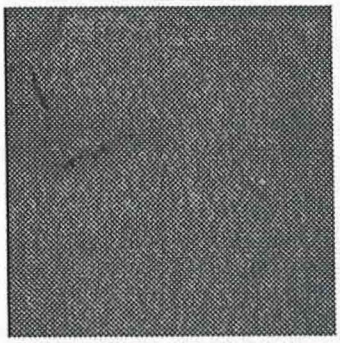

Figure C12a. 128x128 Pixel Image of Painted Crushed Limestone.

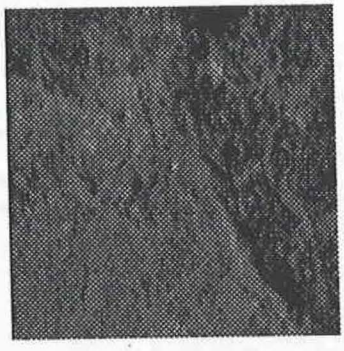

Figure C12b. 128x128 Pixel Image of Washed Limestone Particle.

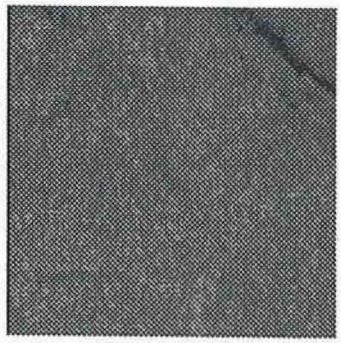

Figure C13a. 128x128 Pixel Image of White Painted, Crushed River Gravel.

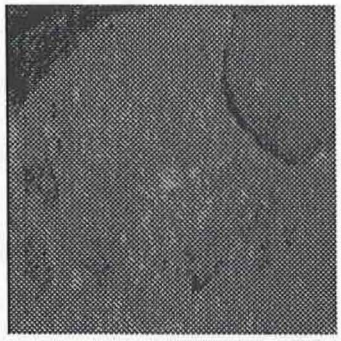

Figure C13b. 128x128 Pixel Image of Washed Crushed River Gravel Particle.

Figure C14a. 128x128 Pixel Image of White Painted Uncrushed River Gravel.

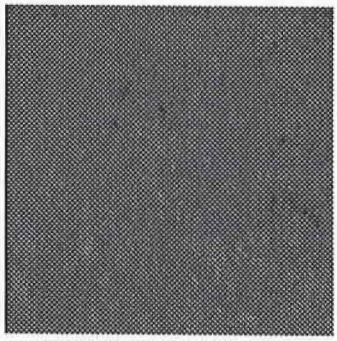

Figure C14b. 128x128 Pixel Image of Washed Uncrushed River Gravel.